CASCADE TESTS OF THE BLADING OF A HIGH-DEFLECTION, SINGLE-STAGE, AXIAL-FLOW IMPULSE TURBINE AND COMPARISON OF RESULTS WITH ACTUAL PERFORMANCE DATA

JOHN EUGENE BARTOCCI

CASCADE TESTS OF THE BLADING OF A HIGH-DEFLECTION, SINGLE-STAGE, AXIAL-FLOW IMPULSE TURBINE AND COMPARISON OF RESULTS WITH ACTUAL PERFORMANCE DATA

by

John Eugene Bartocci
Lieutenant Commander, United States Navy
B.S., United States Naval Academy, 1957

Submitted in partial fulfillment
for the degree of

AERONAUTICAL ENGINEER

from the

UNITED STATES NAVAL POSTGRADUATE SCHOOL
May 1966

ABSTRACT

Cascade tests were performed on models of the stator (nozzles) and rotor blade rows of a high deflection, single-stage, axial-flow impulse turbine. The tests were performed at the Rectilinear Cascade Test Facility of the Propulsion Laboratories, United States Naval Postgraduate School. The results of these tests were compared with the performance data of the actual turbine. The comparison showed that profile and mixing losses, though not negligible, constitute only a small percentage of the overall rotor loss. Also, the inlet flow angle at which the minimum loss occurred for the Cascade flow was significantly different from the inlet flow angle at which minimum actual rotor loss occurred.

TABLE OF CONTENTS

LIST OF ILLUSTRATIONS

TABLE OF SYMBOLS

a	speed of sound, ft./sec.
c	chord of test blade, ft.
C_D	drag coefficient, dimensionless
C_L	lift coefficient, dimensionless
c_p	specific heat at constant pressure, BTU/lbm ^oR.
D	drag force, lb./ft.
dms	mass flow rate, lb. sec./ft.
g	gravitiational constant, ft./sec.^{2}
h	test blade height, ft.
$\hat{\imath}$	unit vector in tangential direction, dimensionless
$\hat{\jmath}$	unit vector in axial direction, dimensionless
J	conversion factor, ft. lb./BTU
L	lift force, lb./ft.
M	Mach number, dimensionless
$\vec{n}$	unit vector normal to control/surface, dimensionless
Ps	absolute static pressure
Pt	absolute total pressure, lb./ft.^{2}
q	dynamic pressure, lb./ft.^{2}
R	gas constant, ft./^oR
$\vec{R}$	force exerted by fluid on test blade, lb./ft.
s	blade spacing, ft.
T	temperature, ^oR or ^oF
V	fluid velocity, ft./sec.
W	flow velocity relative to rotor blades, ft./sec.

x	distance in tangential direction, ft.
y	distance along blade height, ft.
z	distance across blade channel at the discharge, ft.
α	gas flow angle, deg.
β	angle between $\hat{1}$ and $\vec{V}$, deg.
γ	ratio of specific heats, dimensionless
ζ	loss coefficient, dimensionless
θ	(subscripted) flow angle between $\hat{j}$ and $\vec{V}$, deg.
Θ	(non-subscripted) angle between $\hat{1}$ and $\vec{R}$, deg.
ρ	mass density, lb. sec.^{2}/ft.^{4}
σ	solidity, c/s, dimensionless
ϕ	stagger angle, deg.
Ψ	velocity coefficient, dimensionless
ξ	area restriction factor, dimensionless
ΔX	total distance traversed, ft.
Δx	distance between measuring points, ft.
μ	viscosity, lb./ft. - sec.

Subscripts

atm	atmospheric
i	tangential direction
j	axial direction
p	plenum
R	rotor
s	static

t	total
o	station o, far ahead of the cascade
1	station 1, measuring plane ahead of cascade
2	station 2, measuring plane aft of cascade
3	station 3, far aft of cascade
∞	vectorial mean of conditions at stations o and 3

1. Introduction

The need for light-weight, efficient gas turbines that are capable of developing large amounts of power has caused much interest in the flow through low-reaction stages having gas deflections in excess of 110^{o}. Very little performance data on such stages are available and the quest for an efficient design in many instances has become an expensive trial and error process.

The cascade testing of blade rows, performend in conjunction with tests on actual turbines that have the same blade row geometry, is a logical way to learn more about the phenomena involved in the flow through these turbine stages. This work compares the results of cascade tests conducted at the Rectilinear Cascade Test Facility with the results of tests performed on the corresponding actual turbine stage. Two cascade tests of the stator or nozzle blade row were made. Both tests were performed at near design inlet flow angle. Five cascade tests of the rotor blade row were made, each at a different flow angle. The actual turbine performance data are obtained from tests with the Transonic Turbine Test Rig. [9]

A method that would predict the losses of high deflection turbine stages with accuracy would indeed be of value to the turbine designer. The purpose of the comparison of results,

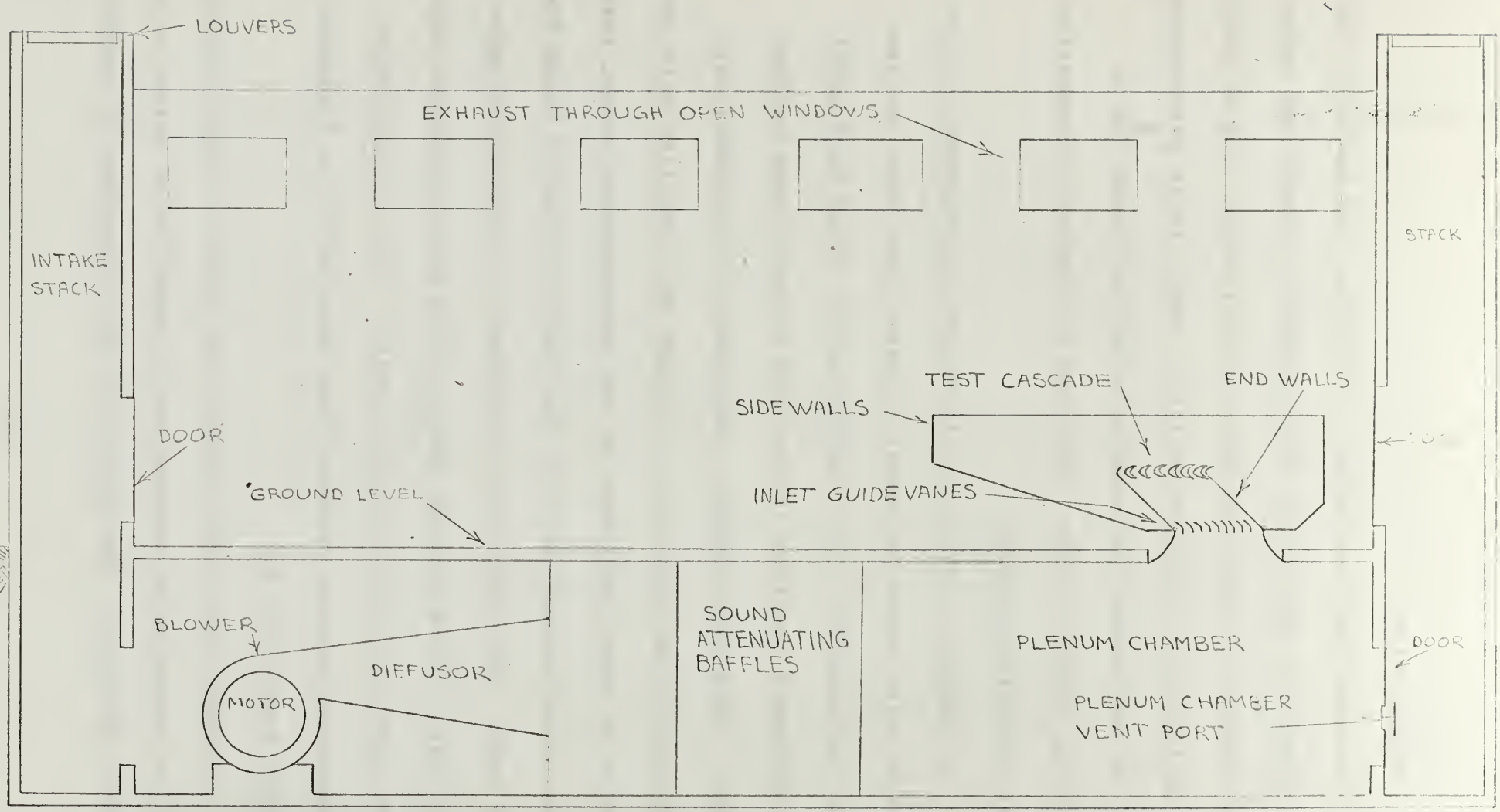

FIGURE 1

SCHEMATIC OF THE CASCADE TEST FACILITY

therefore, is to seek possible ways in which cascade test results may be related to actual turbine performance and to determine a basis on which recommendations for future study may be made. It is hoped that future research in this area will eventually lead to the formulation of some means of accurate turbine performance prediction and a more thorough understanding of the flow through turbomachines.

2. Description of Apparatus

The Rectilinear Cascade Test Facility is an open-cycle wind tunnel designed for the specific purpose of flow testing of rectilinear cascades of axial-flow turbomachines. A schematic diagram of the Cascade Test Facility is shown in Fig. 1. A detailed description of the Cascade Laboratory and associated equipment is given by Rose and Guttormson in a thesis on the installation and initial tests of the Cascade Test Facility. [10] Modifications to the plenum chamber are described in a United States Naval Postgraduate School, Department of Aeronautics, Technical Note by the writer. [6]

The blade shapes used in this investigation were models of the stator and rotor of an actual single-stage turbine which is being tested concurrently in the Transonic Turbine Test Rig, also located at the Propulsion Laboratories of the U. S. Naval Postgraduate School. The stator or nozzle profile

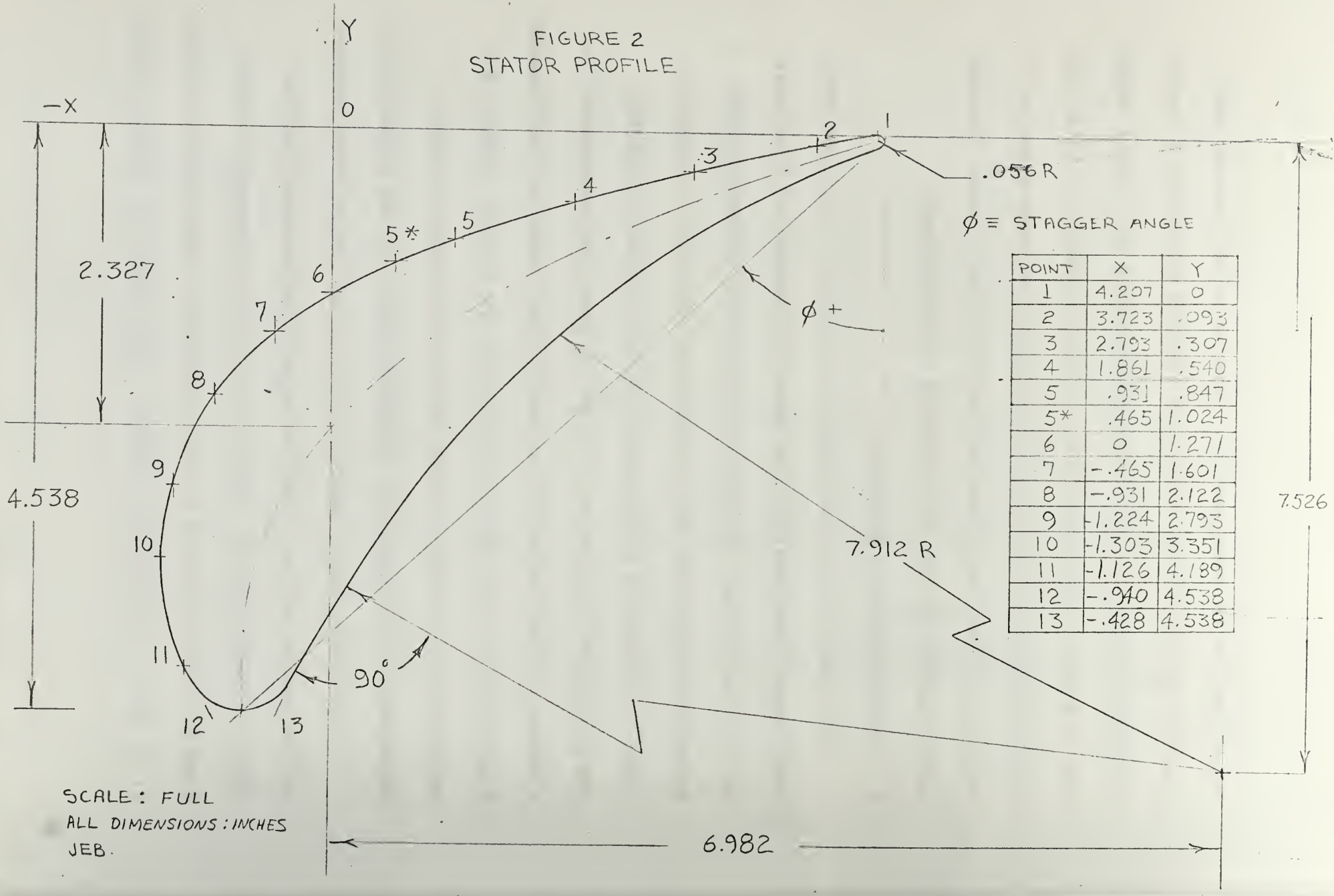

POINT	X	Y
1	4.207	0
2	3.723	.093
3	2.793	.307
4	1.861	.540
5	.931	.847
5*	.465	1.024
6	0	1.271
7	-.465	1.601
8	-.931	2.122
9	-1.224	2.793
10	-1.303	3.351
11	-1.126	4.189
12	-.940	4.538
13	-.428	4.538

is shown in Fig. 2. The stators are of the converging nozzle type with a chord of 6.66 inches, a blade spacing of four inches and a stagger angle of 48°. Stagger angle is defined as shown in Fig. 2.

The rotor profile geometry is shown in Fig. 3. Of note is the fact that the shape geometry is composed solely of straight lines and circular arcs, that the leading and trailing edges are not rounded, and that the blade shape is designed for large flow deflection, namely 132°. The rotor blade models have a chord of 6.657 inches and a blade spacing of four inches. The stagger angle is -4.5°.

The arrangement of the cascade test section for the stator blading is shown schematically in Fig. 4. Straight inlet guide vanes were used and the end walls were positioned vertically so that the flow would come straight up to the stator profiles. The stator cascade had a total of 15 blades. There were 30 inlet guide vanes spaced two inches apart. End walls were not installed aft of the blade models, however, metal fairings were arranged between the lower end walls and the adjacent blade models. Fig. 5 is a view of the stator cascade with the removable side wall installed. Rubber gasket material was cut to the shape of the profile and cemented to the end of the model. This was done to prevent the passage of air between the model and the removable side wall.

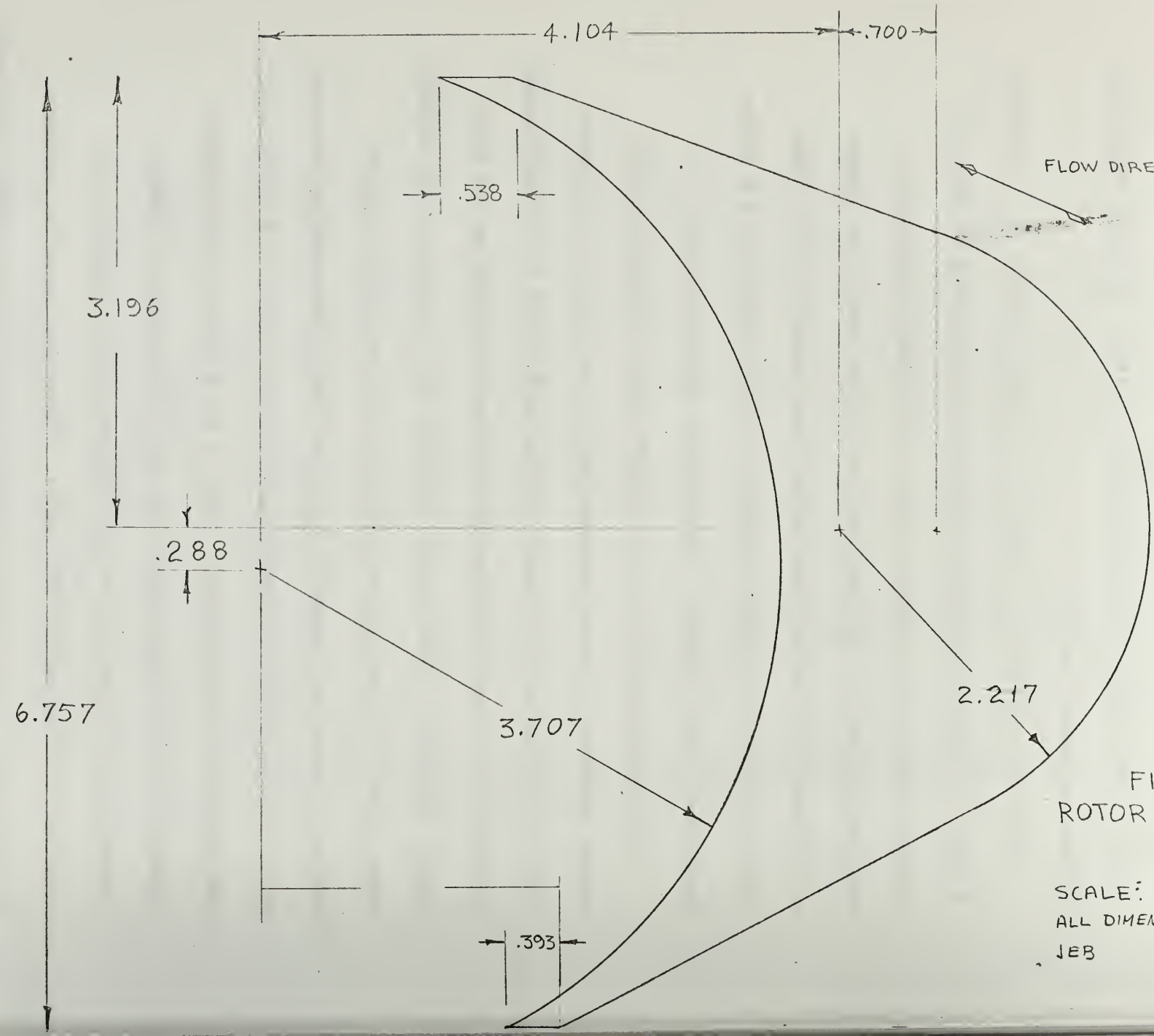

FIGURE 3
ROTOR PROFILE

SCALE: FULL
ALL DIMENSIONS: INCHES
JEB

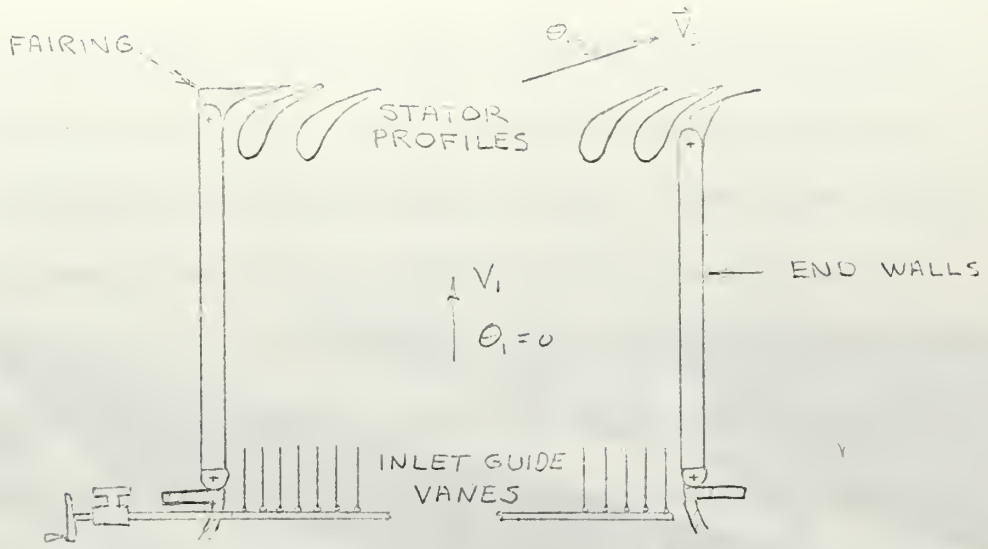

FIGURE 4

TEST SECTION CONFIGURATION : STATOR CASCADE

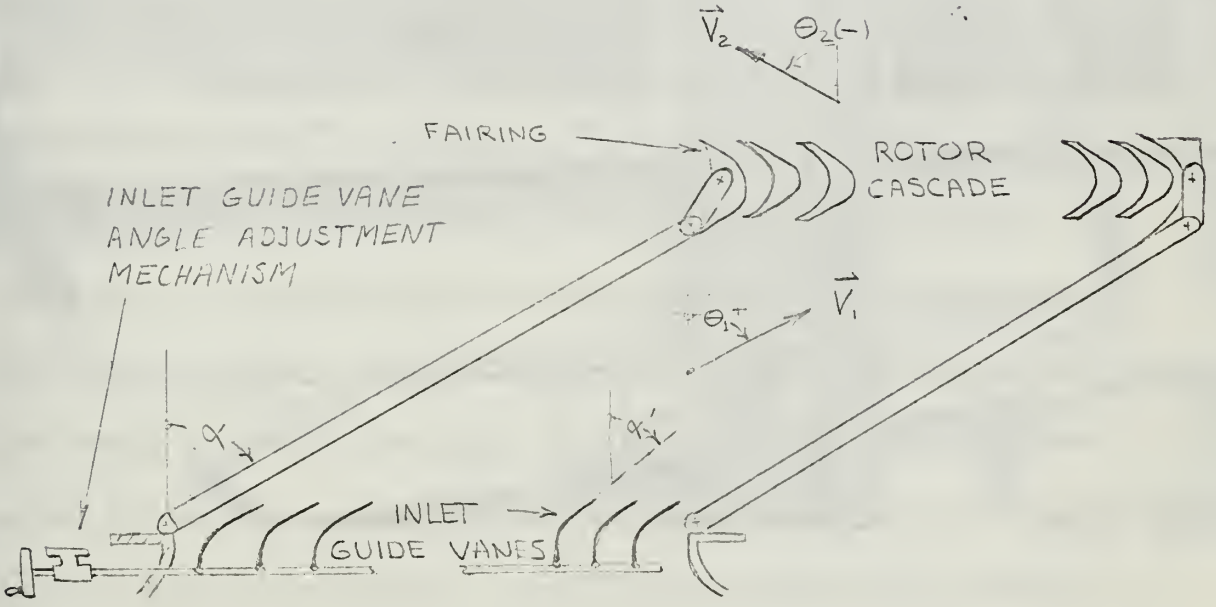

FIGURE 6

TEST SECTION CONFIGURATION : ROTOR CASCADE

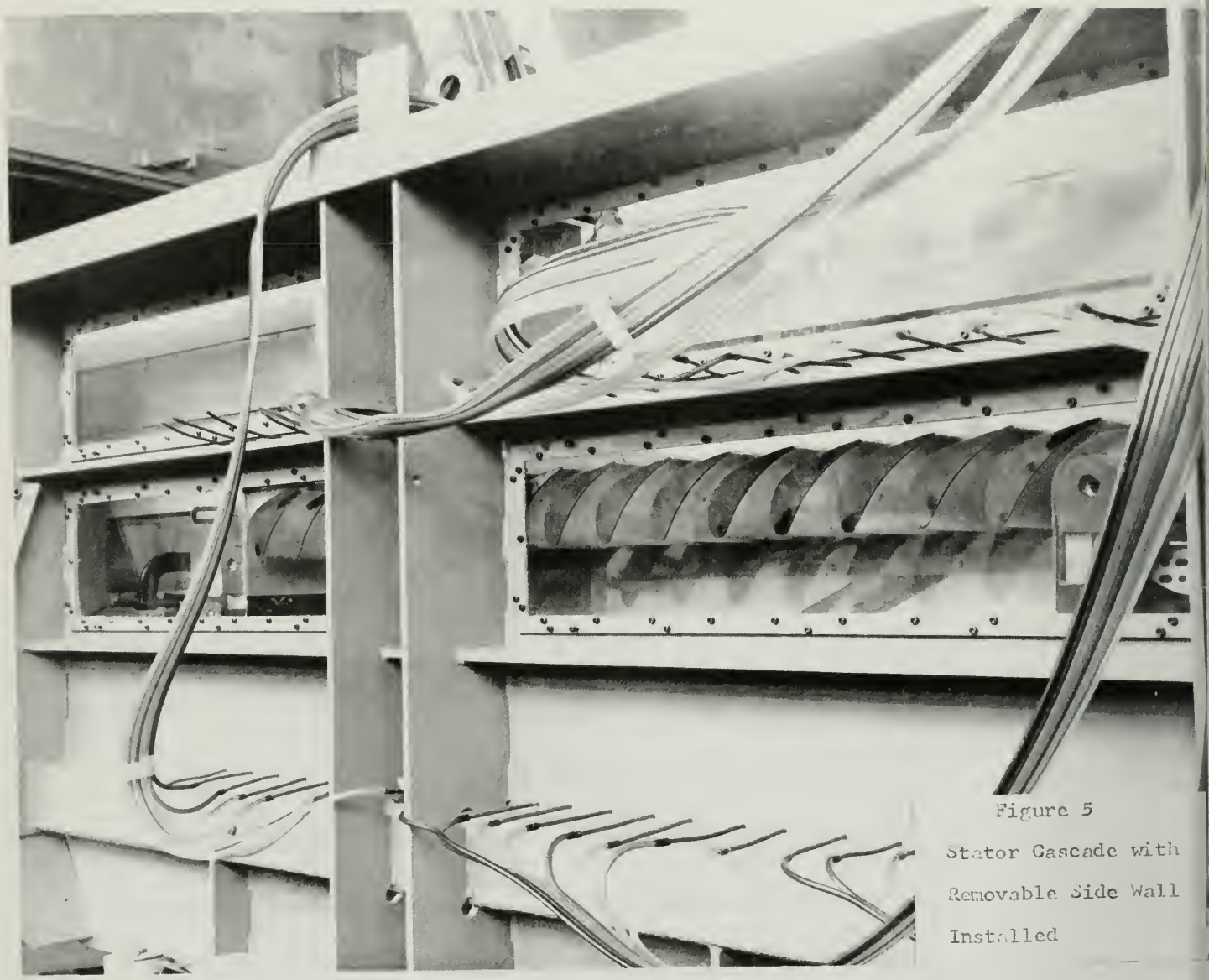

Figure 5

Stator Cascade with Removable Side Wall Installed

The arrangement for the rotor cascade tests is shown schematically in Fig. 6. Inlet guide vanes with 60 degree nominal deflection were installed. Inlet guide vane spacing was two inches. The total number of guide vanes was 30, and there were 15 blades in the rotor cascade. The end walls were positioned parallel to each other. Different inlet flow angles Θ_1 were obtained by changing the angle α of the end walls and by adjusting the angle α' of the inlet guide vanes. The inlet guide vanes are mechanically linked so that angular positioning of all the inlet guide vanes can be accomplished simultaneously.

3. Instrumentation

Pressure and flow angle measurements of the flow in the cascade test section were made by using two United Sensor and Control Corporation YC-120 probes. These probes are designed to measure total pressure, static pressure and yaw angle. The wedge-type probe head has one total pressure sensing port (P1), and two static pressure sensing ports (P2 and P3). When the probe is inserted into a flow, the total pressure sensing port is oriented into the flow direction when P2 and P3 are equal. The YC-120 probes were mounted in the upper and lower carriages in the manner described in [10]. Pressures which were measured directly were total pressure (Pt) and the difference between total and static pressure (q).

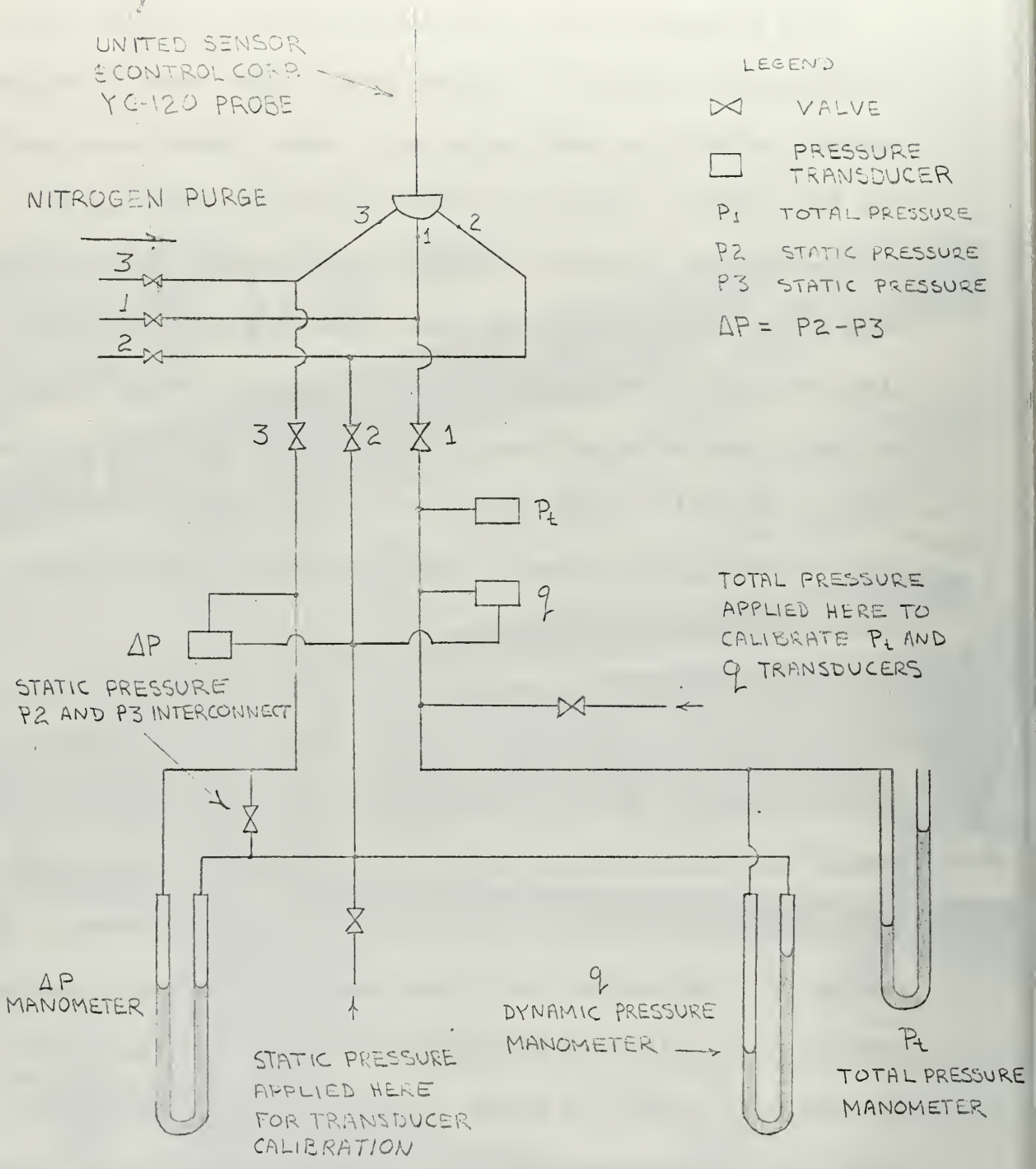

FIGURE 7

INSTRUMENTATION SYSTEM SCHEMATIC. TYPICAL FOR BOTH UPPER AND LOWER TRAVERSES

The probes are connected to an automatic data logging system which utilizes electric pressure transducers, and to a back-up system with water manometers as pressure gages. The system has provisions for calibrating the automatic data logging system by applying pressures to the transducers which can be read on the water manometers. A protractor was installed on the probe carriage housing so that flow angle calibration of the automatic data logging system could be accomplished, and that flow angle could be read directly. A schematic diagram of the system is given in Fig. 7. The system shown is typical for both the upper and lower traverse. The system has provisions for blowing out the probes with Nitrogen to insure that foreign particles do not clog their capillary tubings. A set of three valves is used to isolate the pressure transducers and water manometers from the Nitrogen system that operates at relatively high pressures.

Static pressure taps located in the test section side walls were used to monitor the static pressure distributions in the test section. There are two rows of taps in each side wall. The rows are parallel to the cascade axis and the taps are spaced three inches apart. The lower rows of static taps are located four inches ahead of the lower traverse, and the upper rows of static taps are located aft of the blade models but four and one quarter inches ahead of the

Figure 8

Vernier Probe Holder Position with Stator Cascade

upper traverse. The static pressure taps are connected to three 97-inch water manometer banks.

A pressure tap located in the plenum chamber and connected to a 40-inch manometer is used to measure the plenum pressure. The fluid used in this manometer has a specific gravity of 1.75. A thermometer probe located in the plenum was used to determine the plenum temperature. Atmospheric pressure was read from a standard mercury column barometer.

In order to investigate the flow within a blade channel, a pitot-static probe was placed in a vernier probe holder. The assembly was then mounted in the cascade test section between the side walls as shown in Fig. 8. The probe holder assembly was positioned so that the probe head could be moved along the exit plane of a blade channel. Fig. 9 and Fig. 10 show the probe positioning for the stator and rotor blade modes respectively. The pitot-static probe head used had a diameter of 0.065 inches. A total pressure probe was also made to fit the vernier probe holder. This probe had a thickness of 0.019 inches at the tip. The vernier probe holder allowed the probe to be moved in increments of 0.01 inch. Total pressure and dynamic pressure were measured using two 40-inch water manometers.

Due to malfunctions in the automatic data logging system, the back-up manual system was used to conduct this investigation.

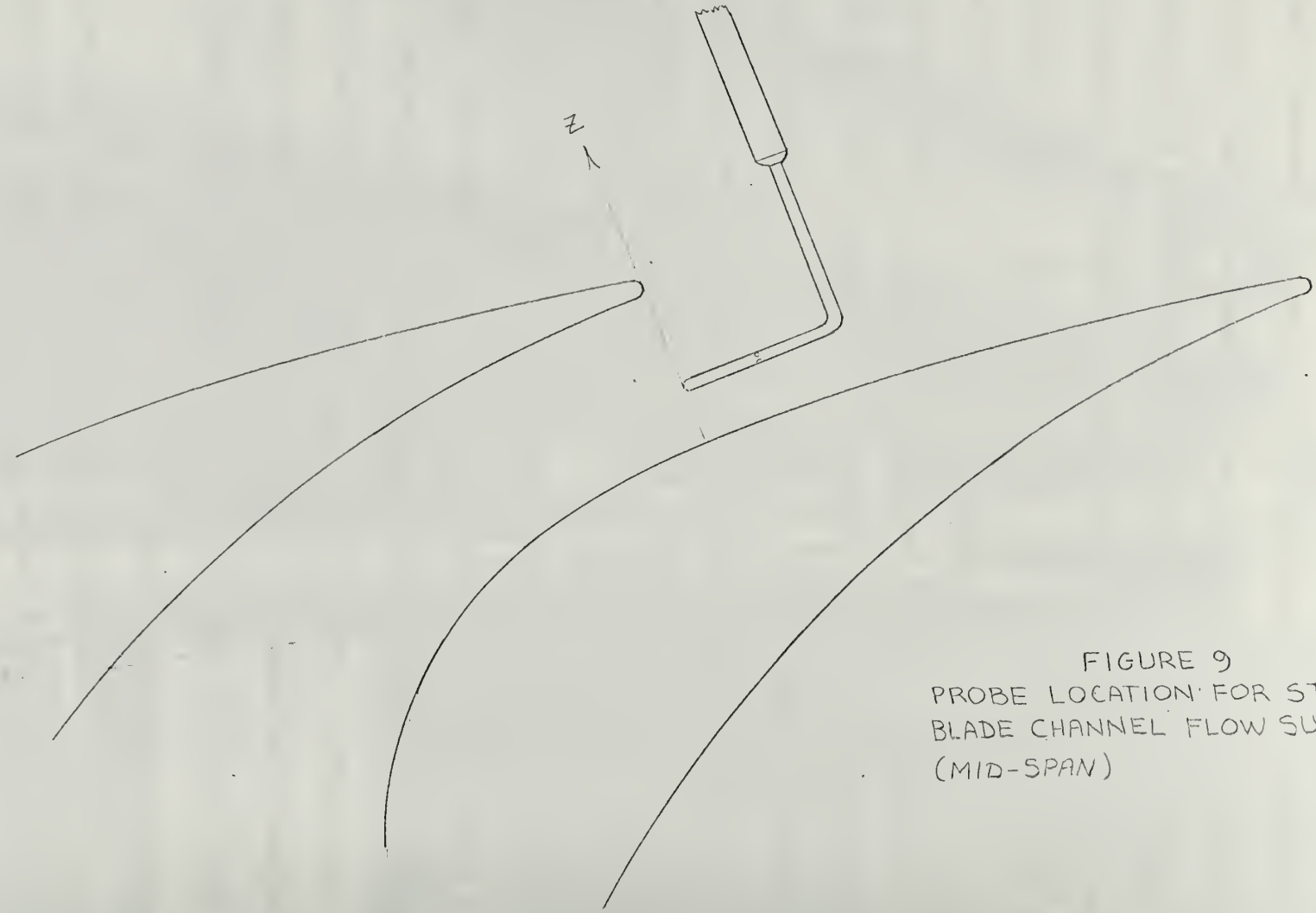

FIGURE 9
PROBE LOCATION FOR STATOR
BLADE CHANNEL FLOW SURVEY
(MID-SPAN)

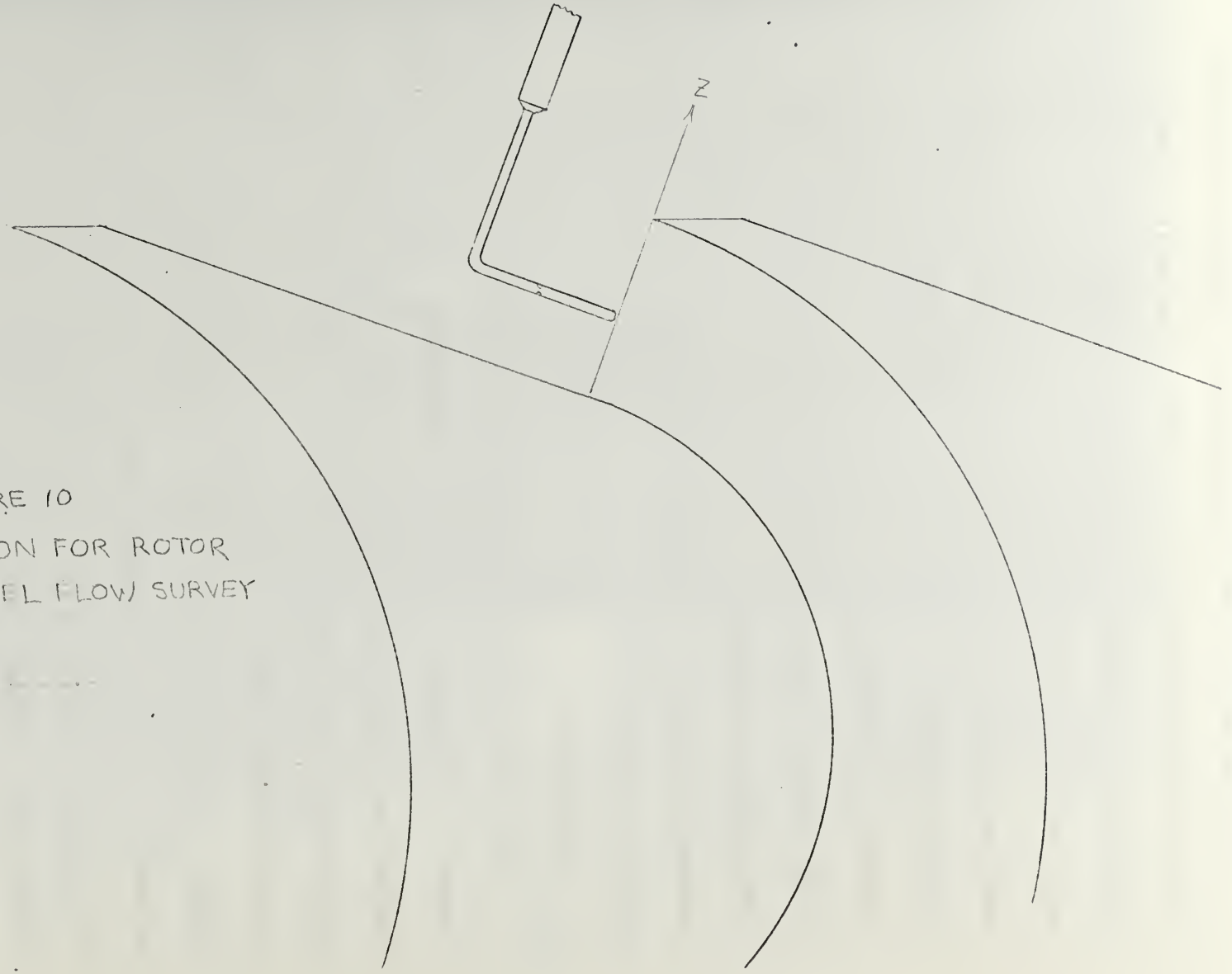

FIGURE 10

PROBE LOCATION FOR ROTOR BLADE CHANNEL FLOW SURVEY (MID-SPAN)

All manometers were graduated in tenths of an inch, and the protractors associated with flow angle readings were graduated in degrees. The pressure measurements could be read accurately to within one-half a graduation. The readings within half a graduation are estimates based on the position of the meniscus at the time of the observation. For instance, a reading of q=25.28 inches of water means 25.30<q< 25.30 but that the pressure reading is closer to 25.30. Flow angle measurement is considered to be accurate to within one-half a degree. A recorded value of $\theta = 62.3^{o}$ means $62^{o}.0 < \theta < 62^{o}.5$.

4. Procedure

The test section was first set up for the stator model tests in the manner previously described. After the blade models, entrance guide vanes, end walls and fairings were positioned, the removable side wall was installed, and the static pressure taps were connected to the 97-inch manometer banks. During the preliminary runs, with the motor running at medium speed, the blower started to surge as the flow rate through the test section was increased by opening the blower inlet vanes. Since the stator blades turn the flow by about 75^{o}, the flow area at the discharge of the stator blades is only about one-fourth of the flow area ahead of them. The pressure required to discharge the whole flow rate of the

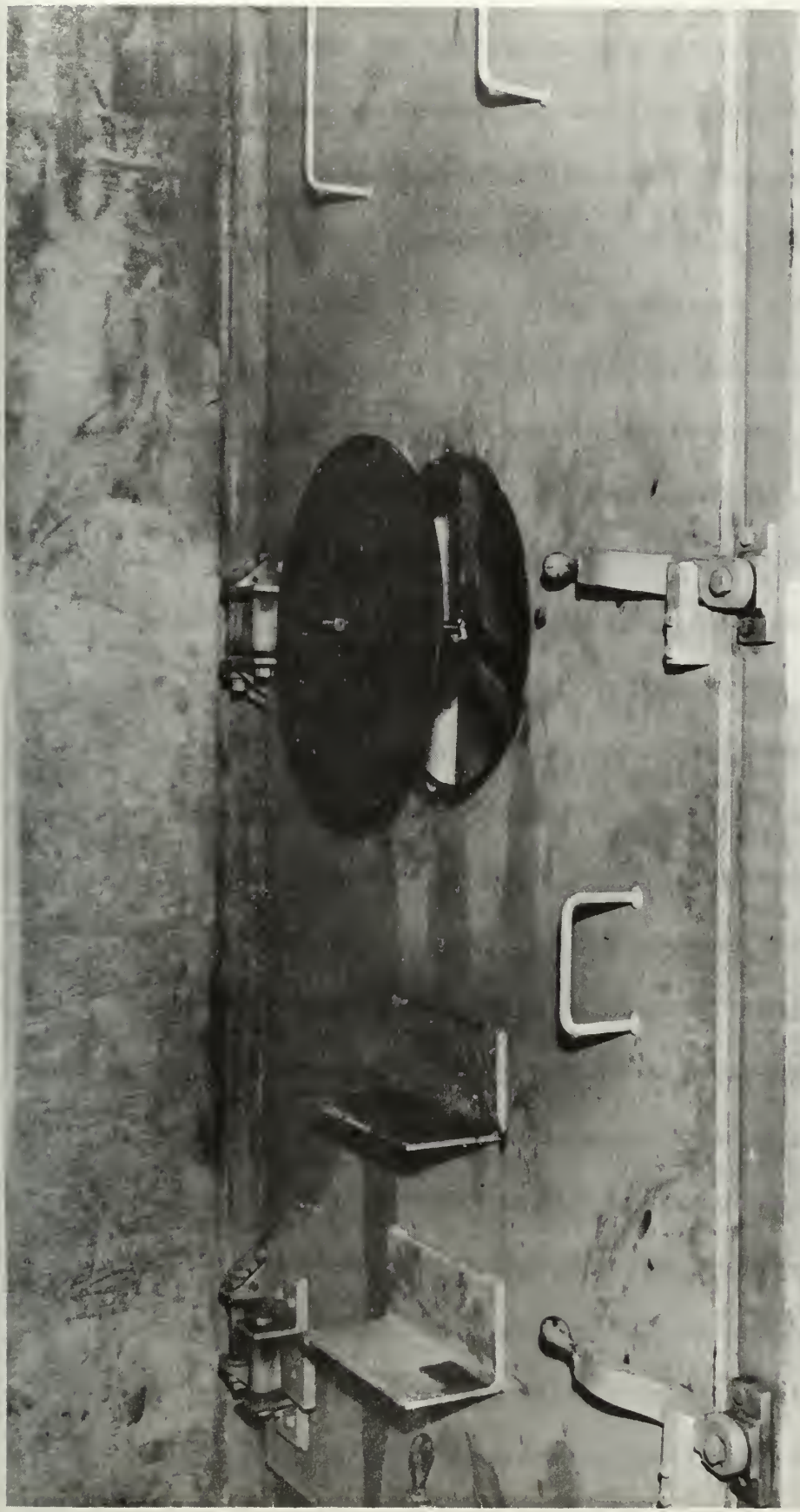

Figure 11

Plenum Chamber Vent Port

blower through the cascade was higher than that which could be produced by the blower without surging. It was therefore necessary to vent part of the flow delivered by the blower directly from the plenum chamber to the atmosphere. This was accomplished by cutting a hole of 16 inches in diameter in each of the two steel doors that give access to the plenum chamber. Cover plates were manufactured for these holes to adjust the effective by-pass flow area. With these plates, one of which is shown in Fig. 11, it was possible to operate the blower at the desired plenum pressure without surging. The location of these vent ports is shown in Fig. 1. It can be seen that the by-pass flow is discharged to the atmosphere through the stack adjacent to the plenum chamber.

Prior to the start of data acquisition, the lower probe was positioned six inches beyond the geometric center of the test section along the cascade axis. The middle probe position along the upper cascade axis was determined by the intersection of a line projected along the design discharge angle from the trailing edge of the center blade and the upper traverse. The starting position for the upper probe was six inches to the same side of center as the lower probe. After the pressure lines of the instrumentation were checked for possible air leaks, the zero flow angle position of the YC-120 probes was set, and the manometers were set at zero.

The blower was then started and the desired plenum pressure set. It was found that an initial decrease in plenum pressure occurred just after start. For instance, with the blower set at medium speed, blower inlet vanes open, the initial plenum pressure was approximately 26.5 inches of H_2O. Within the first half hour of blower operation, the plenum pressure would generally drop 0.8 to 1.2 inches of H_2O and then stabilize.

Once a test run was initiated, the probes were moved along the cascade axis (in the x direction) by manually turning the traverse carriage drive screw instead of using the electric drive. A hand crank was attached to the gearing of the electric motor that moves the carriage along the cascade axis. One turn of the hand crank moved the carriage (and consequently the probe) 0.01 inch. This method of incremental movement of the probe was used since exact positioning of the probe by means of the electric drive motor controlled by the toggle switch located on the automatic data logging system console was difficult.

The positioning of the probes in yaw was accomplished by means of the motor drive arrangement incorporated in the carriage mechanism with control from the console. The yaw seeking feature of the automatic data acquisition system was not used.

It was decided to set the angular position of the probe by hand since with the automatic nulling device of the data logging system the difference between pressures P_2 and P_3 was not zero, but between about 0.5 and 1.0 inches of water.

The data acquisition procedure at each probe position consisted of:

a. Rotating the probe in yaw until the ΔP manometer indicated $\Delta P = 0$.

b. Reading and recording Pt, q and θ.

c. Moving the probe the desired x increment to the next probe position.

At each probe position the data recorded were:

a. Point number

b. Δx (in.)

c. θ (deg.)

d. Pt (in. of H_20)

e. q (in. of H_20)

Periodic recordings of plenum temperature (^oF), plenum pressure (in. of 1.75 specific gravity manometer fluid), and atmospheric pressure (in. of Hg) were also made.

The incremental distance Δx that the probe should be moved depends on the rate of change of the pressures (Pt or q) with x. The x increment used for all rotor cascade tests was 0.05 inches for both upper and lower traverses. For the

stator cascade tests the value of Δx along the lower traverse was 0.05 inches. The x increment was increased to 0.10 inches along the upper traverse once it was established that there was very little variation of Pt or q with x.

Since for both stator models and rotor models the blade spacing was four inches, the total x distance traversed for upper and lower data was 12 inches or three blade spacings (six inches either side of the middle position). Inasmuch as some time had to be allowed at each probe position for the water manometers to seek new levels, the time required to obtain a complete set of data was approximately six to seven hours per traverse. With the manual mode of data acquisition, upper and lower traverse data could be taken simultaneously. Data was recorded directly on computer coding forms in the format required by the data reduction computer program.

Two stator cascade tests were made; one at a plenum pressure of 26.3 ± 0.3 inches of H_2O, and one at 11.4 ± 0.4 inches of H_2O. The former was conducted at medium motor speed, blower inlet vanes open, and the latter at low motor speed, blower inlet open. End walls and test section inlet guide vanes were positioned so as to yield a flow angle of zero ahead of the stator models. Test section geometry was the same for both stator model runs. Plenum chamber vent ports were set wide open for the stator profile tests.

Five tests were made with the rotor cascade, namely at inlet flow angles between 56.1° and 68.6°. For each of the tests, the motor was run at medium speed with blower inlet vanes open which yielded a plenum pressure of approximately 26.0 inches of H_2O. With the test section configured for the design flow angle ahead of the cascade, a preliminary run was made at a plenum pressure of about 35.0 inches of H_2O. To obtain this plenum pressure, high motor speed was used with blower inlet vanes adjusted to yield 35.0 inches of H_2O pressure in the plenum. Plenum chamber vent ports were full open. At this setting, however, plenum pressure fluctuated $\pm$ 0.45 inches of H_2O, and the static pressure readings on the 97-inch manometer banks had a periodic fluctuation of approximately 0.75 inches of water. This was considered excessive in view of the fact that static pressure fluctuations at the intermediate plenum pressure were less than $\pm$ 0.2 inches of water. The decision was therefore made to conduct the rotor profile tests at a plenum pressure of approximately 25.0 inches of H_2O.

Rotor profile tests subsequent to the initial test at near design inlet flow angle involved changing the test section end wall angles and adjustment of inlet guide vanes to give cascade inlet flow angles greater than and less than design flow angle.

At the completion of each run, the data sheets were submitted to the computer facility where the data was punched on IBM cards for use as input to the data reduction computer program.

Surveys of the flow conditions across the blade channel at the discharge were conducted for both rotor and stator blading. The vernier probe holder with the pitot-static probe was aligned so that the probe would traverse across the discharge throat area of the blade channel at the mid-span of the blade model. The incremental distance that the probe was moved, total pressure, and static pressure were recorded for each probe position. At the completion of the throat area traverses with the pitot-static probe, the thinner total pressure probe was installed and total pressure readings close to the blade surfaces were recorded in an effort to define the boundary layer thicknesses at the throat station. The above surveys were made at a blade channel adjacent to the central blade in the cascade.

5. Results and Discussion

The results of the cascade tests are given in Appendix C. Tables 1 and 2 are summaries of these results.

The Reynold's number for both stator and rotor cascade is

$$Re_Y = \frac{\rho_3 V_3 C}{\mu}$$

Table 1

STATOR CASCADE TEST RESULTS

RUN #	300	301
ζ	0.045	0.051
ζ'	0.044	0.049
α_i °	0.3	0.0
α_o °	0.3	0.0
α_3 °	78.5	78.7
$\Delta\alpha$ °	78.2	78.7
$C_{L\infty}$	2.30	2.30
$C_{D\infty}$	0.095	0.133
Rey	1.22×10^6	0.81×10^6
M_3	0.3	0.2
$\sim\theta_1$	±0.5	0
$\sim\theta_2$	±0.5	±0.6

Table 2

ROTOR CASCADE TEST RESULTS

RUN #	302	303	304	305	306
ζ	0.063	0.062	0.081	0.103	0.074
ζ'	0.060	0.059	0.076	0.094	0.070
α_i °	+0.4	+4.2	-2.6	-5.9	+6.6
α_o °	62.4	66.2	59.4	56.1	68.6
α_3 °	-71.9	-71.6	-72.4	-71.9	-70.4
$\Delta\alpha$ °	134.3	137.3	131.8	128.1	139.0
$C_{L\infty}$	5.22	5.86	4.79	4.41	6.29
$C_{D\infty}$	0.231	0.233	0.253	0.257	0.277
Rey	1.16×10^6	1.16×10^6	1.12×10^6	1.12×10^6	1.15×10^6
M_o	0.19	0.21	0.16	0.15	0.24
$\sim\theta_1$	±0.6	±0.8	±0.4	±0.3	±0.9
$\sim\theta_2$	±0.3	±0.4	±0.2	±0.2	±0.2

NOTE: $\sim\theta$ INDICATES THE MAXIMUM VARIATION OF THE MEASURED FLOW ANGLE ALONG THE DISTANCE TRAVERSED

while Mach number is defined as follows:

For the stator cascade,

$$M = \frac{V_3}{\sqrt{\gamma g R T_3}}$$

For the rotor cascade,

$$M = \frac{V_o}{\sqrt{\gamma g R T_o}}$$

Since in turbine calculations and for the turbine tests mentioned earlier, a loss coefficient $\zeta_R = 1 - \Psi^2$ is used, where

$$\Psi = \frac{W_2}{W_{2\,theoretical}}$$

a loss coefficient

$$\zeta' = 1 - \left(\frac{V_3}{V_{3\,theoretical}} \right)^2$$

is determined for the cascade tests.

The flow conditions in the test section during the stator cascade tests are considered to be good. Fig. C1 shows the static pressure distribution (over three blade spacings) at the lower traverse for Run #300. The maximum static pressure reading was approximately one percent higher than the average static pressure. Fig. C2 shows that the total pressure distribution ahead of the cascade is also quite uniform. The presence of wakes due to the inlet guide vanes is evident in Fig. C3. Since the average value of q_1, shown in Fig. C3 is about 1.3 inches of water, errors due to fluctuations in pressure, plus errors in measurement form a greater percentage of the true average value of q

than the same for Ps. Therefore, the plot of q_1 versus x is more irregular than that of Ps_1 versus x.

Fig. C5 shows that the flow aft of the cascade is practically mixed by the time it reaches the upper traverse probe location. The constriction factor

$$PSI = \frac{\int_{(1)} \rho_1 V_1 \cos\theta_1 \, dx}{\int_{(2)} \rho_2 V_2 \cos\theta_2 \, dx} = 1.11$$

indicates that flow constriction due to wall boundary layer growth is not too pronounced. It is reasonable to conclude then, that the flow across the stator cascade is, for all practical purposes, two-dimensional.

Figs. C7 through C12 give corresponding graphs for Run #301. The reason for making a stator cascade test at a lower plenum pressure was to compare the loss coefficients of the same flow at a different Reynold's number. Table 1 shows that the lower loss occurs at the higher Reynold's number, but that the loss coefficients are about the same. Since errors in the pressure readings of Run #301 constitute a greater percentage of the average values, no conclusions can be drawn from the comparison.

Errors in the pressure readings may be classified as:

1. Errors due to the precision limits of the manometer.
2. Errors due to fluctuation in pressure which are caused by a slight unsteady flow condition.

Unless the amplitude and frequency of the pressure fluctuation are known, the accuracy of a reading is difficult to determine. If, however, the fluctuations in pressure are random, statistical methods may be used to estimate an interval in which the actual mean value will lie. This is a so-called confidence interval for the mean.[1] The assumptions made are that the pressure fluctuations are random, and that for a constant plenum pressure, the fluctuations have a normal distribution about the mean value. By observing n pressure readings at the same probe location, a confidence interval is determined by utilizing the t-statistic.[2]

Let Pm be the mean value of pressure, then

$$\bar{P} - t_{\alpha/2} \frac{S}{\sqrt{n}} < P_m < \bar{P} + t_{\alpha/2} \frac{S}{\sqrt{n}}$$

where

$$\bar{P} = \frac{1}{n} \sum_{i=1}^{n} P_i$$

$$S^2 = \frac{\sum_{i=1}^{n} (P_i - \bar{P})^2}{n-1}$$

[1]Miller, I., and Freund, J. E., Probability and Statistics for Engineers (Prentice-Hall, Inc., 1965) p. 146.

[2]Ibid., pp. 136-139.

and S is the variance of the sample of n readings. The quantity $t_{\alpha/2}$ is the value of the t-statistic with a probability of $1-\alpha$ that Pm will fall in the prescribed interval.

Twenty pressure readings of q_2 and Pt_2 were observed. Utilizing the above equations,

$$\bar{q}_2 = 25.20 \quad \text{in. of } H_2O$$

$$S_q = \pm 0.06 \quad \text{in. of } H_2O$$

and

$$25.17 < q_{2_{mean}} < 25.22 \quad \text{in. of } H_2O$$

for a 95% confidence interval. This means that for the assumptions made, and for repeated sampling, the mean value of q_2 will be within the interval 95% of the time. By comparison, the variation for the total pressure observations was 0.01 and is considered negligible. It may be assumed further that the variation in pressure is about the same throughout the test section. The statistical method used merely serves to point out that, although the observed variation was 0.06 inches of water (which is small) during the course of a cascade test, the pressure fluctuations are probably less than 0.06 most of the time.

The results of tests made with the actual stator in the

Transonic Turbine Test Rig[3] show that the total loss coefficient for the stator or nozzle is generally larger than the value obtained by cascade tests. Values of the stator loss coefficient from actual turbine tests varied from 0.095 to 0.11 for a large range of pressure ratios. The geometric scale factor, cascade models to actual nozzle profiles, is 4.65: 1.

The loss coefficient ζ' accounts for two-dimensional profile losses and mixing losses. The mixing loss is due to the decrement of kinetic energy incurred when the wakes aft of the cascade smooth out to a uniform flow. The mixing loss is included, and the conditions far ahead and far aft are determined because most three-dimensional analyses of axial-flow turbomachines are based on the so-called actuator-disc theory.[4] According to this theory, it is assumed that the blade row acts as a line of discontinuity at which the flow direction and velocity are changed, and on either side of which, total or stagnation conditions are different.

[3]Eckert, R. H., Performance Analysis and Initial Tests of a Transonic Turbine Test Rig. (Thesis, United States Naval Postgraduate School, Monterey, California, 1966)

[4]Horlock, J. H., Axial Flow Compressors (London: Butterworths Scientific Publications, 1958) p. 105.

Included in the stator losses of the actual machine are three-dimensional profile loss, secondary flow loss,[5] wall boundary layer loss and mixing loss. In addition, there is the effect of compressibility which, in this analysis, is undetermined since the flow in the stator of the actual machine was choked for most of the tests.

From a method of turbine performance estimation, based on experimental data, by Ainley and Mathieson, the profile loss coefficient, Yp, for the stator is predicted to be 0.05. [4] This loss coefficient is defined by

$$Y = \frac{P_{t_0} - P_{t_3}}{P_{t_3} - P_{s_3}}$$

Calculating Y from the results of Run #300 (Table C1), it is found that Y = .049 which is a loss coefficient based on pressure drop and in which mixing loss is included. The value of Yp derived by the method of Ainley and Mathieson and the value of Y, from cascade data are close. Although it is generally recognized that mixing losses are small compared to profile loss, the mixing loss is not known from the cascade tests of this investigation.

It would be of interest to know how to correlate the two-dimensional loss obtained from cascade tests to the

[5]Vavra, M. H., Aerothermodynamics and Flow in Turbomachines (New York: John Wiley and Sons, Inc., 1960) pp. 374-384.

overall profile loss of a blade of finite height. N. Scholz suggests that the mean loss coefficient of a cascade is one that accounts also for secondary flow losses due to wall boundary layer. [11] The above reference gives a total loss coefficient as follows:

$$\zeta_{total} = \frac{1}{h}\int_0^h \zeta_{local}(y)\, dy = \zeta_{two\text{-}dimensional} + \frac{c}{h}\zeta_{wall}$$

Scholz relates the two dimensional loss to the total loss as a function of h/c, the blade aspect ratio. With ζ' = .044 = ζ two-dimensional (from Run #300) then from results given by Scholz,

$$\zeta_{total} \cong 0.088$$

for the stator cascade. Now by the method of Ainley and Mathieson,

$$\zeta_s + \zeta_p = 0.088$$

where ζ_s is the secondary flow loss and ζ_p is the profile loss coefficient. This interesting correlation of results suggests areas for future experimental studies with the Cascade Test Facility; namely, the verification of the total cascade loss coefficient relationship given by Scholz, and the effect of Reynold's number on losses near the blade-wall juncture. The latter would be particularly applicable to the prediction of three-dimensional blade loss coefficients of

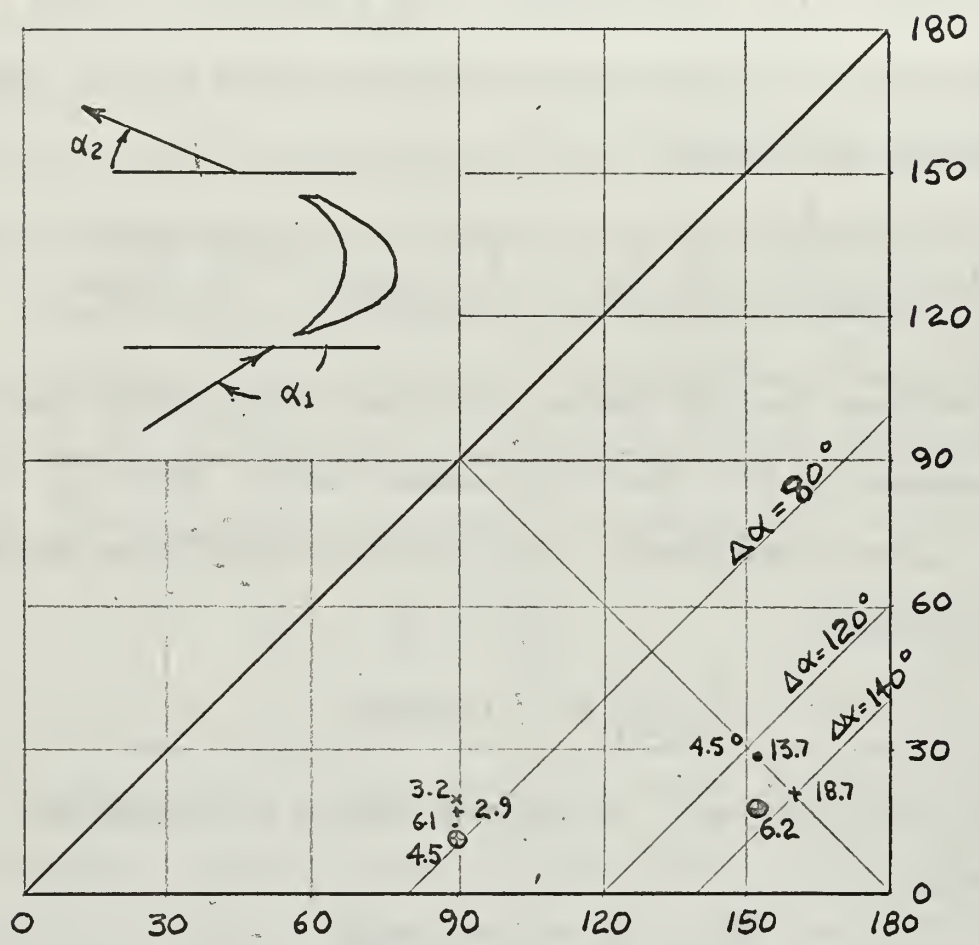

Figure 12

Variation of Loss Coefficients

With Total Flow Deflection

Adapted from Bolte [7]

blade with a varying chord.

Fig. 12 shows the stator cascade loss coefficient with regard to the total turning angle of the flow ($\Delta \alpha$). Also shown are a few loss coefficients for blading of similar deflection as given by Bolte. [7]

Figs. 13, 14, and 15 are the results of the stator cascade throat area survey using the pitot static probe. Fig. 31, the dynamic pressure distribution across the throat shows the influence of the difference in curvature of the two blade surfaces (see Fig. 9), with the higher q occurring near the surface with the most curvature. Fig. 16 shows the velocity distribution in the wake boundary layer near the trailing edge of the stator blade model. The boundary layer thickness was determined from the total pressure distribution.

The area restriction factor (ξ)[6] is important to the determination of flow areas in turbomachine design. ξ is defined by

$$\xi = 1 - \frac{\delta^*}{o}$$

for a cascade, where o is the throat dimension and δ^* is the sum of the displacement thicknesses in the channel. For

[6]Vavra, M. H. Von Karman Institute for Fluid Dynamics Lecture Series, Problems of Fluid Mechanics in Radial Turbomachines. Part III, March, 1965.

Figure 13

Distribution of Dynamic Pressure

Across Stator Throat Area

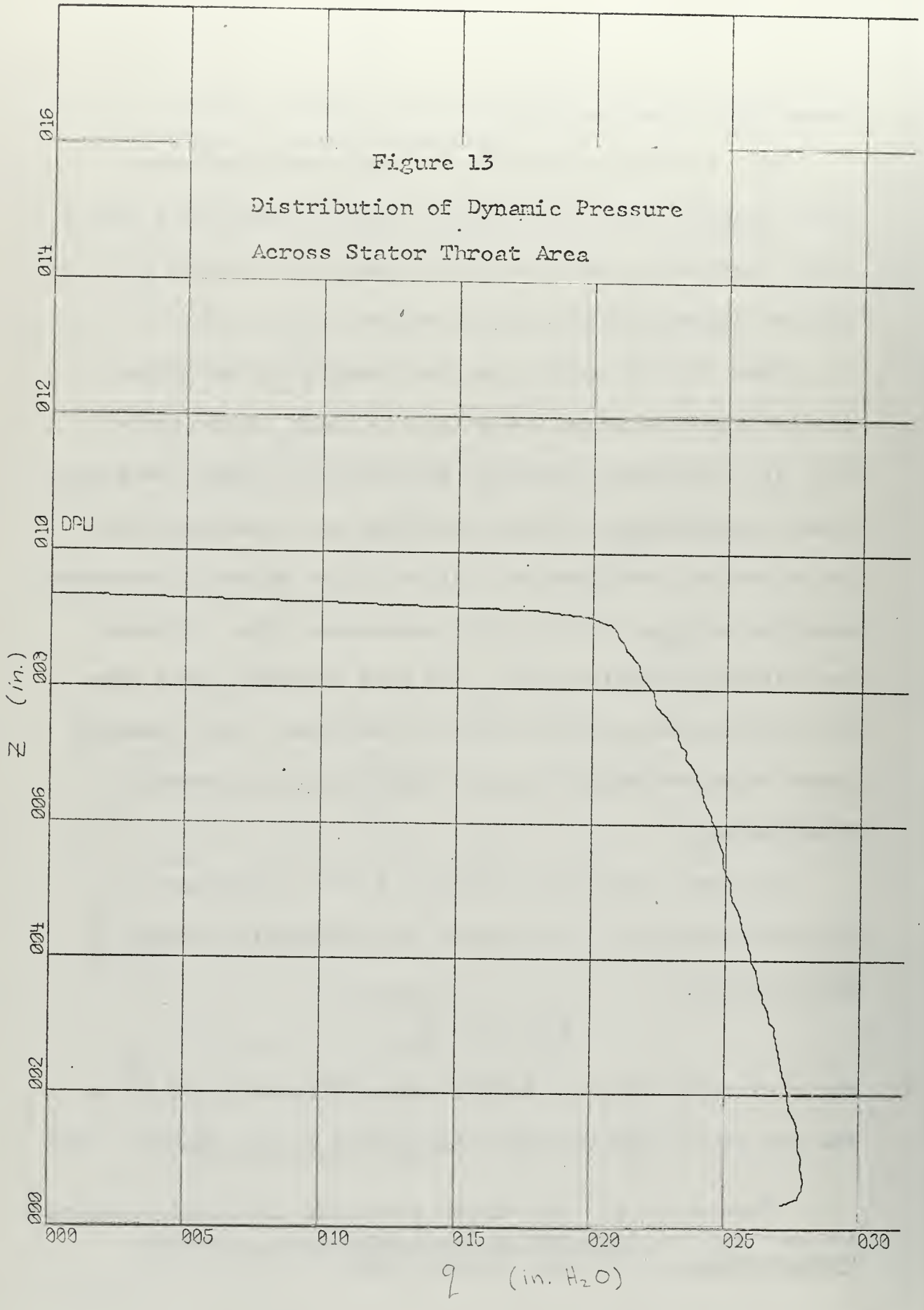

X-SCALE = 5.00E+00 UNITS/INCH.
Y-SCALE = 2.00E-01 UNITS/INCH.

STATOR PROFILES

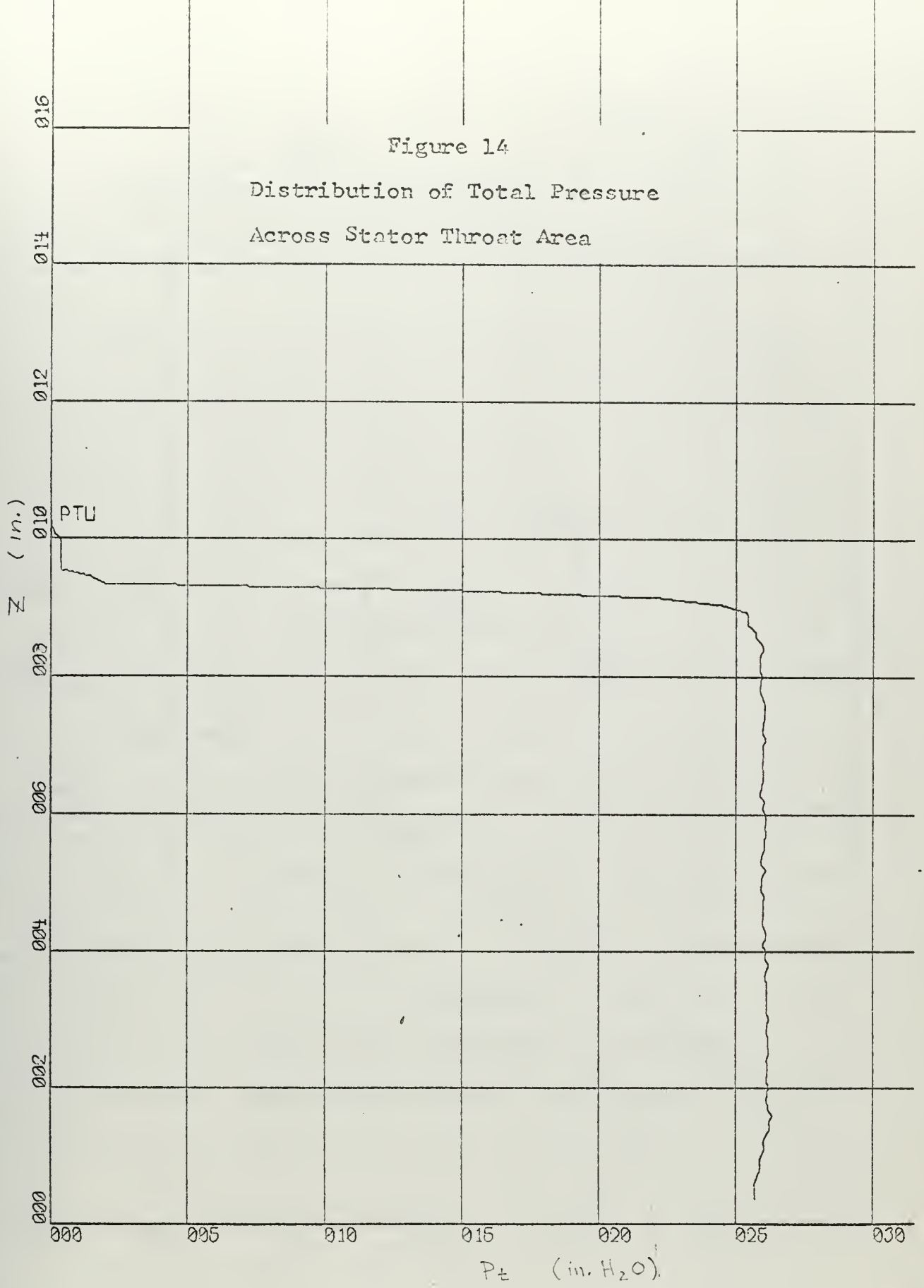

Figure 14

Distribution of Total Pressure

Across Stator Throat Area

X-SCALE = 5.00E+00 UNITS/INCH.
Y-SCALE = 2.00E-01 UNITS/INCH. STATOR PROFILES

Figure 15

Distribution of Static Pressure

Across Stator Throat Area

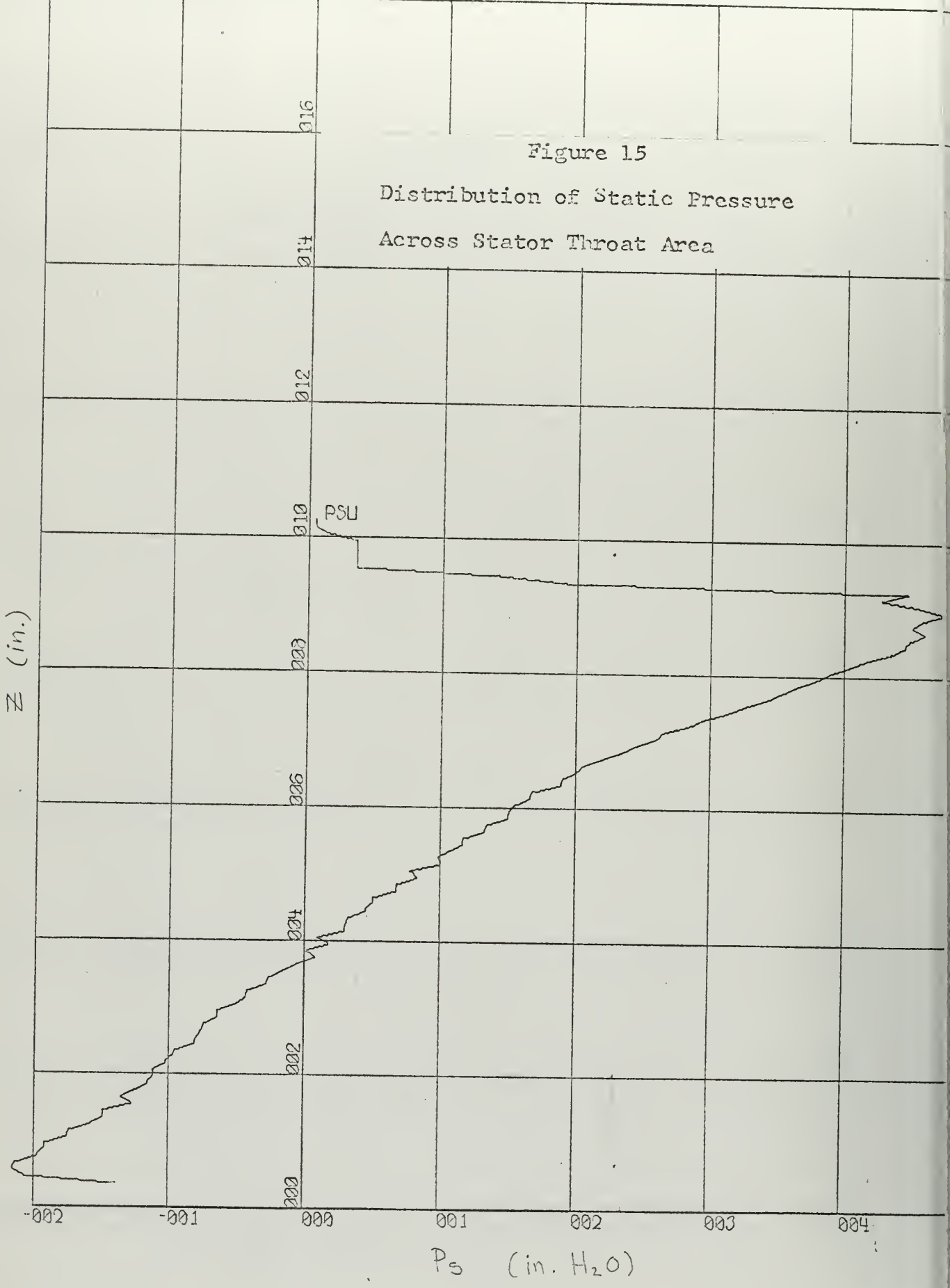

X-SCALE = 1.00E+00 UNITS/INCH.
Y-SCALE = 2.00E-01 UNITS/INCH.

STATOR PROFILES

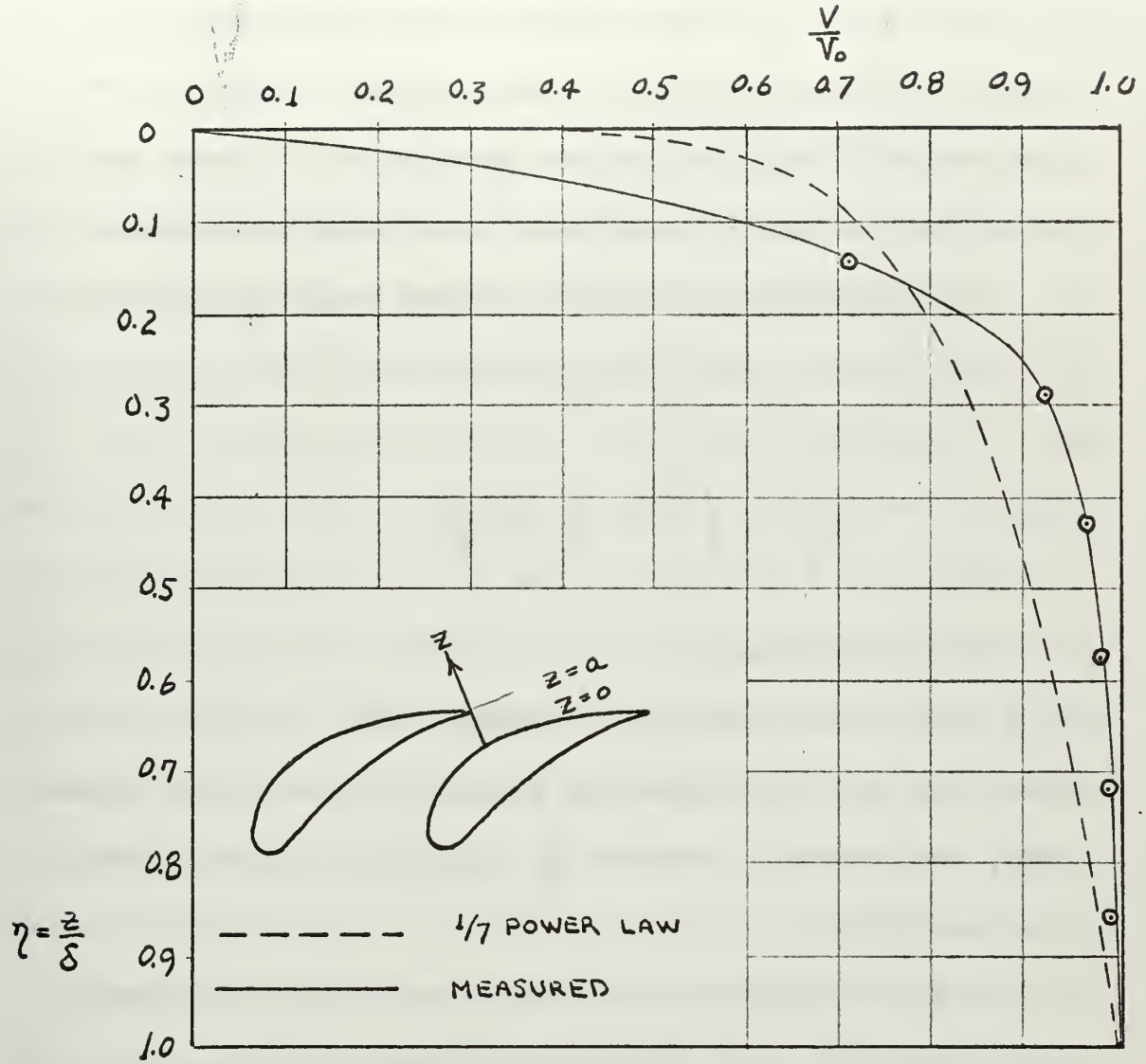

Figure 16

Dimensionless Boundary Layer Velocity Distribution, Stator Throat Area

the stator cascade, δ^* was estimated by performing a graphical integration of the dimensionless velocity distribution of Fig. 16, and by assuming a 1/7 power law distribution in the vicinity of z = o. From measurement, δ = .07 inches in the vicinity of the trailing edge and δ = .056 inches in the vicinity of z = 0.

With

$$\frac{\delta_i^*}{\delta} = \int_o^1 \left(1 - \frac{V}{V_o}\right) d\left(\frac{z}{\delta}\right)$$

and σ = 0.916 inches,

then ξ = 0.98 for the stator cascade. This value is higher than that calculated by Eckert for the actual stator blades. The average value of ξ calculated for the actual stator was 0.95.

The flow conditions in the test section for the rotor cascade tests are also considered to be good. Figs. C13, C19, C25, C31 and C37 all show static pressure distributions ahead of the cascade which are fairly regular. The graphs of q_1 versus x show that the wake patterns due to the inlet guide vanes are not quite as evenly distributed over the distance traversed as they were for the straight inlet guide vanes of the stator cascade. The fact that the flow entering the test section from the plenum must effect a change in direction through the inlet guide vanes probably causes

vortices (associated with the secondary flow through a curved channel). These vortices, in turn, would tend to increase flow turbulence and cause irregularities in the wake patterns at the lower traverse. The values of the constriction factor, however, indicate favorable flow conditions across the cascade.

Fig. 17 shows the change of the loss coefficient with incidence angle. The minimum loss coefficient computed from measured data is 0.06 at $\alpha_i = -4.2^{\circ}$. Fig. 18 shows the variation of the actual rotor loss coefficient with incidence angle.[7] The minimum rotor loss coefficient is 0.35 at $\alpha_i = -3.1^{\circ}$. The loss coefficient ζ for Run #302 is shown also in Fig. 12 for comparison with results from other cascade tests on blading of similar deflection.

Losses in the actual rotor include secondary flow loss, tip losses, three dimensional profile loss, disc friction loss, and an additional loss due to small dead-water regions near the leading edge of the blades close to the tip. Streaks on the rotor blades caused by impurities in the air flow gave evidence of these regions. The loss associated with this phenomen will be called windage loss. To date, there are no analytical theories that can predict values for

[7]Eckert, op. cit.

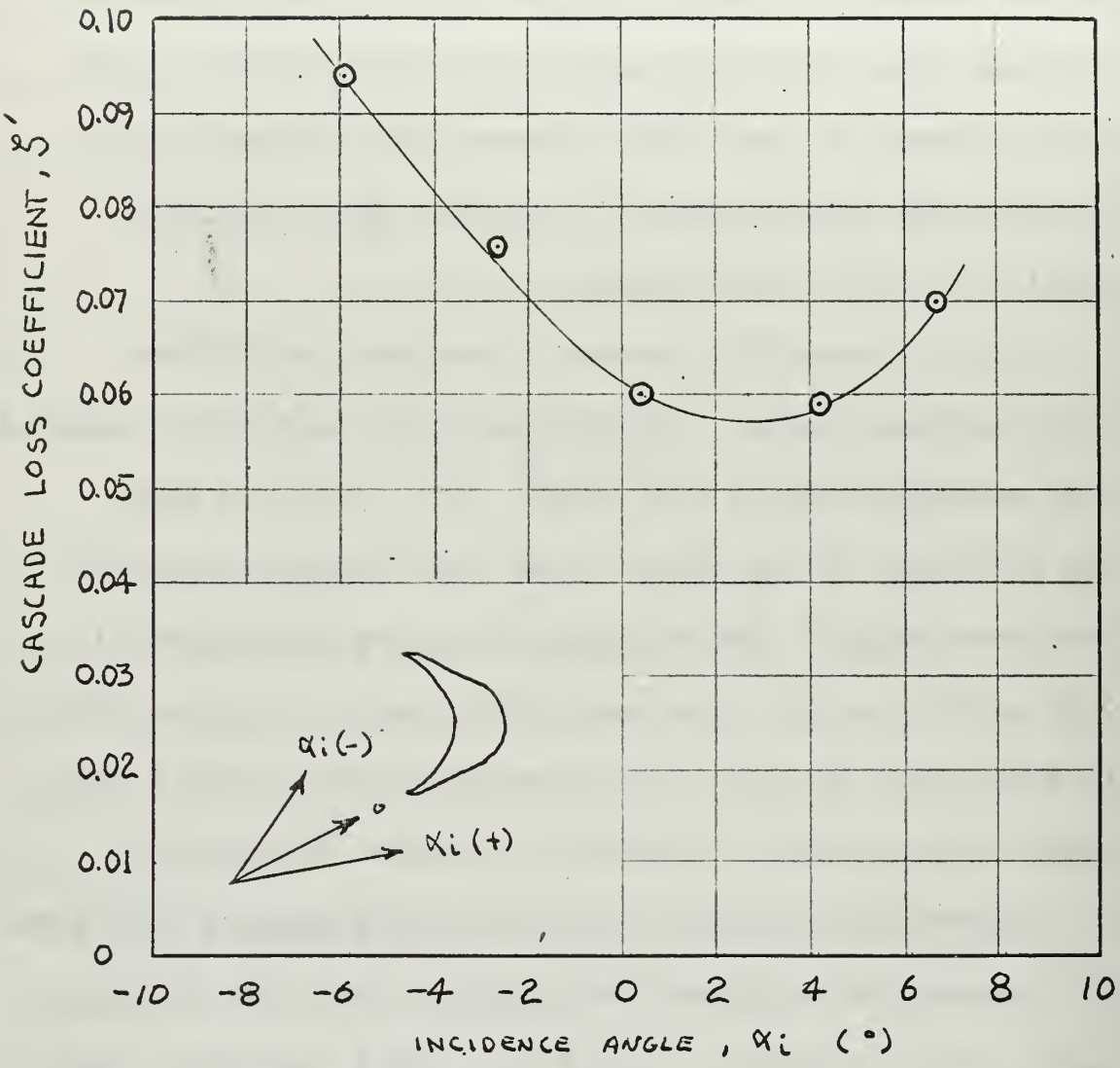

Figure 17

Variation of Rotor Cascade Loss Coefficient with Incidence Angle

the various losses with any degree of assuredness. Theoretical methods of loss prediction that are available, and which have demonstrated correlation with experimental tests, are only applicable to blading of small deflection.

The difference in magnitude between loss coefficients obtained from cascade tests and those obtained from turbine tests indicates that profile losses are not the dominant factor in the overall rotor losses.

The assumption is made that the profile and mixing losses that exist in the actual rotor are those that were determined from the cascade tests. The effect of Reynold's number differences is assumed to be negligible. Mach number effects are assumed also to be negligible, although this is not quite true since the Mach number of the rotor was about 0.6 as opposed to about 0.2 for the cascade flow. Let the following loss coefficient be defined

$$\zeta^* = \zeta_R - \zeta'$$

Values of ζ^* were computed from the data of Fig. 17 and Fig. 18. Fig. 19 shows the variation of ζ^* with incidence angle. The losses represented by the quantity ζ^* seem to increase sharply as the incidence angle becomes more positive. The variation of C_{L_∞} with incidence angle (from cascade test data) is also shown in Fig. 19.

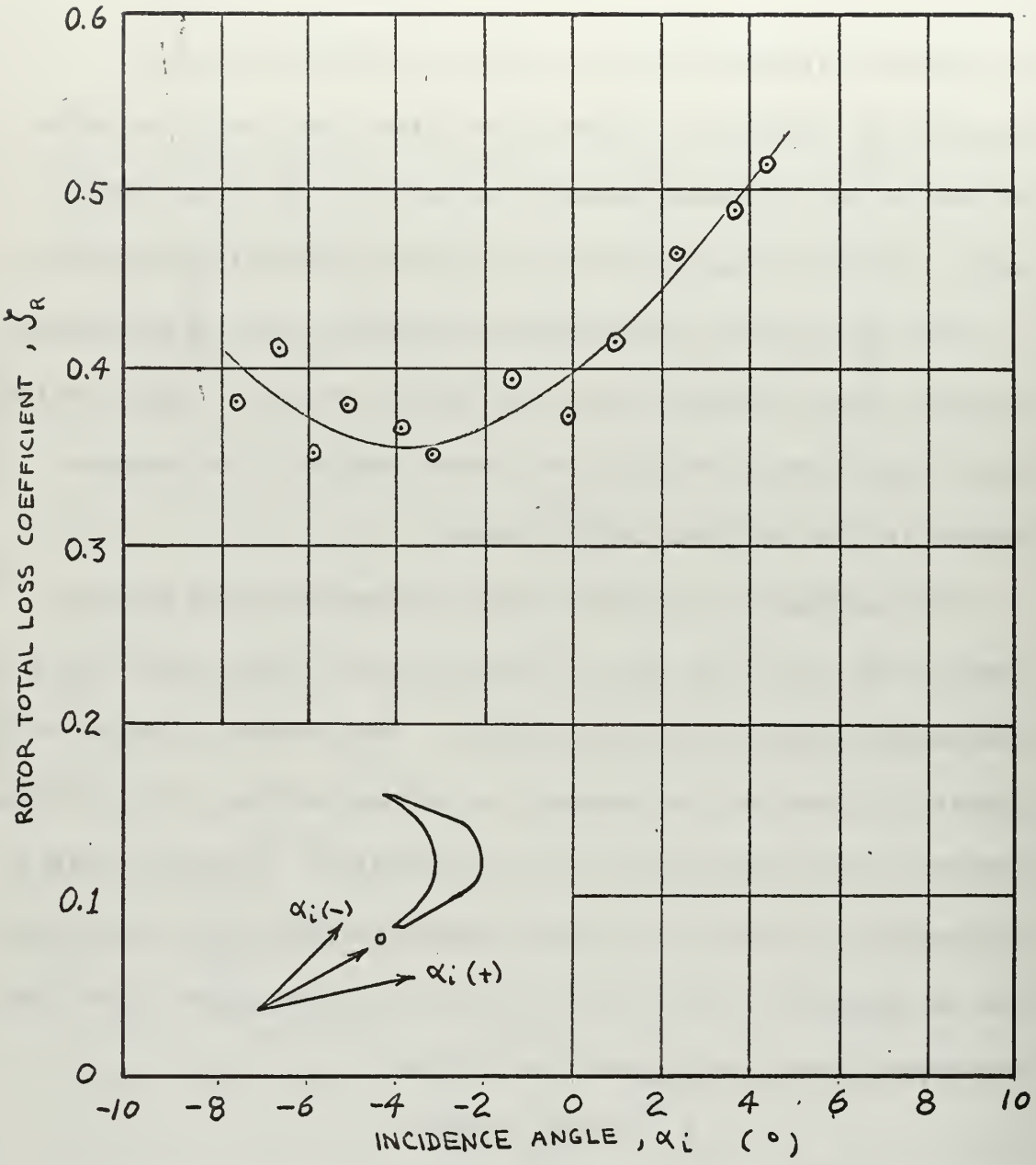

Figure 18

Variation of Actual Rotor Loss

Coefficient with Incidence Angle

Adapted from Eckert [9]

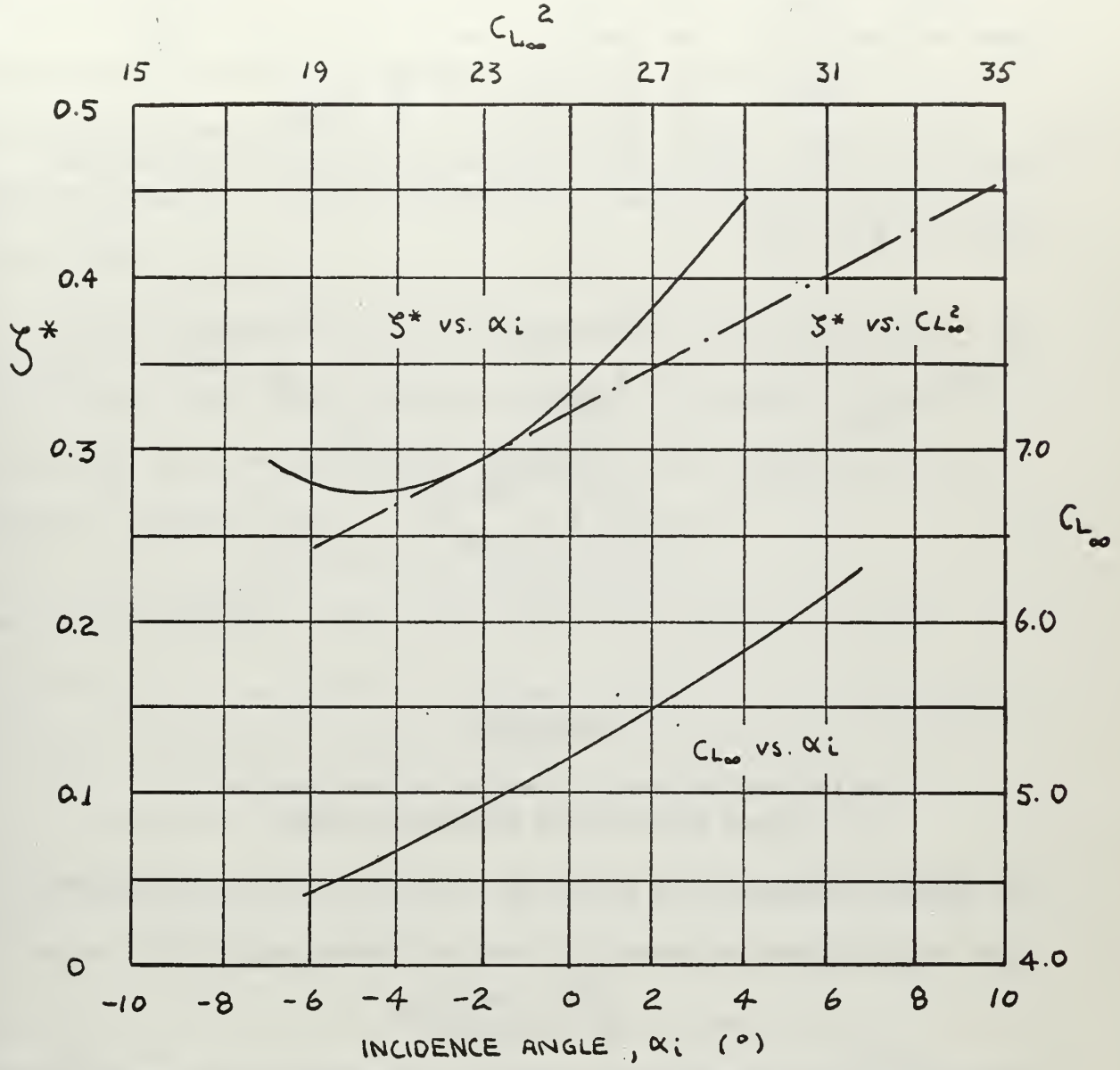

Figure 19

Variation of Loss Coefficient ζ^* with Incidence Angle and the Square of the Lift Coefficient. Variation of Lift Coefficient with Incidence Angle.

An equation that expresses secondary and tip clearance loss in the form of an induced drag coefficient[8] is

$$C_{D_i} = .055\, C_{L_\infty}^2\, \sigma \frac{s}{h} + \frac{1}{4} C_{L_\infty}^2\, \sigma \frac{\delta}{h} \frac{1}{\cos\beta_2}$$

where δ is the radial tip clearance and β_2 is defined as shown in Fig. 20.

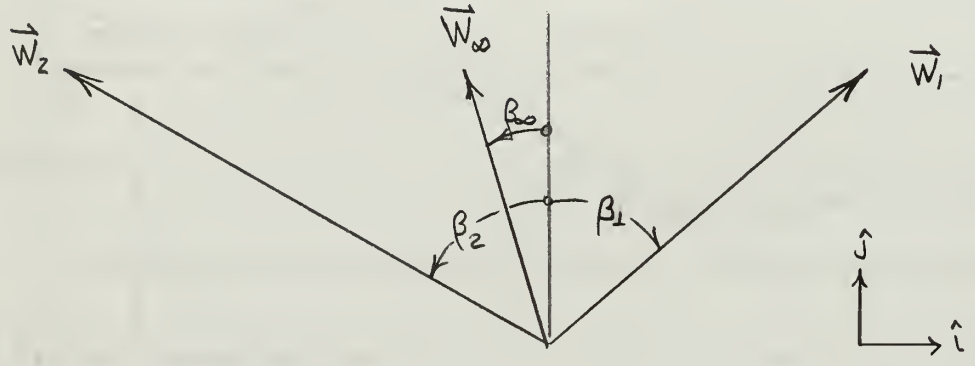

Figure 20

Relative Velcoity Diagram of an Impulse Type Axial-Flow Turbine Rotor

The drag coefficient C_{D_i} may be converted to an equivalent loss coefficient by means of the following equation[9]

$$C_{D_i} = \frac{\zeta^{**} \cos^3\beta_\infty}{\sigma \cos^2\beta_2}$$

where ζ^{**} is the secondary and tip clearance loss coefficient. The above two equations combined give,

$$\zeta^{**} = \frac{.055\, C_{L_\infty}^2}{\cos^3\beta_\infty} \sigma^2 \frac{s}{h} \cos^2\beta_2 + \frac{1}{4} \frac{C_{L_\infty}^2 \sigma^2}{\cos^3\beta_\infty} \frac{\delta}{h} \cos\beta_2$$

[8] Varva, op. cit., p. 379.

[9] Ibid., p. 336.

This equation has application to blade rows of small camber only, but could possibly supply a basis for an empirical relation for secondary and tip clearance loss. Ainley and Mathieson make a similar suggestion involving only secondary loss. [5]

To make a qualitative determination of the variation of ζ^{**} with $C_{L_\infty}^2$, the following procedure is used. First, it is assumed that secondary and tip clearance losses are the dominant losses. Then

$$\zeta^* \cong \zeta^{**}$$

The two-dimensional lift coefficient C_{L_∞} from the cascade test results is assumed to be proportioned to the corresponding lift coefficient (based on $|\vec{W}_\infty|$) of the actual rotor. At the incidence angles which correspond to the cascade test points, values of ζ^* are computed and plotted against corresponding values of $C_{L_\infty}^2$ from cascade test data. The variation of ζ^* with $C_{L_\infty}^2$ is shown in Fig. 19. The fact that ζ^* seems to be linearly related to $C_{L_\infty}^2$ is interesting, but inconclusive. Implied, however, is the possibility of predicting the losses of impulse turbine blading from empirical relations based on the two-dimensional loss and lift coefficients obtained from cascade tests. The facilities for the acquisition of data needed to investigate this possibility are available at the U. S. Naval Postgraduate School, and further studies along these lines should be pursued.

Figure 21

Distribution of Dynamic Pressure

Across Rotor Channel Discharge Area

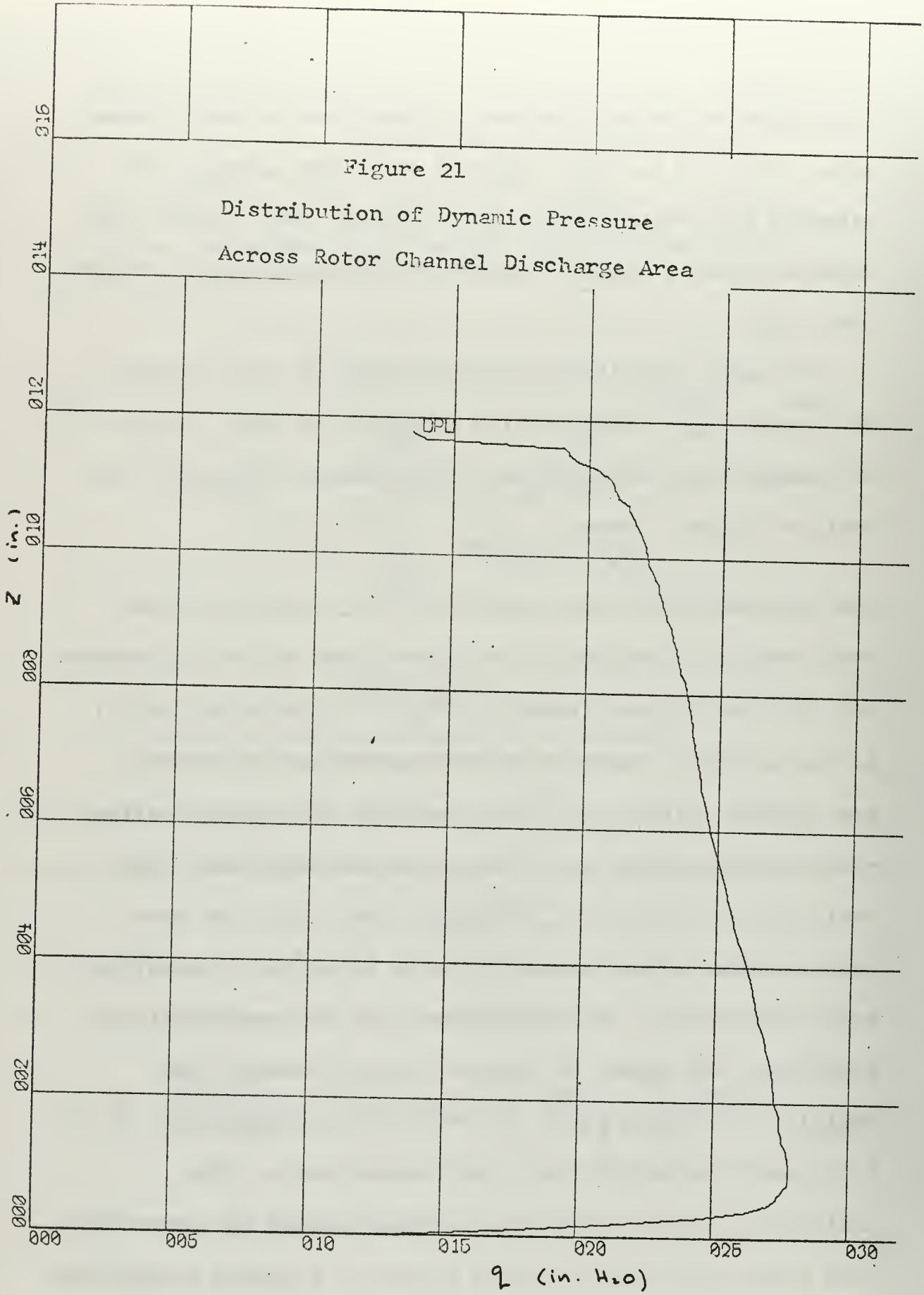

X-SCALE = 5.00E+00 UNITS/INCH.

Y-SCALE = 2.00E-01 UNITS/INCH.

RUN 302 ROTOR PROFILES

Figure 22

Distribution of Total Pressure Across

Rotor Channel Discharge Area

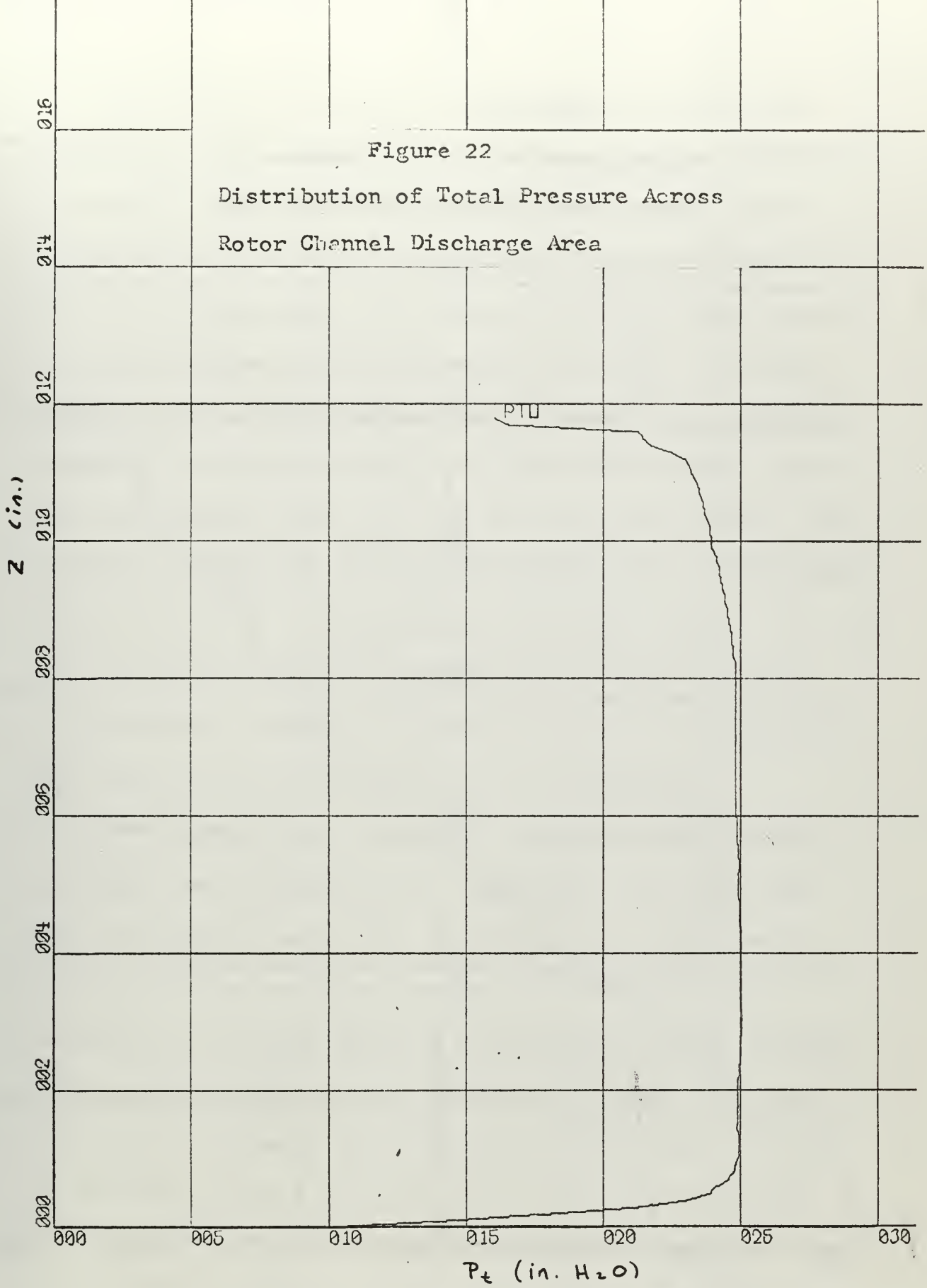

X-SCALE = 5.00E+00 UNITS/INCH.

Y-SCALE = 2.00E-01 UNITS/INCH.

RUN 302 ROTOR PROFILES

Figure 23

Distribution of Static Pressure

Across Rotor Channel Discharge Area

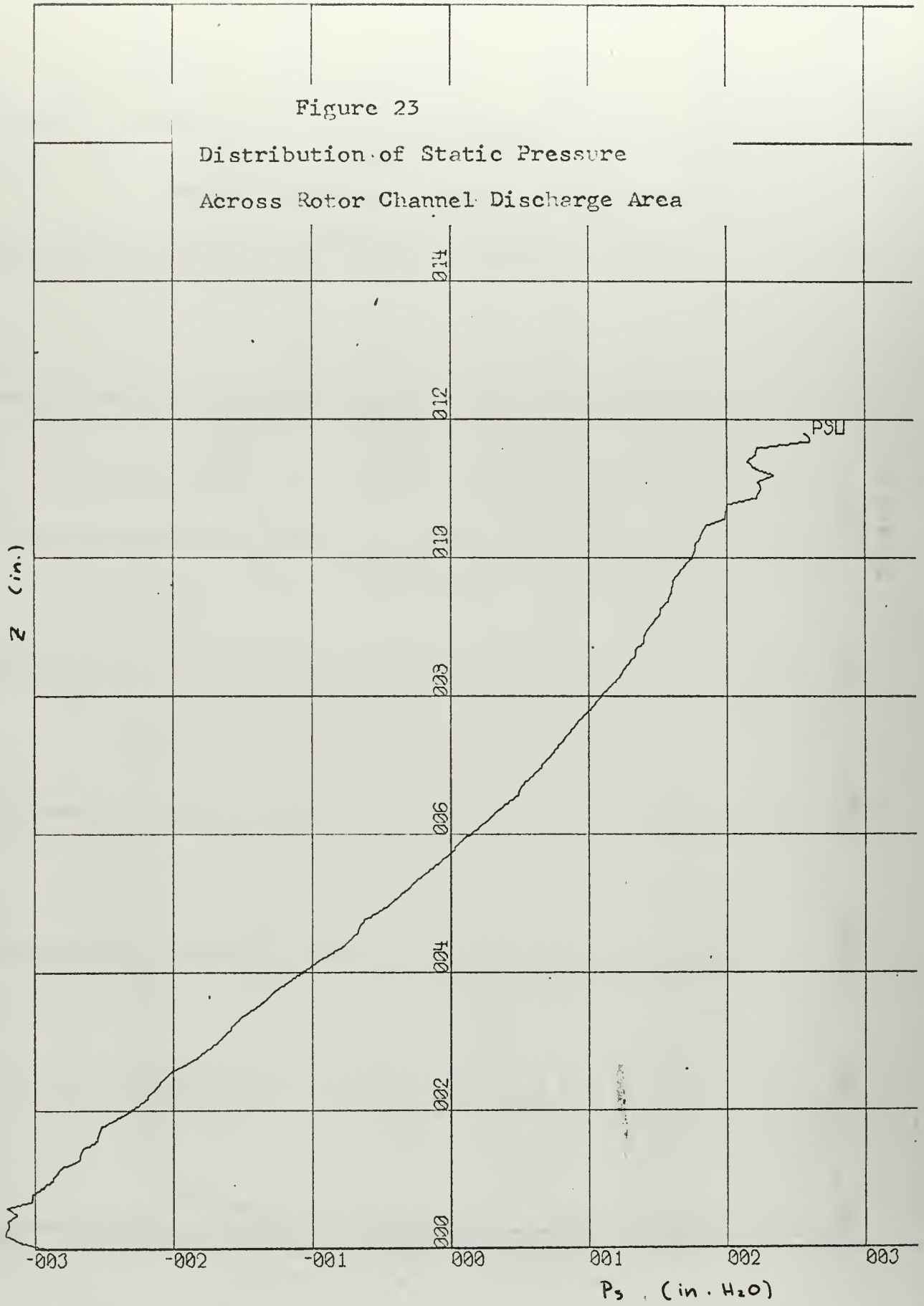

X-SCALE = 1.00E+00 UNITS/INCH.

Y-SCALE = 2.00E-01 UNITS/INCH.

RUN 302 ROTOR PROFILES

The results of the flow survey across the discharge area of a rotor cascade blade channel are shown in Figs. 21, 22 and 23. Figs. 24 and 25 are the dimensionless velocity distribution close to the coordinate $z = 0$, and in the wake near the trailing edge. The distributions are based on total pressure readings and the assumption that $\frac{dP_s}{dz} = 0$ in the boundary layer. The boundary layer thickness, δ, is 0.14 inches in the vicinity of $z = 0$, while the boundary layer near the trailing edge ($z = a$) is 0.36 inches thick. The velocity distribution of Fig. 24 indicates that the boundary layer has started to separate from the blade surface. The area restriction factor calculated for the rotor cascade at near design incidence (Run #302) is 0.94. A corresponding value for the actual rotor was not available.

The boundary layer measuring techniques used in this investigation, although crude, demonstrate that this type of investigation can be made because of the large size of the test section and blade models. The use of hot wire anemometry to measure velocity distributions in the boundary layer would eliminate probe interferance errors. The fact that the flow appears to be separated at the point $z = 0$ in the blade channel is of interest especially since the loss coefficient is not high. Further investigations of the boundary layer behavior on the blade surface may be of value.

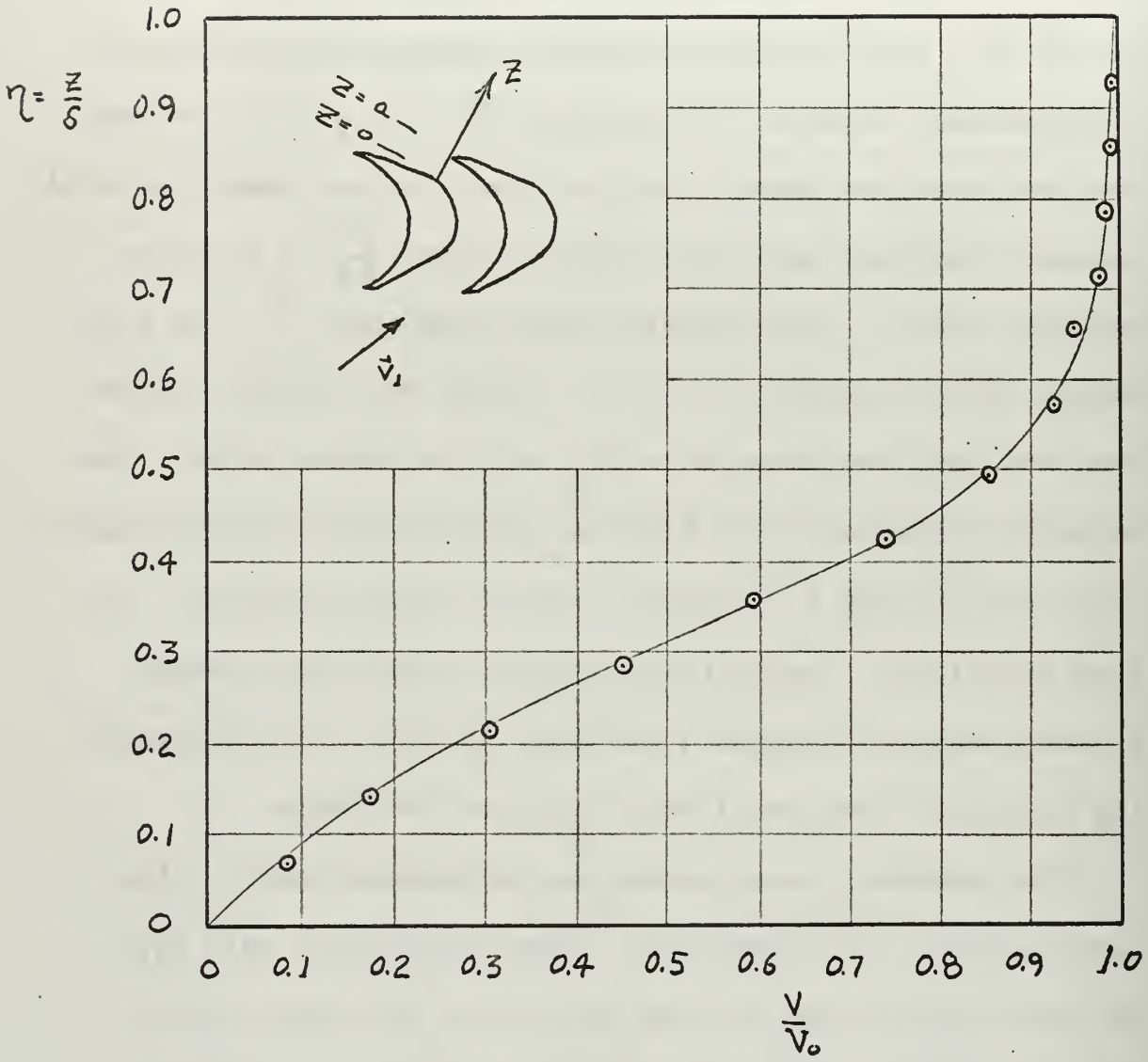

Figure 24

Dimensionless Boundary Layer Velocity Distribution, Rotor Discharge Area (in the vicinity of z = 0)

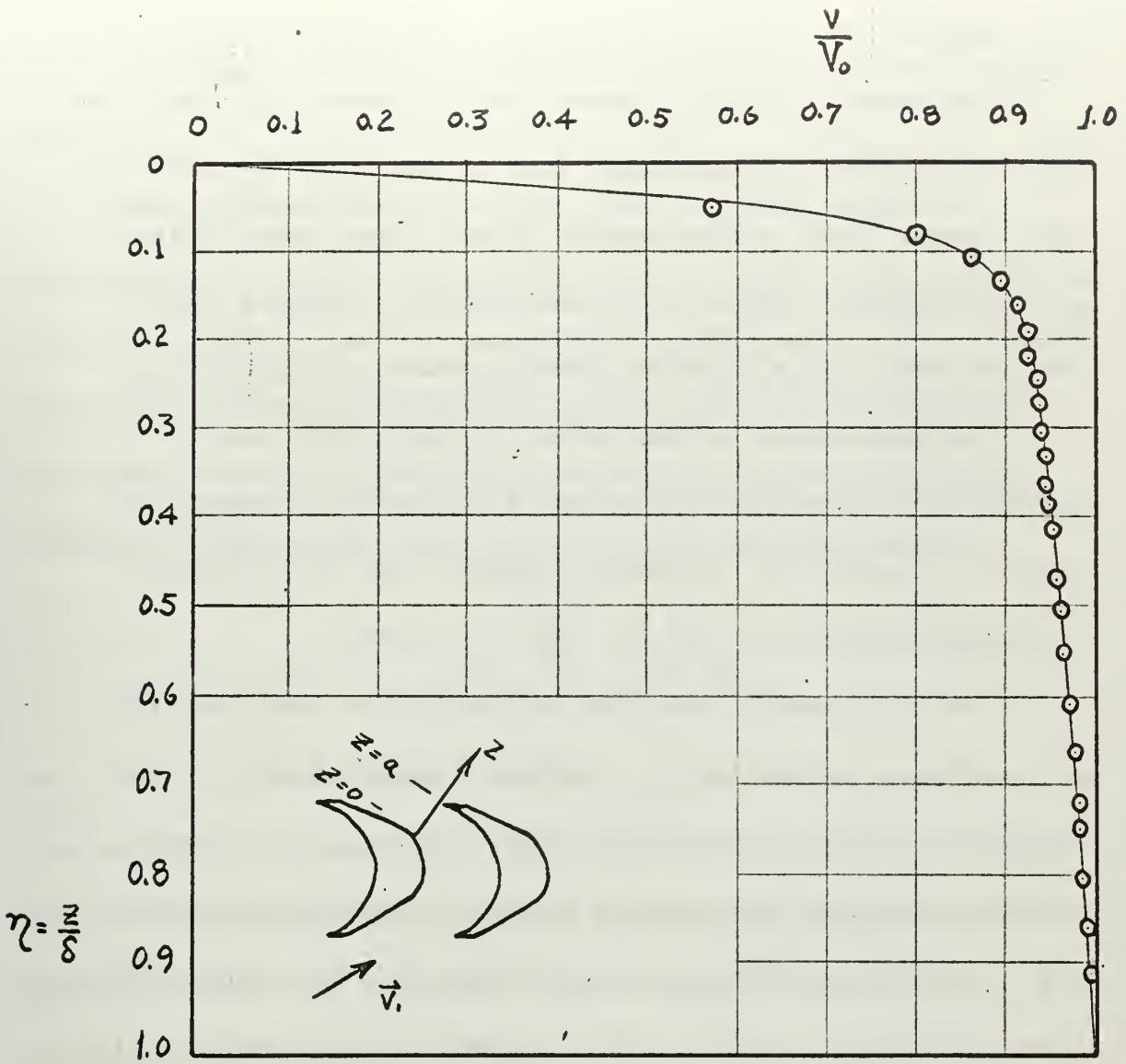

Figure 25

Dimensionless Boundary Layer Velocity Distribution in the Wake, Rotor Discharge Area. (In the vicinity of z = a)

6. Conclusions

The results of this investigation show that the stator loss coefficient, determined from actual turbine tests with choked flow at the nozzle throat, was about twice as large at the stator loss coefficient obtained from cascade tests at a discharge Mach number of about 0.3.

The percentage of the total actual rotor loss coefficient attributed to profile and mixing losses is greater at negative incidence angles than at positive incidence angles for $-6^{\circ} < \alpha_i < +6^{\circ}$.

The flow conditions that exist in the test section are quite satisfactory for turbine cascade tests. The degree of flow non-uniformity that exists in the test section ahead of the cascade depends largely on how much the flow must be deflected after entering the test section from the plenum chamber. The stator cascade test section set-up, with straight inlet guide vanes and end walls positioned vertically, exhibited the most favorable inlet flow conditions.

7. Recommendations and Acknowledgements

As far as the correlation of cascade test results with actual turbine performance is concerned, more can be implied from this investigation than can be definitely concluded. But the implications of any experimental results

must necessarily be the basis of recommendations for future study.

The recommendation is made that cascade tests be performed to measure loss coefficients at planes y = constant along the blade span. A mean loss coefficient, $\bar{\zeta}$, could then be calculated from the relation previously mentioned as given by Scholz. [11] In like manner, a mean value of incidence angle could be determined by the expression

$$\bar{\alpha}_i = \frac{1}{h} \int_{y=0}^{y=h} \alpha_{i_{LOCAL}}(y)\, dy$$

The mean loss coefficient thus calculated would include the influence of secondary flow due to wall boundary layer. Now by varying the angle of the flow ahead of the cascade, the variation of $\bar{\zeta}$ with $\bar{\alpha}_i$ could be established for comparison with actual turbine test data similar to those shown in Fig. 18. This would be a step toward more thorough understanding of the influence of secondary flows on the efficiency of turbine blades of large deflection.

In conjunction with secondary flow investigations, a means of flow visualization in the cascade test section is desirable and recommended. An attempt to introduce smoke streams into the test section was made but was not successful. The smoke, which was generated from heated

mineral oil, "condensed" in the tube that transported it into the air flow. By devising a means to electrically heat the tube, the "condensation" process may be precluded.

In order to separate the loss attributed to mixing from the profile loss, it is recommended that flow conditions aft of the cascade be measured close to the trailing edge of the blade row. A suggestion as to how this might be accomplished is given in the previously mentioned report by the writer. [6]

Acquisition of a hot-wire anemometer probe and associated read-out equipment is recommended for future boundary layer studies of the flow through cascades.

Possible ways of maintaining a constant plenum pressure should be investigated. The first step is to monitor the blower speed and find out if a constant RPM is maintained.

Finally, every effort should be made to utilize the Automatic Data Logging System. In fact, the use of two such systems simultaneously for upper and lower traverse data acquisition would reduce the test time considerably.

The writer wishes to express his appreciation to Mr. R. W. Savage for the patience, loyalty, skill and assistance he provided during the course of this investigation. The writer also wishes to thank Dr. M. H. Vavra for his guidance in this work.

BIBLIOGRAPHY

1. Horlock, J. H. Axial Flow Compressors. Butterworth Publications, 1958.

2. Miller, I. and Freund, J. E. Probability and Statistics for Engineers. Prentice-Hall, 1965.

3. Varva, M. H. Aero-Thermodynamics and Flow in Turbomachines. John Wiley and Sons, 1960.

4. Ainley, D. G. and Mathieson, G. C. R. A Method of Performance Estimation for Axial-Flow Turbines, Aeronautical Research Council. R. and M. No. 2974, 1957.

5. Ainley, D. G. and Mathieson, G. C. R. An Examination of the Flow and Pressure Losses in Blade Rows of Axial-Flow Turbines, Aeronautical Research Council. R. and M. No. 2891, 1955.

6. Bartocci, J. E. An Investigation of the Flow Conditions at the Lower Measuring Plane, and in the Plenum Chamber of the Rectilinear Cascade Test Facility, United States Naval Postgraduate School, Department of Aeronautics. TN No. 66T3, 1966.

7. Bolte, W. Zur Berechnung and Optimierung des Wirkungsgrades axialer Stromungsmaschinen. VDI - Forschungsheft 501, 1964.

8. Dunavant, J. C. and Erwin, J. R. Investigation of a Related Series of Turbine Blade Profiles in Cascade. NACA TN 3802, October, 1956.

9. Eckert, R. H. Performance Analysis and Initial Tests of a Transonic Turbine Test Rig. United States Naval Postgraduate School, Thesis, 1966.

10. Rose, C. C. and Guttormson, D. L. Installation and Test of a Rectilinear Cascade. United States Naval Postgraduate School, Thesis, 1964.

11. Scholz, N. Secondary Flow Losses in Turbine Cascades, Journal of the Aeronautical Sciences. v. 21, October, 1954.

12. Vavra, M. H. Von Karman Institute for Fluid Dynamics Lecture Series, Problems of Fluid Mechanics in Radial Turbomachines. Part III, March, 1965.

APPENDIX A

DERIVATION OF FORMULAE USED IN THE REDUCTION OF DATA

The recorded results of a cascade test include the following constants: atmospheric pressure (Patm), plenum temperature (Tp), blade spacing (s), blade chord (c), and the number of blade spacings traversed (BN). The coordinate (y) is a constant for a particular run, but is not used in the data reduction.

The following quantities are recorded for both the upper and the lower traverse (stations (1) and (2)), and are functions of the probe position (x): Pt, q, Θ , ΔX.

Thermodynamic Relations

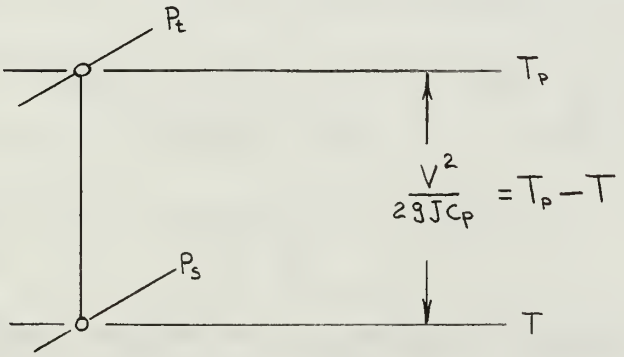

Using the isentropic relationship for a perfect gas,

$$P v^{\gamma} = \text{constant}$$

and

$$C_p = \frac{R}{J} \frac{\gamma}{\gamma - 1}$$

then

$$\frac{V^2}{2gJC_p} = \left[1 - \left(\frac{P_s}{P_t} \right)^{\frac{\gamma-1}{\gamma}} \right] T_p = \frac{(\gamma-1) V^2}{2 R \gamma g}$$

with

$$P_s = P_t - q$$

yields

$$V^2 = \gamma g R T_p \frac{2}{\gamma-1}\left[1-\left(1-\frac{q}{P_t}\right)^{\frac{\gamma-1}{\gamma}}\right] \qquad (1)$$

Let $a_p=\sqrt{\gamma g R T_p}$, where a_p is the sonic velocity in the plenum. Expanding the term $\left(1-\frac{q}{P_t}\right)^{\frac{\gamma-1}{\gamma}}$ in a binomial expansion and ignoring terms with powers of $\frac{q}{P_t}$ higher than two, $V_1 = V_1(x)$ and $V_2 = V_2(x)$ can be computed. Thus from Eq. (1), the flow velocities as point functions of the probe position along the x coordinate are obtained from

$$V^2 = \frac{2}{\gamma-1} a_p^2\left[\frac{\gamma-1}{\gamma}\frac{q}{P_t}\left(1+\frac{1}{2\gamma}\frac{q}{P_t}\right)\right] \qquad (2)$$

also, from $\rho = p^{-1/\gamma}$

$$\rho = \rho_t\left(\frac{P_s}{P_t}\right)^{1/\gamma} = \rho_t\left(\frac{P_t-q}{P_t}\right)^{1/\gamma}$$

$$\rho = \rho_t\left(1-\frac{q}{P_t}\right)^{1/\gamma} \qquad (3)$$

With the same binomial expansion as before, and the equation of state for an ideal gas,

$$\rho_t = \frac{P_t}{gRT_p}$$

there is

$$\rho = \frac{P_t}{gRT_p}\left[1-\frac{1}{\gamma}\frac{q}{P_t}\left(1+\frac{\gamma-1}{2\gamma}\frac{q}{P_t}\right)\right]$$

or

$$\rho = \frac{P_t}{a_p^2}\left[\gamma - \frac{q}{P_t}\left(1 + \frac{\gamma-1}{2\gamma}\frac{q}{P_t}\right)\right] \qquad (4)$$

From Eq. (4), $\rho_1 = \rho_1(x)$ and $\rho_2 = \rho_2(x)$ can be computed.

The static pressures at the lower and upper measuring planes are

$$P_{s_1} = P_{t_1} - q_1 \quad \text{and} \quad P_{s_2} = P_{t_2} - q_2$$

where

$$P_{s_1} = P_{s_1}(x) \quad \text{and} \quad P_{s_2} = P_{s_2}(x)$$

Conditions Far Ahead of the Cascade

Up to this point, the derivation of the equations is similar to that given by Rose and Guttormson with only the difference that q is a measured quantity and not Ps. [10] In the determination of the flow character far ahead of the cascade, the above reference makes use of the momentum theorem. The control volume used consisted of two streamlines bounded by the lower measuring plane (1) near the cascade, and of a reference plane far ahead of the cascade (o) at which uniform flow conditions were considered to exist.

Figure A1

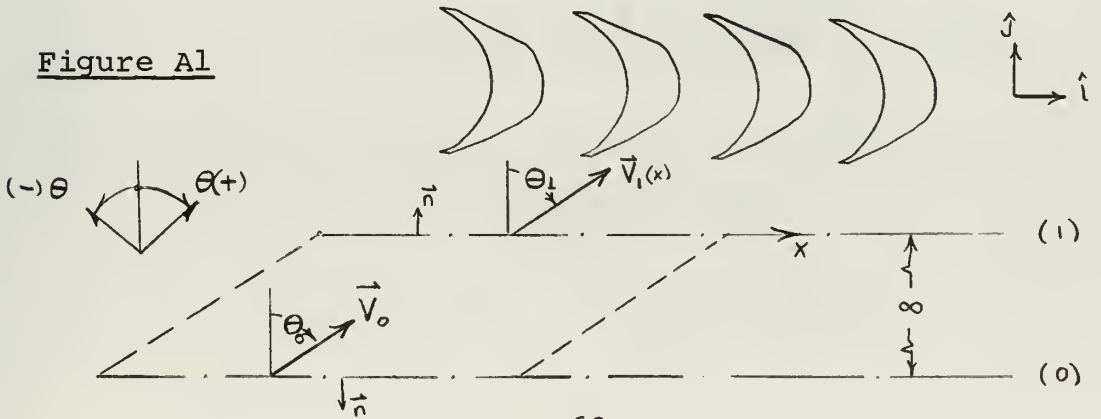

The resultant force on the control volume was considered to be equal to zero. Since the flow at station (1) can never be exactly uniform, this model assumed that a flow of uniform conditions was by some means becoming non-uniform without guiding surfaces to cause it to do so. The following derivations will show that this concept violates the energy equation.

Consider the flow between two parallel streamlines, as shown below, where V_1 is constant and $V_2 = f(y)$

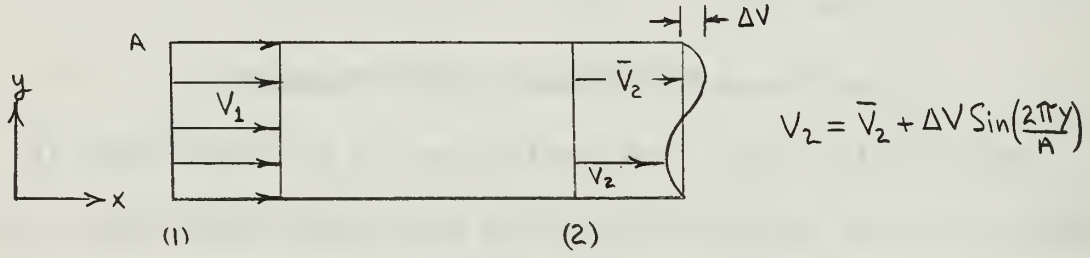

Figure A2

For constant mass densities $\rho = \rho_1 = \rho_2$, from continuity,

$$V_1 = \frac{1}{A}\int_0^A V_2\, dy$$

From the Momentum equation in the x-direction, and assuming that the static pressure Ps_2 at station (2) is constant,

$$ms_1 V_1 - \int_0^A dms_2\, V_2 + Ps_1 A - Ps_2 A = 0$$

with

$$ms_1 = \rho V_1 A$$

and

$$dm_{s_2} = \rho V_2 \, dy$$

$$P_{s_2} = \rho V_1^2 + P_{s_1} - \frac{\rho}{A} \int_0^A V_2^2 \, dy$$

The average total pressure at station (2) is

$$\bar{P}_{t_2} = \frac{\int_0^A \left(P_{s_2} + \frac{\rho}{2} V_2^2\right) \rho V_2 \, dy}{\int_0^A \rho V_2 \, dy} = \frac{\int_0^A \left(P_{s_2} + \frac{\rho}{2} V_2^2\right) V_2 \, dy}{A V_1}$$

$$\bar{P}_{t_2} = \frac{P_{s_2} \int_0^A V_2 \, dy}{A V_1} + \frac{\rho/2 \int_0^A V_2^3 \, dy}{A V_1} = P_{s_2} + \rho/2 \, \frac{\int_0^A V_2^3 \, dy}{A V_1}$$

Further,

$$P_{t_2} = \rho V_1^2 + P_{s_1} - \rho/A \int_0^A V_2^2 \, dy + \frac{\rho}{2A} \int_0^A \frac{V_2^3}{V_1} \, dy$$

with $P_{t_1} = \rho/2 \, V_1^2 + P_{s_1}$

$$\bar{P}_{t_2} = P_{t_1} + \rho/2 \, V_1^2 - \rho/A \int_0^A V_2^2 \, dy + \frac{\rho}{2A} \int_0^A \frac{V_2^3}{V_1} \, dy$$

Assume now that, as shown in Fig. A2,

$$V_2 = \bar{V}_2 + \Delta V \sin\left(\frac{2\pi y}{A}\right)$$

Clearly, $\bar{V}_2 = V_1$ from the equation of continuity, and, with

$$a = \frac{\Delta V}{\bar{V}_2}$$

$$V_2 = V_1 \left[1 + a \sin\left(\frac{2\pi y}{A}\right)\right]$$

then,

$$\bar{P}_{t_2} = P_{t_1} + \rho/2\, V_1^2 - \rho/A \int_0^A V_1^2 \left[1 + 2a \sin\left(\frac{2\pi y}{A}\right) + a^2 \sin^2\left(\frac{2\pi y}{A}\right)\right] dy$$

$$+ \frac{\rho}{V_1 2 A} \int_0^A V_1^3 \left[1 + 3a \sin\left(\frac{2\pi y}{A}\right) + 3a^2 \sin^2\left(\frac{2\pi y}{A}\right) + a^3 \sin^3\left(\frac{2\pi y}{A}\right)\right] dy$$

and,

$$\bar{P}_{t_2} = P_{t_1} + \rho/2\, V_1^2 \left(\tfrac{5}{2} a^2\right)$$

Thus $P_{t_2} > P_{t_1}$ for $a \neq 0$

Conditions far ahead of the cascade are assumed to be the average values of the conditions measured at the lower measuring plane (1). The following quantities are obtained:

$$P_{s_o} = \frac{\int_{(1)} P_{s_1} V_1 \cos\theta_1 \, dx}{\int_{(1)} V_1 \cos\theta_1 \, dx} \tag{5}$$

$$P_{t_o} = \frac{\int_{(1)} P_{t_1} V_1 \cos\theta_1 \, dx}{\int_{(1)} V_1 \cos\theta_1 \, dx} \tag{6}$$

$$\rho_o = \frac{1}{\Delta X_1} \int_{(1)} \rho_1 \, dx \tag{7}$$

$$\theta_o = \frac{1}{\Delta X_1} \int_{(1)} \theta_1 \, dx \tag{8}$$

Conditions Far Aft of the Cascade

The derivation of the following relations is given in [10] and listed here for convenience.

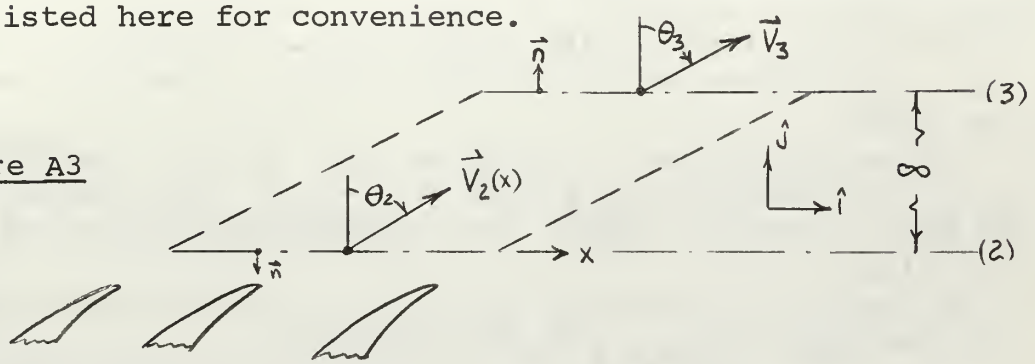

Figure A3

From the Momentum equation:

$$\int_{(2)} dm_{s_2}\,\vec{V}_2 - \int_{(3)} dm_s\,\vec{V}_3 + \hat{j}\int_{(2)} P_{s_2}\,dx - \hat{j}\int_{(3)} P_{s_3}\,dx = 0 \qquad (9)$$

From continuity

$$m_s = \int_{(2)} \rho_2 V_2 \cos\theta_2\,dx = \rho_3\,\Delta X_3\,V_3\cos\theta_3 \qquad (10)$$

$$\vec{V}_2 = \hat{i}\,V_2\sin\theta_2 + \hat{j}\,V_2\cos\theta_2$$

$$\vec{V}_3 = \hat{i}\,V_3\sin\theta_3 + \hat{j}\,V_3\cos\theta_3$$

Substituting the above relations in Eq. (9),

$$\int_{(1)} \rho_2 V_2\cos\theta_2\,(\hat{i}\,V_2\sin\theta_2 + \hat{j}\,V_2\cos\theta_2)\,dx - m_s\,(\hat{i}\,V_3\sin\theta_3 + \hat{j}\,V_3\cos\theta_3)$$
$$= \hat{j}\,P_{s_3}\Delta X_3 - \hat{j}\int_{(2)} P_{s_2}\,dx \qquad (11)$$

The $\hat{i}$ components of Eq. (11) give

$$\int_{(2)} \rho_2 V_2^2 \cos\theta_2 \sin\theta_2\,dx = m_s\,V_3\sin\theta_3$$

With Eq. (10)

$$V_3 \sin\theta_3 = \frac{\frac{1}{2}\int_{(2)} \rho_2 V_2^2 \sin 2\theta_2 \, dx}{\int_{(2)} \rho_2 V_2 \cos\theta_2 \, dx} \tag{12}$$

The $\hat{J}$ components of Eq. (11) give

$$\int_{(2)} \rho_2 V_2^2 \cos^2\theta_2 \, dx - ms V_3 \cos\theta_3 = P_{s_3} \Delta X_3 - \int_{(2)} P_{s_2} dx$$

with Eq. (10),

$$P_{s_3} = \frac{1}{\Delta X}\int_{(2)} \rho_2 V_2^2 \cos^2\theta_2 \, dx + \frac{1}{\Delta X_3}\int_{(2)} P_{s_2} dx - \frac{1}{\rho_3 (\Delta X_3)^2}\left[\int_{(2)} \rho_2 V_2 \cos\theta_2 \, dx\right]^2 \tag{13}$$

From Eq. (10)

$$V_3 \cos\theta_3 = \frac{1}{\rho_3 \Delta X_3}\int_{(2)} \rho_2 V_2 \cos\theta_2 \, dx \tag{14}$$

Eqs. (12) and (14) combined, give

$$V_3^2 = \frac{1}{4}\frac{\left[\int_{(2)} \rho_2 V_2^2 \sin 2\theta_2 \, dx\right]^2}{\left[\int_{(2)} \rho_2 V_2 \cos\theta_2 \, dx\right]} + \frac{1}{\rho_3^2 (\Delta X_3)^2}\left[\int_{(2)} \rho_2 V_2 \cos\theta_2 \, dx\right]^2 \tag{15}$$

and,

$$\theta_3 = \arctan\left\{\frac{\rho_3 \Delta X_3}{2}\,\frac{\int_{(2)} \rho_2 V_2^2 \sin 2\theta_2 \, dx}{\left[\int_{(2)} \rho_2 V_2 \cos\theta_2 \, dx\right]^2}\right\} \tag{16}$$

$$\Delta X_3 = \Delta X_2$$

The Mass Density Far Aft of the Cascade

The assumption of constant density between stations (2) and (3) is usually made in view of the fact that the mixing losses are small. Hence, the difference between (V_3) and the average velocity (V_2) is small. However, since the whole data reduction procedure of this study attempts to take into account compressibility effects, an iteration procedure to determine ρ_3 is used.

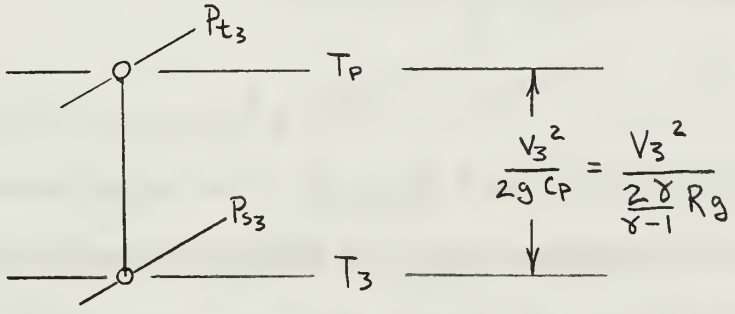

There are:

$$T_P - T_3 = \frac{\gamma-1}{2\gamma R g} \frac{V_3^2}{T_P}$$

$$\frac{T}{T_P} = \left[\frac{P_{s_3}}{P_{t_3}}\right]^{\frac{\gamma-1}{\gamma}} = 1 - \frac{\gamma-1}{2} \frac{V_3^2}{\gamma g R T_P}$$

and,

$$\frac{P_{s_3}}{P_{t_3}} = \left[1 - \frac{\gamma-1}{2} \frac{V_3^2}{a_P^2}\right]^{\frac{\gamma}{\gamma-1}} \qquad (17)$$

also,

$$\frac{P_{s_3}}{P_{t_3}} = \left[\frac{\rho_3}{\rho_t}\right]^{\gamma} = \left[\frac{\rho_3 g R T_P}{P_{t_3}}\right]^{\gamma}$$

and,

$$\rho_3 = \left(\frac{P_s}{P_t}\right)^{1/\gamma} \frac{P_t}{g R T_p}$$

Let $\rho_3 = \rho_3'$ then with

$$\frac{P_s}{P_t} = 1 - \frac{(P_t - P_s)}{P_t}$$

then,

$$\rho_3' = \frac{P_{t_3}}{g R T_p}\left[1 - \frac{(P_{t_3} - P_{s_3})}{P_{t_3}}\right]^{1/\gamma}$$

By selecting a trial value of ρ_3, with the measured quantities at station (2) and Eqs. (15) and (13), V_3^2 and P_{s_3} are calculated. Then, with Eq. (17),

$$P_{t_3} = P_{s_3} / \left(P_{s_3}/P_{t_3}\right)$$

Now, with the values of P_{s_3} and P_{t_3}, ρ_3' is calculated from Eq. (18). When the absolute value of the difference between ρ_3' and the trial value of ρ_3 is less than or equal to a pre-selected tolerance, the value of ρ_3 is established.

Loss Coefficients

Considering first a compressor cascade

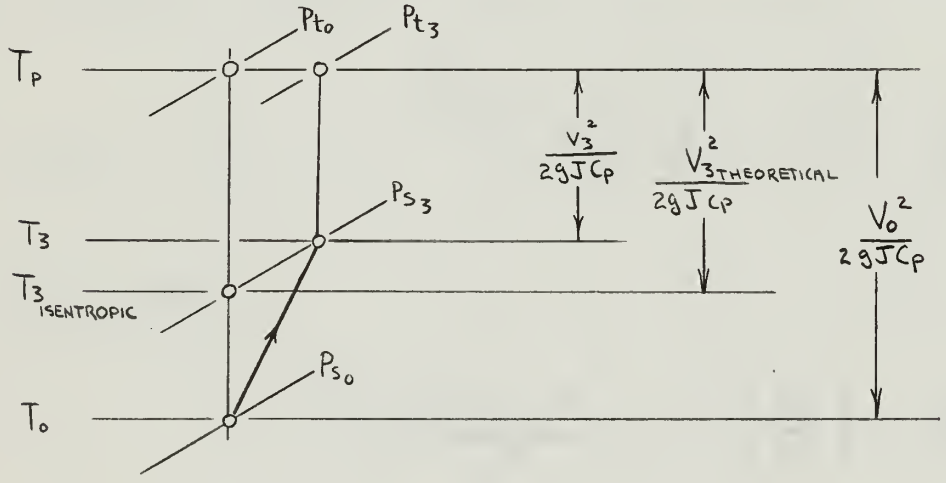

Let: $$\zeta = \frac{V_{3_{THEORET}}^2 - V_3^2}{V_3^2}$$

$$\zeta = \frac{V_{3theor.}^2}{V_3^2} - 1 \qquad (19)$$

$$\frac{V_{3theoret.}^2}{2gJc_p} = T_p\left[1 - \left(\frac{P_{s_3}}{P_{t_0}}\right)^{\frac{\gamma-1}{\gamma}}\right]$$

$$\frac{V_3^2}{2gJc_p} = T_p\left[1 - \left(\frac{P_{s_3}}{P_{t_3}}\right)^{\frac{\gamma-1}{\gamma}}\right]$$

$$\zeta = \frac{1 - \left(\frac{P_{s_3}}{P_{t_0}}\right)^{\frac{\gamma-1}{\gamma}}}{1 - \left(\frac{P_{s_3}}{P_{t_3}}\right)^{\frac{\gamma-1}{\gamma}}} - 1 \qquad (21)$$

For a turbine cascade,

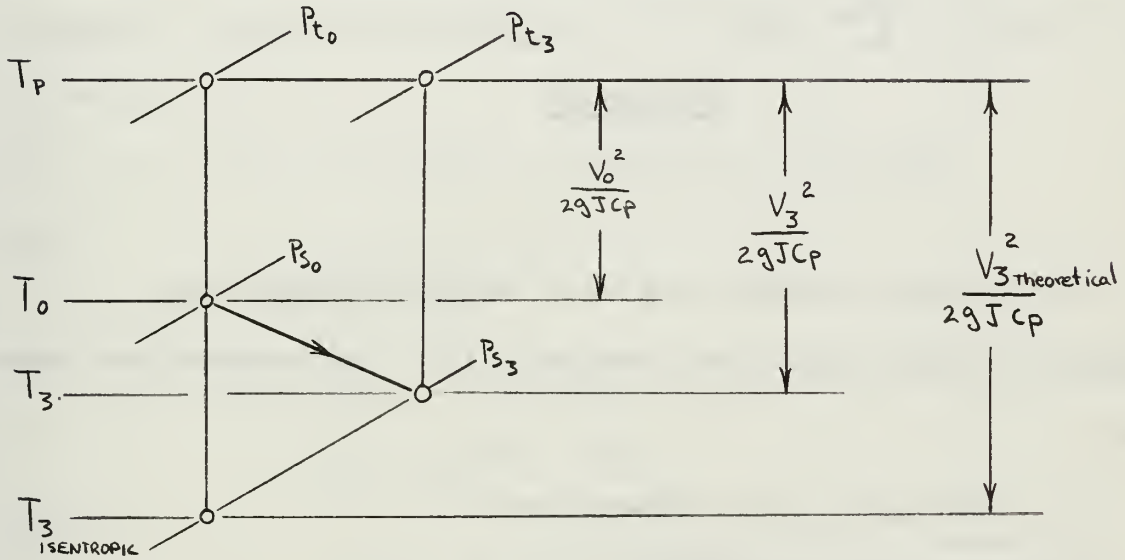

$$\zeta = \frac{V_{3theoret.}^2 - V_3^2}{V_3^2}$$

$$\zeta = \frac{V_{3theoret.}^2}{V_3^2} - 1$$

and, similar to Eq. (20),

$$\zeta = \frac{1 - \left(\frac{P_{s_3}}{P_{t_0}}\right)^{\frac{\gamma-1}{\gamma}}}{1 - \left(\frac{P_{s_3}}{P_{t_3}}\right)^{\frac{\gamma-1}{\gamma}}} \qquad -- 1$$

Forces Acting on the Blades

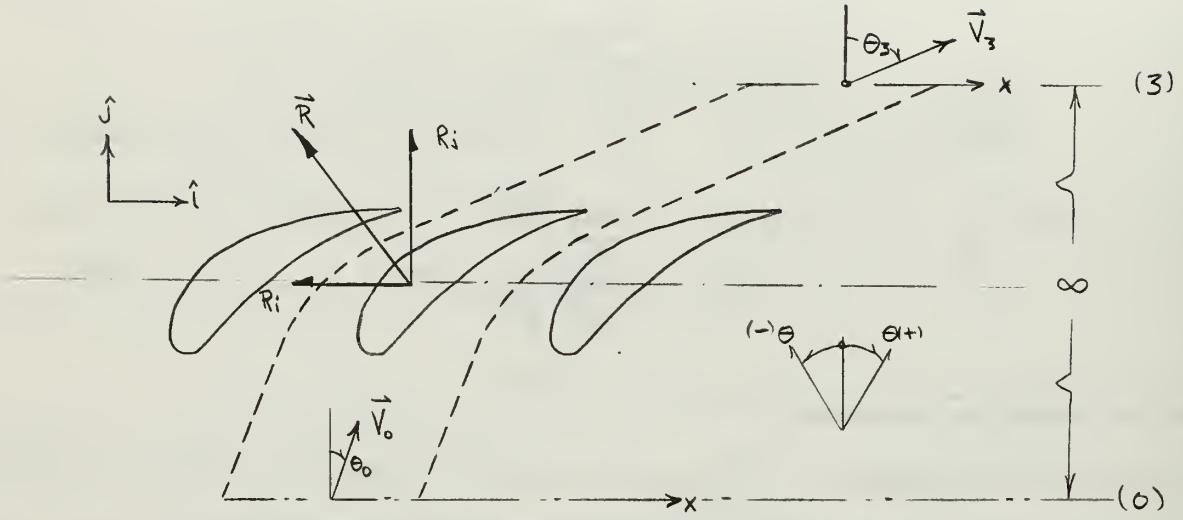

Figure A4

The control volume used will be that bounded by station (o) far ahead, and station (3). The assumptions made are:

(a) The flow is two dimensional.

(b) The flow is steady.

The Momentum equation (ignoring shear stress integrals)

gives

$$\int_{(0)} dm_s \vec{V}_0 - \int_{(3)} dm_s \vec{V}_3 + \hat{\imath} \int_{(0)} P_{s_0} dx - \hat{\imath} \int_{(3)} P_{s_3} dx = \vec{R} \qquad (21)$$

and

$$\vec{V}_0 = \hat{\imath} V_0 \sin\theta_0 + \hat{\jmath} V_0 \cos\theta_0$$

$$\vec{V}_3 = \hat{\imath} V_3 \sin\theta_3 + \hat{\jmath} V_3 \cos\theta_3$$

The force acting on the blade per unit height and the axial direction is

$$R_j = \rho_0 V_0^2 \cos^2\theta_0 \Delta X - \rho_3 V_3^2 \cos^2\theta_3 \Delta X + P_{s_0} \Delta X - P_{s_3} \Delta X \qquad (22)$$

for uniform flow conditions at station (o) and (3). The force per unit height acting on the blade in the tangential direction is

$$R_i = \tfrac{1}{2} \rho_0 V_0^2 \sin 2\theta_0 \Delta X - \tfrac{1}{2} \rho_3 V_3^2 \sin 2\theta_3 \Delta X \qquad (23)$$

and

$$|\vec{R}| = \sqrt{R_i^2 + R_j^2}$$

The mean vectorial velocity is

$$\vec{V}_\infty = \tfrac{1}{2} (\vec{V}_0 + \vec{V}_3)$$

or

$$V_\infty = \frac{1}{2} \sqrt{[V_0 \sin\theta_0 + V_3 \sin\theta_3]^2 + [V_0 \cos\theta_0 + V_3 \cos\theta_3]^2} \qquad (24)$$

where $\vec{V}_\infty$ is as shown in Fig. A5.

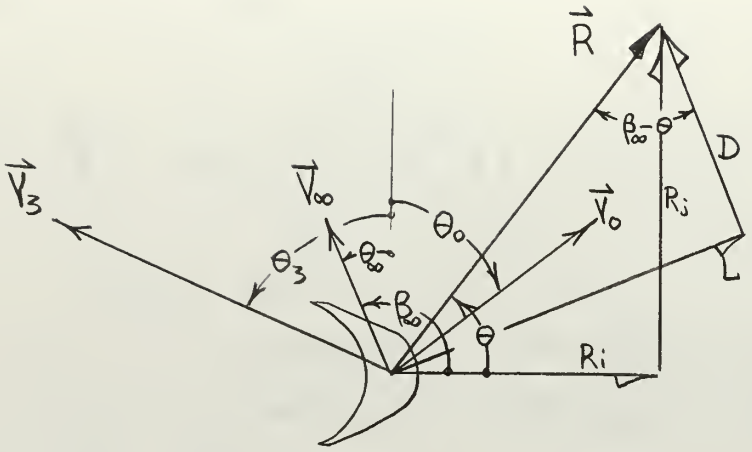

Figure A5

Also

$$\theta_\infty = \arctan \frac{[V_0 \cos\theta_0 + V_3 \cos\theta_3]}{[V_0 \sin\theta_0 + V_3 \sin\theta_3]} \qquad (25)$$

The drag force then is that component of $\vec{R}$ which is parallel to $\vec{V}_\infty$ and the lift force is that component of $\vec{R}$ perpendicular to V_∞. Then,

$$\vec{R} = \vec{L} + \vec{D}$$

$$L = R \sin(\beta_\infty - \theta)$$

$$D = R \cos(\beta_\infty - \theta)$$

where L, and D are the lift and drag force per unit height acting on the blade.

The lift and drag coefficients are defined as

$$C_L = \frac{L}{\frac{1}{2} \rho V_\infty^2 c} \qquad (26)$$

and

$$C_D = \frac{D}{\frac{1}{2}\rho V_\infty^2 c} \tag{27}$$

where c is the blade chord and

$$\rho = \frac{1}{2}\left[\rho_0 + \rho_3\right]$$

The lift and drag coefficients may also be defined as [8]

$$C_{L_0} = \frac{L}{\frac{1}{2}\rho_0 V_0^2 c}$$

and

$$C_{D_0} = \frac{D}{\frac{1}{2}\rho_0 V_0^2 c}$$

APPENDIX B

PROGRAM CASCADE

The data reduction computer program, entitled CASCADE, utilizes FORTRAN 60. Program CASCADE reads in the measured data of a cascade test in the form of input data cards, utilizes the equations developed in Appendix A, and displays the results in printed and graphical form. Output from CASCADE includes the following:

1. Conditions far ahead of the cascade
   a. Vo (ft./sec.)
   b. α_o (deg.)
   c. Pto (lbs./sq.ft.)
   d. Pso ((lbs./sq.ft.)
2. Conditions far aft of the cascade
   a. V_3 (ft./sec.)
   b. α_3 (deg.)
   c. Pt_3 (lbs./sq.ft.)
   d. Ps_3 (lbs./sq.ft.)
3. Average conditions at the measuring planes
   a. Pt_1 (lbs./sq.ft.)
   b. Ps_1 (lbs./sq.ft.)
   c. Pt_2 (lbs./sq.ft.)
   d. Ps_2 (lbs./sq.ft.)

4. Forces on the blades models (lbs. per ft.)

   a. Axial force

   b. Tangential force

   c. Lift

   d. Drag

5. Total turning angle of the flow (deg.).

6. Dimensionless loss coefficient of Eq. (20) between station (o) and station (3) which includes the mixing losses.

7. Lift and Drag coefficients based on the vectorial mean of V_o and V_3 (i.e., V_∞); (dimensionless).

8. Lift and Drag coefficients based on V_o; (dimensionless).

9. Constriction factor; equal to

$$\frac{\int_{(1)} \rho_1 V_1 \cos\Theta_1 \, dx}{\int_{(2)} \rho_2 V_2 \cos\Theta_2 \, dx} \qquad \text{(dimensionless)}$$

10. Total distance traversed, Δ X for both upper and lower traverse (in.).

11. Density far ahead and far aft (slugs/cu.ft.).

12. Reynolds number based on blade chord and V_3; (dimensionless).

13. Mach number based on V_o for the rotor cascade and V_3 for the stator cascade. (dimensionless).

FORTRAN Symbols

Symbols which are followed by an L to indicate association with the lower traverse or a U to indicate association with the upper traverse are as follows:

FORTRAN Symbol	Definition
X	x
DX	Δ x
PS	Ps
PT	Pt
DP	q
THETA	θ
TX	Total distance traversed
PCM	Probe Mach number correction factor
PCP	Probe pitch angle correction correction

Symbols which are followed by an A for station(o)or a B for station(3)are:

FORTRAN Symbol	Definition
PT	Pt
PS	Ps
DELP	Pt - Ps
THETA	θ
RHO	ρ
V	V

VCT	$V \cos \theta$
VST	$V \sin \theta$

Symbols which are followed by a 1 for station(1) (lower traverse) or a 2 for station(2)(upper traverse) are:

FORTRAN Symbol	Definition
PT	Average total pressure
PS	Average static pressure
RHO	ρ

Symbols associated with the various integrals involved are:

FORTRAN Symbol	Definition
CC1	$\int \rho_1 V_1 \cos\theta_1 \, dx$
EE1	$\int \rho_1 \, dx$
FFA	$\int P_{s_1} V_1 \cos\theta_1 \, dx$
FF1	$\int P_{t_1} V_1 \cos\theta_1 \, dx$
GG1	$\int V_1 \cos\theta_1 \, dx$
HH1	$\int V_1 \, dx$
TT1	$\int \theta_1 \, dx$
AA2	$\int P_{s_2} \, dx$
BB2	$\int \rho_2 V_2^2 \cos\theta_2 \, dx$

FORTRAN Symbol	Definition
CC2	$\int \rho_2 V_2 \cos\theta_2 \, dx$
DD2	$\int \rho_2 V_2^2 \sin 2\theta_2 \, dx$
EE2	$\int \rho_2 \, dx$
FFB	$\int p_{s_2} V_2 \cos\theta_2 \, dx$
FF2	$\int p_{t_2} V_2 \cos\theta_2 \, dx$
GG2	$\int V_2 \cos\theta_2 \, dx$

Symbols used without suffix:

FORTRAN Symbol	Definition
A	Conversion unit; 5.2022 $(lb./ft.^2)/(in.\ H_2O)$
AP2	$\gamma g R T_p$
AP3	$\frac{\gamma - 1}{\gamma}$
BETAIN	β_∞
BN	Number of blade spacings traversed
BP	P atm
B	$1 - \frac{2V_3^2}{\gamma g R T_p}$

FORTRAN Symbol	Definition
C	Chord
CD	Coefficient of drag based on V_∞ and RHO
CL	Coefficient of lift based on V_∞ and RHO
CDl	Coefficient of drag based on V_o and ρ_o
CLl	Coefficient of lift based on V_o and ρ_o
CB	$\left[1 - \frac{q_3}{Pt_3}\right]^{1/\gamma}$
DR	$\lvert\vec{R}\rvert$
DRA	R_j
DRU	R_i
DELB	$\theta_o - \theta_3$
DRAG	Drag
DRHO	$\Delta\rho$
G	g
GAMMA	γ

FORTRAN Symbol	Definition
K	Run number
L	Number of lower data points
M	Number of upper data points
MO	Mach number
PSI	$\dfrac{\int_{(1)} \rho_1 V_1 \cos\theta_1 \, dx}{\int_{(2)} \rho_2 V_2 \cos\theta_2 \, dx}$
R	R . g
REO	Reynolds Number
RHO	$\frac{1}{2}\left[\rho_0 + \rho_3\right]$
RHOBC	$\dfrac{\gamma P_{t3}}{\gamma g R T_p}\left[1 - \dfrac{q_3}{P_{t3}}\right]^{1/\gamma}$
S	Blade spacing
SIGMA	Solidity = c/s
STAN	Stagger angle
TA	Tp (^{o}R)
TF	Tp (^{o}F)
TA	T_3 (^{o}R)

FORTRAN Symbol	Definition
T1	T_o (^oR)
TLIFT	Lift
THETAIN	Θ_∞
VA^2	V_o^2
VB^2	V_3^2
VIN	V_∞
VISC	μ

The statements in program CASCADE are indexed by a six-digit number which appears at the extreme right of the program printout (see Table C1); i.e., in columns 74 to 80 of the IBM card format. In referring to these indices, all zeros will be neglected. For instance, index number 101 will appear in the program printout as 001010. In other words, the statements are numbered consecutively within digits three through five of the six-digit index. Reference to statement numbers will mean the numbers which appear in columns one through six of the IBM card format.

Statements 0 through 12 establish the arrays used in the program arithmetic and provide for the graph output titles in accordance with subroutine draw of the FORTRAN 60 library

(associated with the CDC 1604 computer). The COMMON statement is required (index #5) since the memory cells reserved by CASCADE in conjunction with subroutine DRAW exceed the present memory capacity of the CDC 1604 system.

Statements 13 through 18 read the input data into the computer. Data input for CASCADE is in the form of data cards. A set of data consists of the following:

(a) First subset: A single card reads in: Run number, Barometic pressure, Plenum temperature, number of blade spacings traversed, the blade spacing.

(b) Second subset: A single card with one number reads in: the total number data points to be read in for the lower traverse data.

(c) Third subset: The set of lower traverse data points: one card per point. The total number of cards in the set must be equal to the number appearing in (b), the second subset.

(d) Fourth subset: A single card with one number: the total number of data points to be read in for the upper traverse data.

(e) Fifth subset: A single card reads in: the blade chord, the stagger angle of the cascade, the pitch angle and Mach number correction factors for the lower and upper YC-120 probes, respectively.

Input data must have the following dimensions:

(a) Temperature: ^{o}F

(b) Barometric pressure: in. of Hg

(c) All other pressures: in. of H_2O

(d) Angles: deg.

(e) Lengths: inches

(f) All other data: non-dimensional

After input data is read in, statements indexed 21 through 40, by means of a sequence of individual DO LOOPS, establish the following data for both upper and lower traverses.

(a) Total distance traversed.

(b) The x coordinate of the individual data points with the first point assigned x = o.

(c) The static pressure at each point.

Subroutine DRAW is summoned by statements 41 through 52 with the appropriate graph label preceding each call statement. The statements for draw exhibited in Table C1 are of the format which allows automatic scale factor adjustment by the CDC 1604. Statements 53 through 58 print out the input data. The graphical and printed output are in the dimensions of the input data (i.e., in. of H_2O, inches, etc.)

Statements 59 through 90 establish constants, correct static pressure readings for probe calibrations in accordance

with equations established by United Sensor and Control Corporation calibration charts, and converts pressures, temperatures, angles, and lengths to the units used in computations. The converted units are:

(a) Pressures: lbs./sq.ft., absolute

(b) Temperature: ^{o}R

(c) Length: ft.

(d) Angles: radians

Using the thermodynamic relations of Appendix A, densities and velocities are computed for each probe position by means of statements 91 through 100. Statements 101 through 150 perform the summation approximations to the various integrals. The form of the integration is:

$$\int f(x)\,dx \cong \sum_{i=1}^{n} \left[f(x_i) + f(x_{i+1})\right] \frac{1}{2}\left(x_{i+1} - x_i\right)$$

The method of determining the mass density of the mixed flow far aft of the cascade given in Appendix A is programmed in statements 151 through 172. In the process of the iteration for density at station (3), the pressures, velocity and flow angle at (3) are also established. Statements 173 through 182 compute flow properties far ahead of the cascade based on the previously computed integrals. In addition, the average pressures at the measuring planes are established.

Statements 183 through 233 compute the remaining output information, namely:

(a) Forces on the blades

(b) Constriction factor

(c) Lift and Drag coefficients

(d) Total turning angle of the flow

(e) Mach and Reynold's numbers

(f) Loss coefficient

The remaining statements through index number 312 are the PRINT and FORMAT statements for the computed output.

Program CASCADE is designed to process more than one set of input data. Statement index number 313 just before STOP starts the computing process at statement number 1; the READ statements. If there is only one set of data, the program will exit the loop normally and stop. If there is more than one set of data, the program will read in the next set. CASCADE will work for both compressor or turbine cascade data. The only difference between the two is the computation of lift and drag from the axial and tangential blade force components, because of possible differences in sign of the leaving flow angle. This is handled by the IF statement index number 197. If multiple sets of input data are used, graphs will be plotted for each set, however, the graph title will not change.

Table B1

PROGRAM LISTING

```
..JOB0322F BARTOCCI                                                    000010
      PROGRAM CASCADE                                                  000020
      DIMENSION XL(900),XU(900),DPL(900),DPU(900),THETAL(900),THETAU(900 000030
     1),PTL(900),PTU(900),PSL(900),PSU(900),RHO1(900),RHO2(900),IN(10),  000040
     2DXL(900),DXU(900),ITITLE(12),VL2(900),VU2(900)                     000050
      COMMON XL,XU,DPL,DPU,THETAL,THETAU                               000060
      DO 1850 I=1,12                                                   000070
 1850 ITITLE(I)=8H                                                     000080
      ITITLE(1)=8HRUN  304                                             000090
      ITITLE(3)=8H ROTOR                                               000100
      ITITLE(4)=8HPROFILES                                             000110
      ITITLE(6)=8HBARTOCCI                                             000120
    1 READ 801,K,RP,TF,BN,S                                            000130
      READ 2,L                                                         000140
      READ 803,(IL,DXL(I),THETAL(I),DPL(I),PTL(I),I=1,L)               000150
      READ 2,M                                                         000160
      READ 803,(IU,DXU(I),THETAU(I),DPU(I),PTU(I),I=1,M)               000170
      READ 3,C,STAN,PCPL,PCVL,PCPU,PCVU                                000180
    2 FORMAT (I3)                                                      000190
    3 FORMAT(6F10.2)                                                   000200
      TXL=0.0                                                          000210
      DO 150 I=2,L                                                     000220
      TXL=TXL+DXL(I)                                                   000230
  150 CONTINUE                                                         000240
      TXU=0.0                                                          000250
      DO 151 I=2,M                                                     000260
       TXU=TXU+DXU(I)                                                  000270
  151 CONTINUE                                                         000280
      XL(1)=0.0                                                        000290
      PSL(1)=PTL(1)-DPL(1)                                             000300
      DO 1800 I=2,L                                                    000310
      XL(I)=XL(I-1)+DXL(I)                                             000320
      PSL(I)=PTL(I)-DPL(I)                                             000330
```

```
 1800 CONTINUE                                                          000340
      XU(1)=0.0                                                         000350
      PSU(1)=PTU(1)-DPU(1)                                              000360
      DO 1801 I=2,M                                                     000370
      XU(I)=XU(I-1)+DXU(I)                                              000380
      PSU(I)=PTU(I)-DPU(I)                                              000390
 1801 CONTINUE                                                          000400
      LABEL=4H PTL                                                      000410
      CALL DRAW(L,XL,PTL,0,0,LABEL,ITITLE,0,0,0,0,0,0,0.9,1,LAST)       000420
      LABEL=4H DPL                                                      000430
      CALL DRAW(L,XL,DPL,0,0,LABEL,ITITLE,0,0,0,0,0,0,0.9,1,LAST)       000440
      LABEL=4H PSL                                                      000450
      CALL DRAW(L,XL,PSL,0,0,LABEL,ITITLE,0,0,0,0,0,0,0.9,1,LAST)       000460
      LABEL=4H PTU                                                      000470
      CALL DRAW(M,XU,PTU,0,0,LABEL,ITITLE,0,0,0,0,0,0,0.9,1,LAST)       000480
      LABEL=4H DPU                                                      000490
      CALL DRAW(M,XU,DPU,0,0,LABEL,ITITLE,0,0,0,0,0,0,0.9,1,LAST)       000500
      LABEL=4H PSU                                                      000510
      CALL DRAW(M,XU,PSU,0,0,LABEL,ITITLE,0,0,0,0,0,0,0.9,1,LAST)       000520
      PRINT 800                                                         000530
      PRINT 801,K,BP,TF,BN,S                                            000540
      PRINT 802                                                         000550
      PRINT 803,(I,XL(I),THETAL(I),DPL(I),PTL(I),PSL(I),I=1,L)          000560
      PRINT 804                                                         000570
      PRINT 805,(I,XU(I),THETAU(I),DPU(I),PTU(I),PSU(I),I=1,M)          000580
C     CONVERT BP(IN HG) TO LB/SQUARE FOOT                               000590
      BP=BP*70.727                                                      000600
C     CONVERT PM(IN H2O) TO LB/SQUARE FOOT                              000610
      A=5.2022                                                          000620
      TA=TF+459.69                                                      000630
      G=32.174                                                          000640
      B=2.*G*778.26*.24                                                 000650
      R=53.35*G                                                         000660
      GAMMA=1.4                                                         000670
      AP2=GAMMA*R*TA                                                    000680
      AP3=(GAMMA-1.)/(2.*GAMMA)                                         000690
```

```
      S=S/12.                                                          000700
      TXL=TXL/12.                                                      000710
      TXU=TXU/12.                                                      000720
      DO 125 I=1,L                                                     000730
      DXL(I)=DXL(I)/12.                                                000740
      THETAL(I)=THETAL(I)/57.2958                                      000750
      PSL(I)=PSL(I)*A+BP                                               000760
      PTL(I)=PTL(I)*A+BP                                               000770
      PSL(I)=(PSL(I)-PCPL*PTL(I))/(1.-PCPL)                            000780
      PSL(I)=(PSL(I)-PCML*PTL(I))/(1.-PCML)                            000790
      DPL(I)=PTL(I)-PSL(I)                                             000800
  125 CONTINUE                                                         000810
      DO 100 I=1,M                                                     000820
      DXU(I)=DXU(I)/12.                                                000830
      PTU(I)=PTU(I)*A+BP                                               000840
      PSU(I)=PSU(I)*A+BP                                               000850
      PSU(I)=(PSU(I)-PCPU*PTU(I))/(1.-PCPU)                            000860
      PSU(I)=(PSU(I)-PCMU*PTU(I))/(1.-PCMU)                            000870
      DPU(I)=PTU(I)-PSU(I)                                             000880
      THETAU(I)=THETAU(I)/57.2958                                      000890
  100 CONTINUE                                                         000900
C     THE FOLLOWING STATEMENTS COMPUTE THE VARIOUS INTEGRALS           000910
      DO 121 I=1,L                                                     000920
      RHO1(I)=(GAMMA-(DPL(I)/PTL(I))-((AP3*DPL(I)*DPL(I)))/(PTL(I)**2))000930
     1*PTL(I)/AP2                                                      000940
      VL2(I)=2.*AP2*DPL(I)/PTL(I)*(1.+DPL(I)/(PTL(I)*2.*GAMMA)) /1.4   000950
  121 CONTINUE                                                         000960
      DO 122 I=1,M                                                     000970
      RHO2(I)=(GAMMA-(DPU(I)/PTU(I))-((AP3*DPU(I)*DPU(I)))/(PTU(I)**2))000980
     1*PTU(I)/AP2                                                      000990
      VU2(I)=2.*AP2*DPU(I)/PTU(I)*(1.+DPU(I)/(PTU(I)*2.*GAMMA))/1.4    001000
  122 CONTINUE                                                         001010
      LL=L-1                                                           001020
      CC1=0.0                                                          001030
      EF1=0.0                                                          001040
      EFA=0.0                                                          001050
```

```
      EE1=0.0                                                           001060
      GG1=0.0                                                           001070
      HH1=0.0                                                           001080
      TT1=0.0                                                           001090
      DO 200 I=1,LL                                                     001100
      RR=RHO1(I)*SQRTF(VL2(I))                                          001110
      RR1=RHO1(I+1)*SQRTF(VL2(I+1))                                     001120
      CC1=CC1+(RR*COSF(THETAL(I))+RR1*COSF(THETAL(I+1)))*DXL(I+1)*.5    001130
      EE1=EE1+(RHO1(I)+RHO1(I+1))*DXL(I+1)*.5                           001140
      FF1=FF1+(PTL(I)*SQRTF(VL2(I))*COSF(THETAL(I))+PTL(I+1)*SQRTF(VL2  001150
     1(I+1))*COSF(THETAL(I+1)))*DXL(I+1)*.5                             001160
      GG1=GG1+(SQRTF(VL2(I))*COSF(THETAL(I))  +SQRTF(VL2(I+1))*COSF(THET 001170
     1AL(I+1)))*DXL(I+1)*.5                                             001180
      FFA=FFA+(PSL(I)*SQRTF(VL2(I))*COSF(THETAL(I))+PSL(I+1)*SQRTF(VL2(I 001190
     1+1))*COSF(THETAL(I+1)))*DXL(I+1)*.5                               001200
      HH1=HH1+(VL2(I)+VL2(I+1))*DXL(I+1)*.5                             001210
      TT1=TT1+(THETAL(I)+THETAL(I+1))*DXL(I+1)*.5                       001220
  200 CONTINUE                                                          001230
      MM=M-1                                                            001240
      AA2=0.0                                                           001250
      BB2=0.0                                                           001260
      CC2=0.0                                                           001270
      DD2=0.0                                                           001280
      EE2=0.0                                                           001290
      FFB=0.0                                                           001300
      FF2=0.0                                                           001310
      GG2=0.0                                                           001320
      DO 300 I=1,MM                                                     001330
      AA2=AA2+(PSU(I)+PSU(I+1))*DXU(I+1)*.5                             001340
      THU=COSF(THETAU(I))**2                                            001350
      THUU=COSF(THETAU(I+1))**2                                         001360
      BB2=BB2+(RHO2(I)*VU2(I)*THU+RHO2(I+1)*VU2(I+1)*THUU)*DXU(I+1)*.5  001370
      RR2=RHO2(I)*SQRTF(VU2(I))                                         001380
      RR3=RHO2(I+1)*SQRTF(VU2(I+1))                                     001390
      CC2=CC2+(RR2*COSF(THETAU(I))+RR3*COSF(THETAU(I+1)))*DXU(I+1)*.5   001400
      DD2=DD2+(-HO2(I)*VU2(I)*SINF(2.*THETAU(I))+RHO2(I+1)*VU2(I+1)*SINF 001410
```

```
     1(2.*THETAU(I+1)))*DXU(I+1)*.5                                          001420
      EE2=EE2+(RHO2(I)+RHO2(I+1))*DXU(I+1)*.5                                001430
      FF2=FF2+(PTU(I)*SQRTF(VU2(I))*COSF(THETAU(I))+PTU(I+1)*SQRTF(VU2(I     001440
     1+1))*COSF(THETAU(I+1)))*DXU(I+1)*.5                                    001450
      GG2=GG2+(SQRTF(VU2(I))*COSF(THETAU(I))  +SQRTF(VU2(I+1))*COSF(THET     001460
     1AU(I+1)))*DXU(I+1)*.5                                                  001470
      FFB=FFB+(PSU(I)*SQRTF(VU2(I))*COSF(THETAU(I))+PSU(I+1)*SQRTF(VU2(I     001480
     1+1))*COSF(THETAU(I+1)))*DXU(I+1)*.5                                    001490
  300 CONTINUE                                                               001500
C     ITERATION TO DETERMINE THE DENSITY FAR AHEAD AND FAR AFT OF THE        001510
C     CASCADE.                                                               001520
      TOL=.000001                                                            001530
      DRHO=.0000001                                                          001540
      EX=1./1.4                                                              001550
      RHOA=EE1/TXL                                                           001560
  202 RHOB=0.001                                                             001570
  306 PSB=(AA2/TXU)+ BB2/TXU     -((CC2**2)/(RHOB*TXU*TXU))                  001580
      VB2=.25*((DD2**2)/(CC2*CC2))+(CC2**2)/(RHOB*RHOB*TXU*TXU)              001590
      VB=SQRTF(VB2)                                                          001600
      THETAB=ATANF(RHOB*TXU*DD2/(2.*CC2**2))                                 001610
       B=1.-.2*VB2/AP2                                                       001620
      PB=B**3.5                                                              001630
      PTB=PSB/PB                                                             001640
      DELPB=PTB-PSB                                                          001650
      CB=(1.-DELPB/PTB)**EX                                                  001660
      RHOBC=1.4*PTB*CB/AP2                                                   001670
      ERR=ABSF(RHOB-RHOBC)                                                   001680
      IF(ERR-TOL) 302,302,304                                                001690
  304 RHOB=RHOB+DRHO                                                         001700
      GO TO 306                                                              001710
  302 CONTINUE                                                               001720
C     DETERMINATION OF FORCES ACTING ON THE BLADES IN CASCADE                001730
      PT1=FF1/GG1                                                            001740
      PS1=FFA/GG1                                                            001750
      PT2=FF2/GG2                                                            001760
      PS2=FFB/GG2                                                            001770
```

```
      PTA=PT1                                                          001780
      PSA=PS1                                                          001790
      THETAA=TT1/TXL                                                   001800
      VA2=HH1/TXL                                                      001810
      VA=SQRTF(VA2)                                                    001820
      PSI=CC1/CC2                                                      001830
      VSTA=VA*SINF(THETAA)                                             001840
      VCTA=VA*COSF(THETAA)                                             001850
      VSTB=VB*SINF(THETAB)                                             001860
      VCTB=VB*COSF(THETAB)                                             001870
      S=4./12.                                                         001880
      DRA=S*(RHOA*VCTA*VCTA-RHOB*VCTB*VCTB)+(PSA-PSB)*S                001890
      DRU=.5*S*(RHOA*VA2*SINF(2.*THETAA)-RHOB*VB2*SINF(2.*THETAB))     001900
      VIN=SQRTF(.25*(VSTA+VSTB)*(VSTA+VSTB)+.25*(VCTA+VCTB)*(VCTA+VCTB)) 001910
      THETAIN=ATANF((VSTA+VSTB)/(VCTA+VCTB))                           001920
      BETAIN=3.14159/2.-THETAIN                                        001930
      TB=TA-VB2*.4/(2.*778.28*GAMMA*R)                                 001940
      T1=TA-VA2*.4/(2.*778.28*GAMMA*R)                                 001950
      IF(THETAB) 500,500,501                                           001960
  500 THETA=ATANF(DRA/DRU)                                             001970
      THETA=ABSF(THETA)                                                001980
      DR=SQRTF(DRA*DRA+DRU*DRU)                                        001990
      DRAG=DR*COSF(BETAIN-THETA)                                       002000
      TLIFT=DR*SINF(BETAIN-THETA)                                      002010
      AMO=VA/SQRTF(GAMMA*R*T1)                                         002020
      GO TO 502                                                        002030
  501 THETA=ATANF(DRU/DRA)                                             002040
      THETA=ABSF(THETA)                                                002050
      TLIFT=DR*COSF(BETAIN-THETA)                                      002060
      DRAG=DR*SINF(BETAIN-THETA)                                       002070
      AMO=VB/SQRTF(GAMMA*R*TB)                                         002080
      GO TO 502                                                        002090
  502 C=C/12.                                                          002100
      RHO=.5*(RHOA+RHOB)                                               002110
      CL=2.*TLIFT/(RHO*C*VIN*VIN)                                      002120
      DPB=PTB-PSB                                                      002130
```

```
      CON=(1.-PSB/PTA)/(2.*GAMMA)                                       002140
      CONS=DPB/(2.*GAMMA*PTB)                                           002150
      ZETA=((PTB*(PTA-PSB)*(1.-CON))/(PTA*DPB*(1.-CONS)))-1.            002160
      CD=2.*DRAG/(RHO*C*VIN*VIN)                                        002170
      CL1=CL*RHO*VIN*VIN/(RHOA*VA2)                                     002180
      CD1=CD*RHO*VIN*VIN/(RHOA*VA2)                                     002190
      THETAA=THETAA*57.3                                                002200
      THETAB=THETAB*57.3                                                002210
      THETAIN=THETAIN*57.3                                              002220
      THETA=THETA*57.3                                                  002230
      BETAIN=BETAIN*57.3                                                002240
C     CONVERT BP(LB/SQ FT) TO IN. HG.                                   002250
      BP=BP/70.727                                                      002260
      TXL=TXL*12.                                                       002270
      TXU=TXU*12.                                                       002280
      SIGMA=C/S                                                         002290
      VISC=0.00001*(TB/400.)**.76                                       002300
      VISC=VISC*.031081                                                 002310
      REO=VB*C*RHOB/VISC                                                002320
      DELB=THETAA-THETAB                                                002330
  800 FORMAT(8H1RUN NO. 5X 2HBP 5X 4HTEMP 5X 2HBN 5X 1HS / )            002340
  801 FORMAT ( I5, F11.2, F8.1, F7.2, F7.1)                             002350
  802 FORMAT(6H0POINT6X2HXL8X6HTHETAL5X3HDPL7X3HPTL7X3HPSL    /)        002360
  803 FORMAT(I6,F14.5,3F10.4)                                           002370
  804 FORMAT(6H0POINT6X2HXU8X6HTHETAU5X3HDPU7X3HPTU7X3HPSU    /)        002380
  805 FORMAT(I5,5F10.2)                                                 002390
  910 FORMAT ( 6HICL1 = F10.5, 5X 5HCD1 = F10.5  )                      002400
      PRINT 400                                                         002410
  400 FORMAT(1H1//32X21HPROPULSION LABORATORY/28X30HU.S. NAVAL POSTGRADU 002420
     1ATE SCHOOL//)                                                     002430
      PRINT 401,K                                                       002440
  401 FORMAT(35X13HTEST RUN NO. I3//)                                   002450
      PRINT 402,BP                                                      002460
  402 FORMAT(27X20HBAROMETRIC PRESS. = F6.2,8H IN. HG.//)               002470
      PRINT 403,TF                                                      002480
  403 FORMAT(29X16H PLENUM TEMP. = F4.1,8H DEG. F.//)                   002490
```

```
      PRINT 404,STAN                                                    002500
  404 FORMAT(29X16HSTAGGER ANGLE = F5.2,4HDEG.//)                       002510
      PRINT 405,SIGMA                                                   002520
  405 FORMAT(33X11HSOLIDITY = F4.2//)                                   002530
      PRINT 406                                                         002540
  406 FORMAT(28X16HBLADE PROFILE = //)                                  002550
      PRINT 407                                                         002560
  407 FORMAT(10X22HFAR AHEAD (STATION 0 )11X22HFAR AFT   (STATION 3 )//)  002570
      PRINT 408                                                         002580
  408 FORMAT(8X2HV03X8HALPHA 0 2X3HPT04X3HPS010X2HV33X8HALPHA 3 2X3HPT34  002590
     1X3HPS3)                                                           002600
      PRINT 409                                                         002610
  409 FORMAT(5X29H(FT/SEC) (DEG)   (PSF)  (PSF)5X29H(FT/SEC) (DEG)   (PS  002620
     1F)  (PSF)//)                                                      002630
      PRINT 410,VA,THETAA,PTA,PSA,VB,THETAB,PTB,PSB                     002640
  410 FORMAT(5XF8.3,F7.2,2F8.1,F12.3,F7.2,2F8.1//)                      002650
      PRINT 411                                                         002660
  411 FORMAT(21X34HCONDITIONS AT THE MEASURING PLANES//)                002670
      PRINT 412                                                         002680
  412 FORMAT(9X27HLOWER TRAVERSE (STATION 1 )5X27HUPPER TRAVERSE (STATIO  002690
     1N 2 )//)                                                          002700
      PRINT 413                                                         002710
  413 FORMAT(14X3HPT19X3HPS117X3HPT220X3HPS2)                           002720
      PRINT 414                                                         002730
  414 FORMAT(13X5H(PSF)7X5H(PSF)15X5H(PSF)7X5H(PSF)//)                  002740
      PRINT 415,PT1,PS1,PT2,PS2                                         002750
  415 FORMAT(5X2F12.1,8X2F12.1//)                                       002760
      PRINT 416                                                         002770
  416 FORMAT(21X36HFORCES ON THE BLADES IN LBS. PER FT.//23X5HAXIAL2X10H  002780
     1TANGENTIAL3X4HLIFT4X4HDRAG//)                                     002790
      PRINT 417,DRA,DRU,TLIFT,DRAG                                      002800
  417 FORMAT(21XF7.2,2F10.2,F7.2//)                                     002810
      PRINT 418,DELB                                                    002820
  418 FORMAT(15X40HTOTAL TURNING ANGLE OF THE FLOW (DEG) = F6.2//)      002830
      PRINT 419,K                                                       002840
  419 FORMAT(1H1//10HRUN NO. = I3,10H CONCLUDED////)                    002850
```

```
      PRINT 420,ZETA                                                    002860
  420 FORMAT(10X42HLOSS COEFFICIENT , MIXING LOSS INCLUDED = F8.5///)   002870
      PRINT 422                                                         002880
  422 FORMAT(22X35HLIFT AND DRAG COEFFICIENTS BASED ON/22X31HTHE VECTORI 002890
     1AL MEAN OF V0 AND V3//27X2HCL16X2HCD//)                           002900
      PRINT 423,CL,CD                                                   002910
  423 FORMAT(14X2F17.4//)                                               002920
      PRINT 424                                                         002930
  424 FORMAT(22X35HLIFT AND DRAG COEFFICIENTS BASED ON/22X35HCONDITIONS  002940
     1EAR AHEAD OF THE CASCADE//27X3HCL015X3HCD0//)                     002950
      PRINT 425,CL1,CD1                                                 002960
  425 FORMAT(14X2F17.4//)                                               002970
      PRINT 426,PSI                                                     002980
  426 FORMAT(20X38HCONSTRICTION FACTOR                  = F6.4//)       002990
      PRINT 427,TXL                                                     003000
  427 FORMAT(20X38HDELTA X LOWER                        = F6.2//)       003010
      PRINT 429,TXU                                                     003020
  429 FORMAT(20X38HDELTA X UPPER                        = F6.2//)       003030
      PRINT 430,RHOA                                                    003040
  430 FORMAT(20X38HDENSITY(SLUGS PER CU.FT.) FAR AHEAD = F9.8//)        003050
      PRINT 431,RHOB                                                    003060
  431 FORMAT(20X38HDENSITY(SLUGS PER CU.FT.) FAR AFT   = F9.8//)        003070
      PRINT 432                                                         003080
  432 FORMAT(20X38HREYNOLDS NUMBER(CHORD) AND MACH NUMBER/24X4H REY14X3H 003090
     1 MO//)                                                            003100
      PRINT 433,REO,AMO                                                 003110
  433 FORMAT(17XF15.0,F15.4)                                            003120
      GO TO 1                                                           003130
      STOP                                                              003140
      END                                                               003150
      END                                                               003160
```

APPENDIX C
RESULTS OF THE CASCADE TESTS

Table C1

PROPULSION LABORATORY
U.S. NAVAL POSTGRADUATE SCHOOL

TEST RUN NO. 300

BAROMETRIC PRESS. = 30.19 IN. HG.

PLENUM TEMP. = 69.0 DEG. F.

STAGGER ANGLE = 68.00DEG.

SOLIDITY = 1.66

BLADE PROFILE =

FAR AHEAD (STATION 0)				FAR AFT (STATION 3)			
V0 (FT/SEC)	ALPHA 0 (DEG)	PT0 (PSF)	PS0 (PSF)	V3 (FT/SEC)	ALPHA 3 (DEG)	PT3 (PSF)	PS3 (PSF)
76.407	.29	2272.2	2264.9	356.496	78.45	2264.6	2110.1

CONDITIONS AT THE MEASURING PLANES

LOWER TRAVERSE (STATION 1)		UPPER TRAVERSE (STATION 2)	
PT1 (PSF)	PS1 (PSF)	PT2 (PSF)	PS2 (PSF)
2272.2	2264.9	2264.8	2109.9

FORCES ON THE BLADES IN LBS. PER FT.

AXIAL	TANGENTIAL	LIFT	DRAG
52.47	-19.69	56.00	2.30

TOTAL TURNING ANGLE OF THE FLOW (DEG) = -78.16

RUN NO. = 300 CONCLUDED

LOSS COEFFICIENT , MIXING LOSS INCLUDED = .04437

LIFT AND DRAG COEFFICIENTS BASED ON THE VECTORIAL MEAN OF V0 AND V3

CL	CD
2.3005	.0943

LIFT AND DRAG COEFFICIENTS BASED ON CONDITIONS FAR AHEAD OF THE CASCADE

CL0	CD0
13.8368	.5674

CONSTRICTION FACTOR = 1.1268

DELTA X LOWER = 12.00

DELTA X UPPER = 12.00

DENSITY(SLUGS PER CU.FT.) FAR AHEAD = .00249808

DENSITY(SLUGS PER CU.FT.) FAR AFT = .00237160

REYNOLDS NUMBER(CHORD) AND MACH NUMBER BASED ON VIN

REY	M0
1221047.	.3162

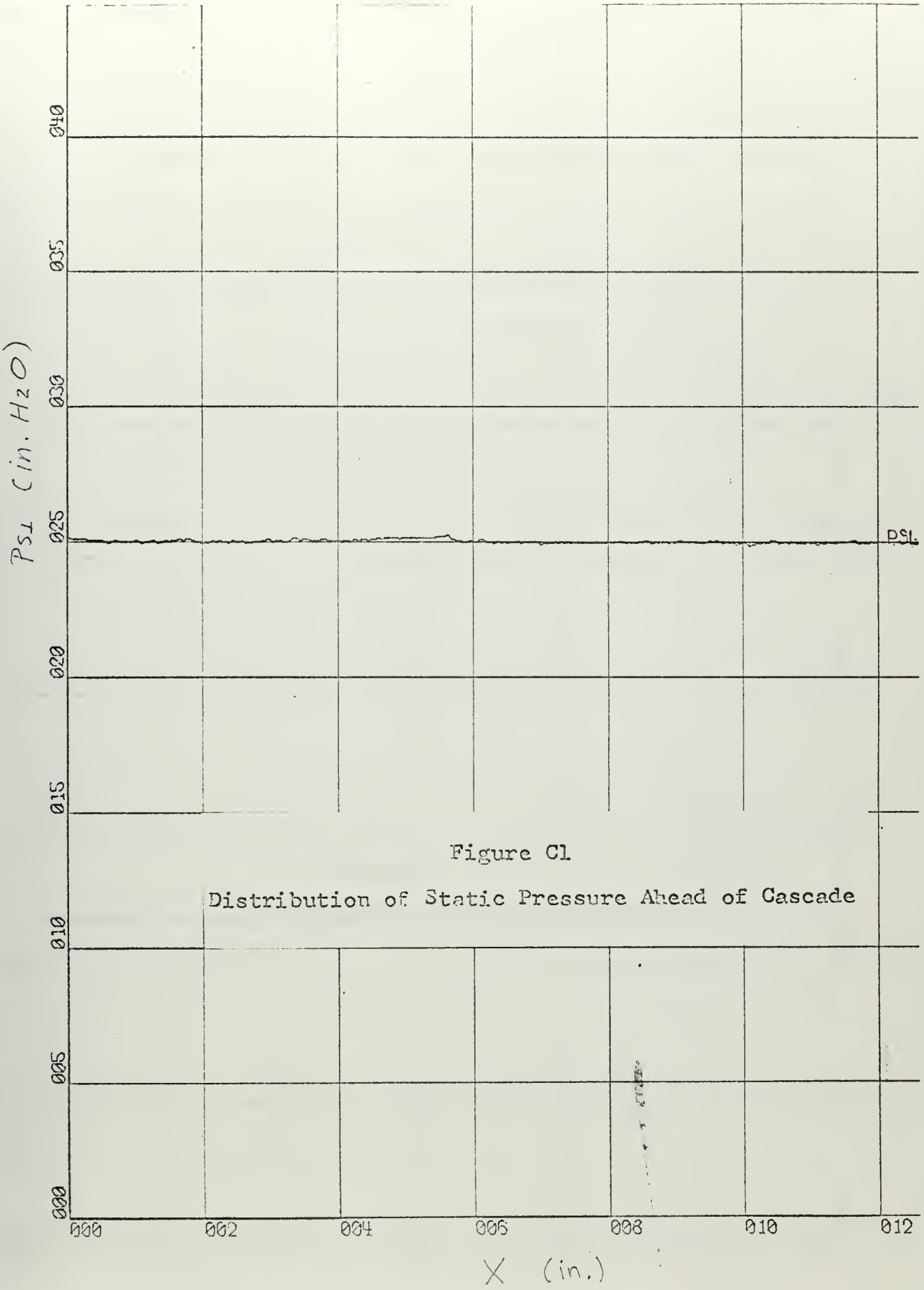

Figure C1

Distribution of Static Pressure Ahead of Cascade

X-SCALE = 2.00E+00 UNITS/INCH.
Y-SCALE = 5.00E+00 UNITS/INCH.

RUN 300 STATOR PROFILES

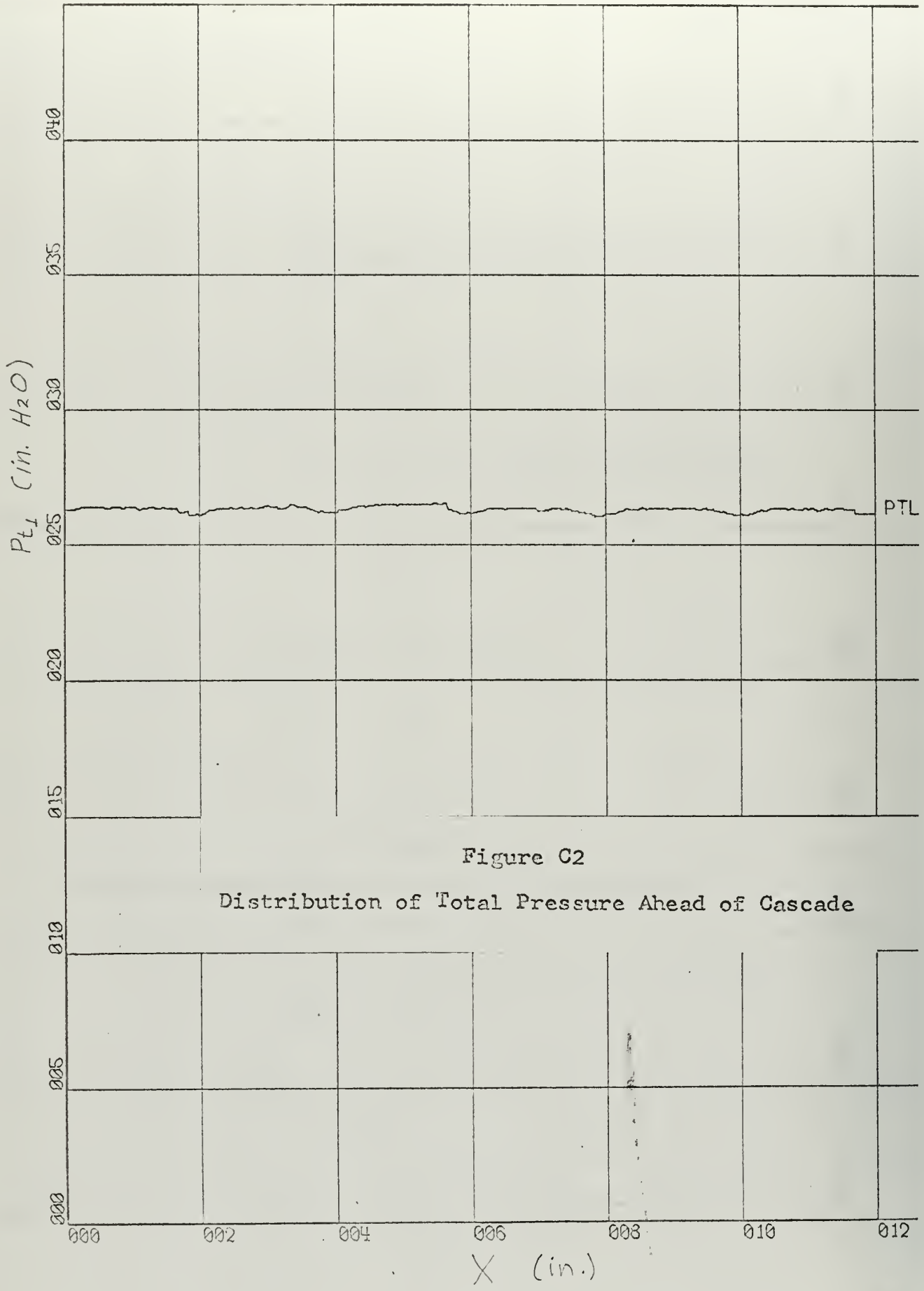

Figure C2

Distribution of Total Pressure Ahead of Cascade

X-SCALE = 2.00E+00 UNITS/INCH.
Y-SCALE = 5.00E+00 UNITS/INCH.

RUN 300 STATOR PROFILES

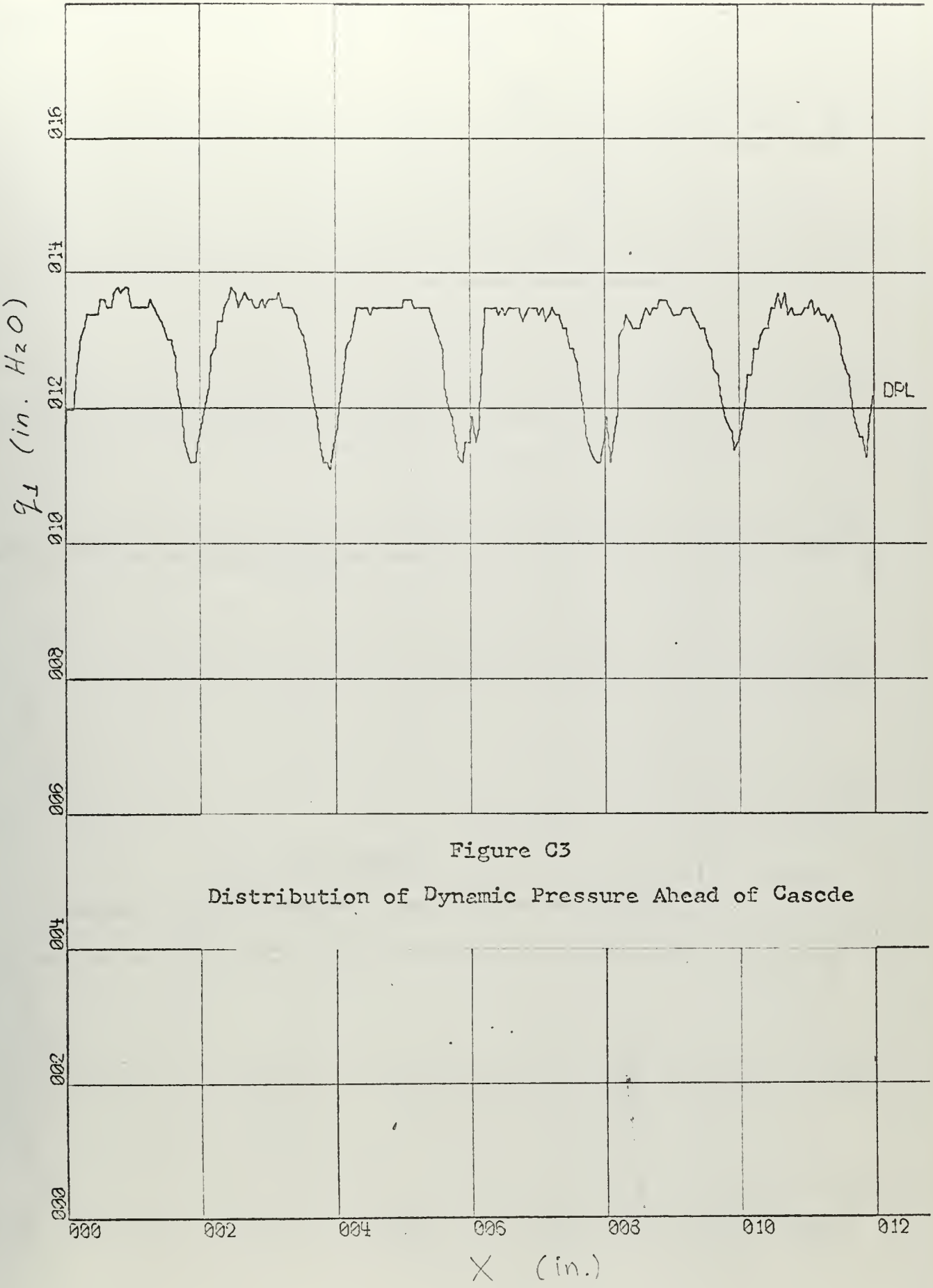

Figure C3

Distribution of Dynamic Pressure Ahead of Cascde

X-SCALE = 2.00E+00 UNITS/INCH.
Y-SCALE = 2.00E-01 UNITS/INCH.

RUN 300 STATOR PROFILES

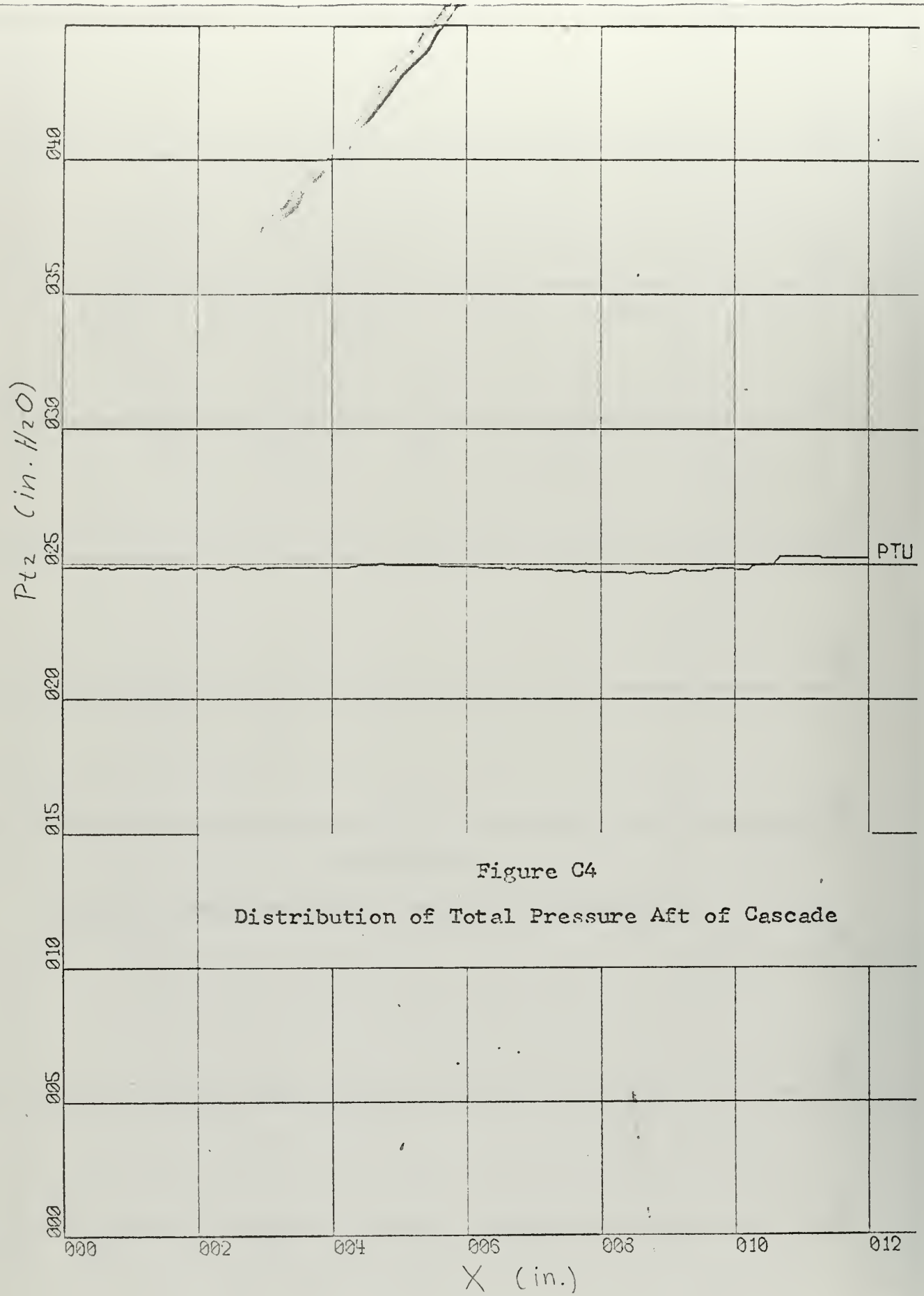

Figure C4

Distribution of Total Pressure Aft of Cascade

X-SCALE = 2.00E+00 UNITS/INCH.
Y-SCALE = 5.00E+00 UNITS/INCH.

RUN 300 STATOR PROFILES

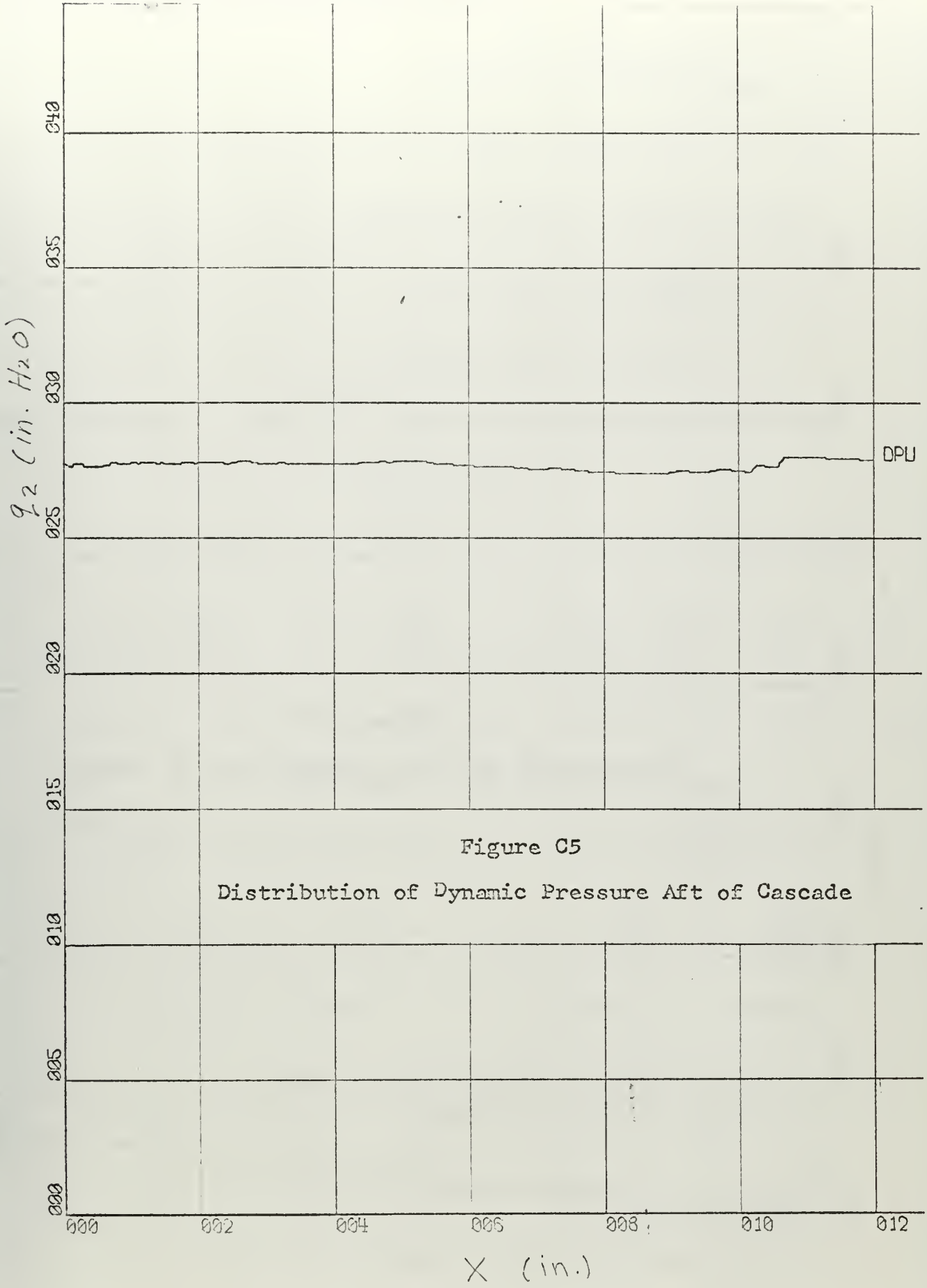

Figure C5

Distribution of Dynamic Pressure Aft of Cascade

X-SCALE = 2.00E+00 UNITS/INCH.
Y-SCALE = 5.00E+00 UNITS/INCH.

RUN 300 STATOR PROFILES

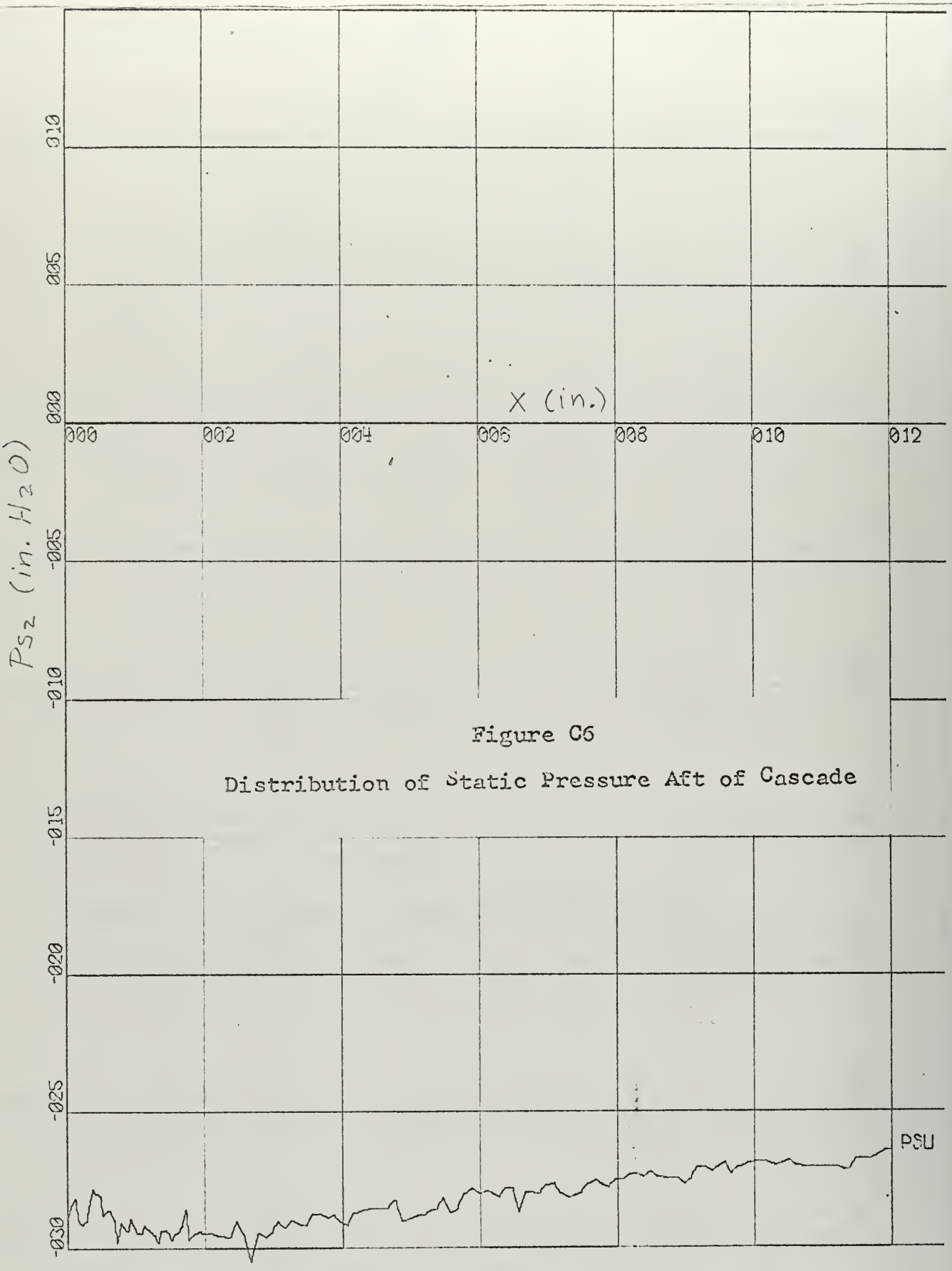

Figure C6

Distribution of Static Pressure Aft of Cascade

X-SCALE - 2.00E+00 UNITS/INCH.
Y-SCALE - 5.00E-01 UNITS/INCH.

RUN 300 STATOR PROFILES

Table C2

PROPULSION LABORATORY
U.S. NAVAL POSTGRADUATE SCHOOL

TEST RUN NO. 301

BAROMETRIC PRESS. = 30.13 IN. HG.

PLENUM TEMP. = 60.1 DEG. F.

STAGGER ANGLE = 48.00DEG.

SOLIDITY = 1.66

BLADE PROFILE =

FAR AHEAD (STATION 0)				FAR AFT (STATION 3)			
V0 (FT/SEC)	ALPHA 0 (DEG)	PT0 (PSF)	PS0 (PSF)	V3 (FT/SEC)	ALPHA 3 (DEG)	PT3 (PSF)	PS3 (PSF)
53.312	.00	2190.0	2186.5	229.918	78.67	2186.6	2122.5

CONDITIONS AT THE MEASURING PLANES

LOWER TRAVERSE (STATION 1)		UPPER TRAVERSE (STATION 2)	
P11 (PSF)	PS1 (PSF)	PT2 (PSF)	PS2 (PSF)
2190.0	2186.5	2186.6	2122.5

FORCES ON THE BLADES IN LBS. PER FT.

AXIAL	TANGENTIAL	LIFT	DRAG
22.02	-8.14	23.44	1.36

TOTAL TURNING ANGLE OF THE FLOW (DEG) = -78.67

RUN NO. = 301 CONCLUDED

LOSS COEFFICIENT , MIXING LOSS INCLUDED = .05088

LIFT AND DRAG COEFFICIENTS BASED ON
THE VECTORIAL MEAN OF V0 AND V3

CL	CD
2.3024	.1332

LIFT AND DRAG COEFFICIENTS BASED ON
CONDITIONS FAR AHEAD OF THE CASCADE

CL0	CD0
12.1233	.7012

CONSTRICTION FACTOR = 1.2054

DELTA X LOWER = 12.00

DELTA X UPPER = 12.00

DENSITY(SLUGS PER CU.FT.) FAR AHEAD = .00245173

DENSITY(SLUGS PER CU.FT.) FAR AFT = .00239820

REYNOLDS NUMBER(CHORD) AND MACH NUMBER

REY	MO
806858.	.2057

TIME, 4 MINUTES AND 43 SECONDS

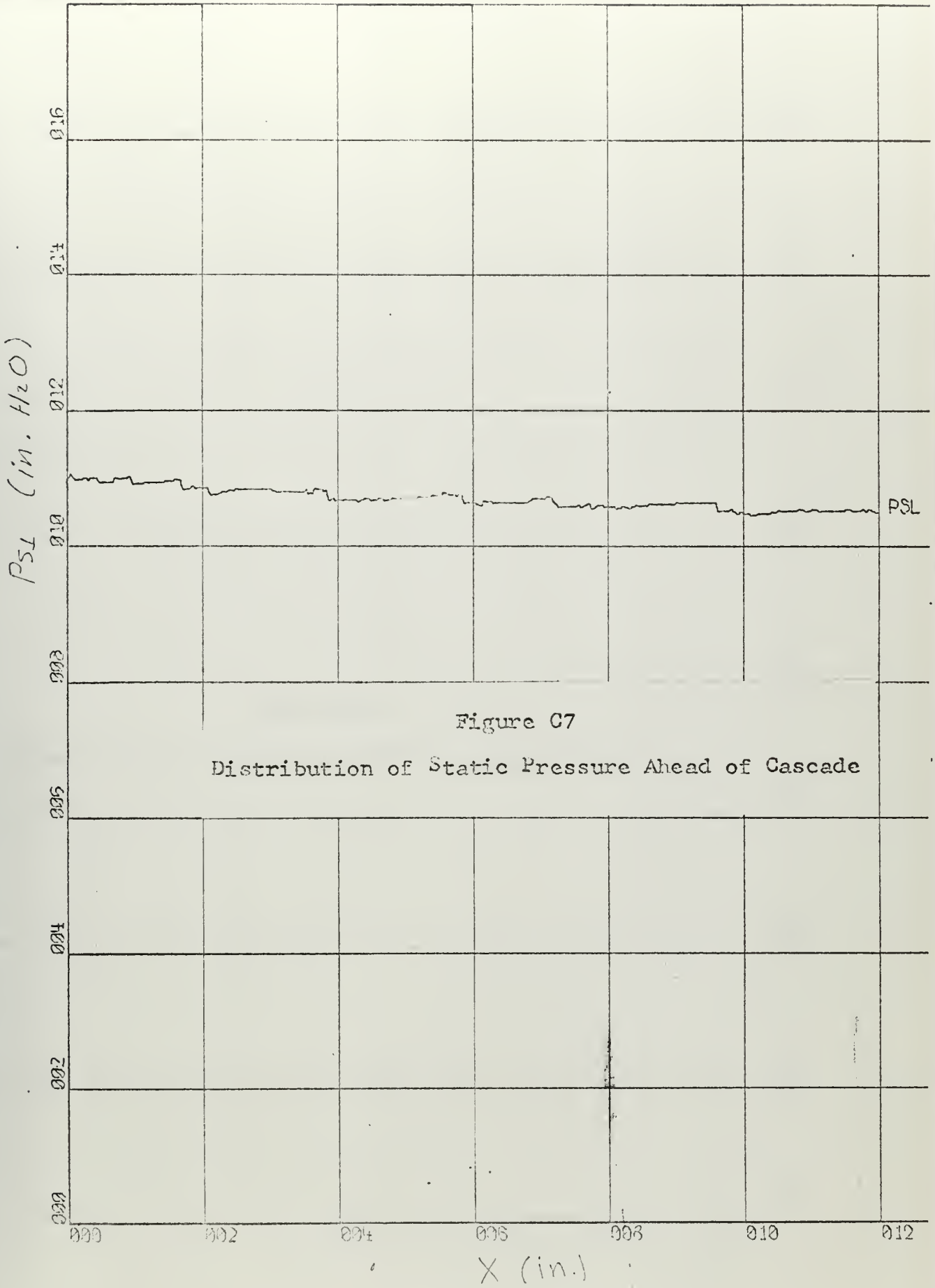

Figure C7

Distribution of Static Pressure Ahead of Cascade

X-SCALE = 2.00E+00 UNITS/INCH.
Y-SCALE = 2.00E+00 UNITS/INCH.

RUN 301

STATOR PROFILES

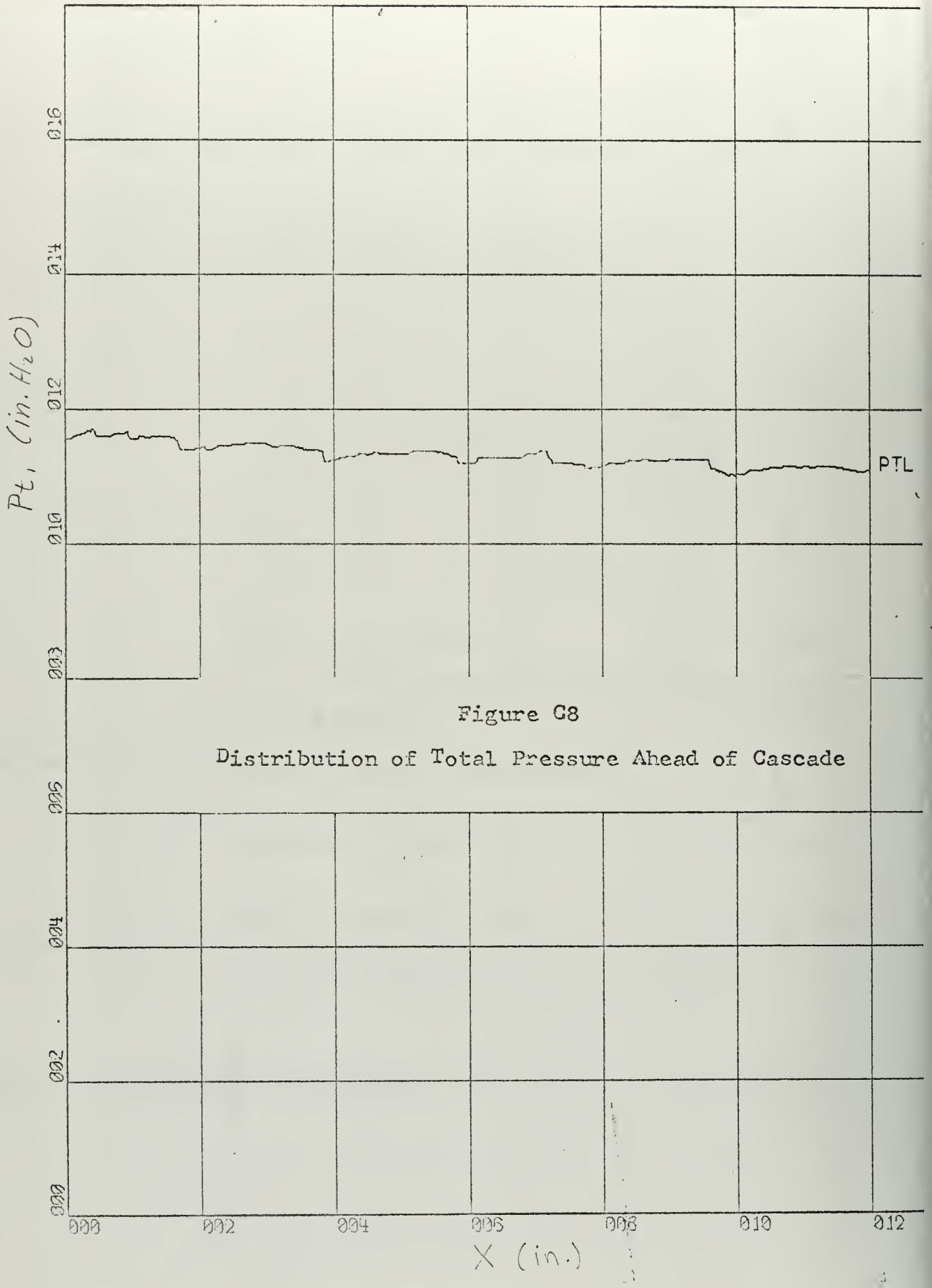

Figure C8

Distribution of Total Pressure Ahead of Cascade

X-SCALE = 2.00E+00 UNITS/INCH.
Y-SCALE = 2.00E+00 UNITS/INCH.

RUN 301 STATOR PROFILES

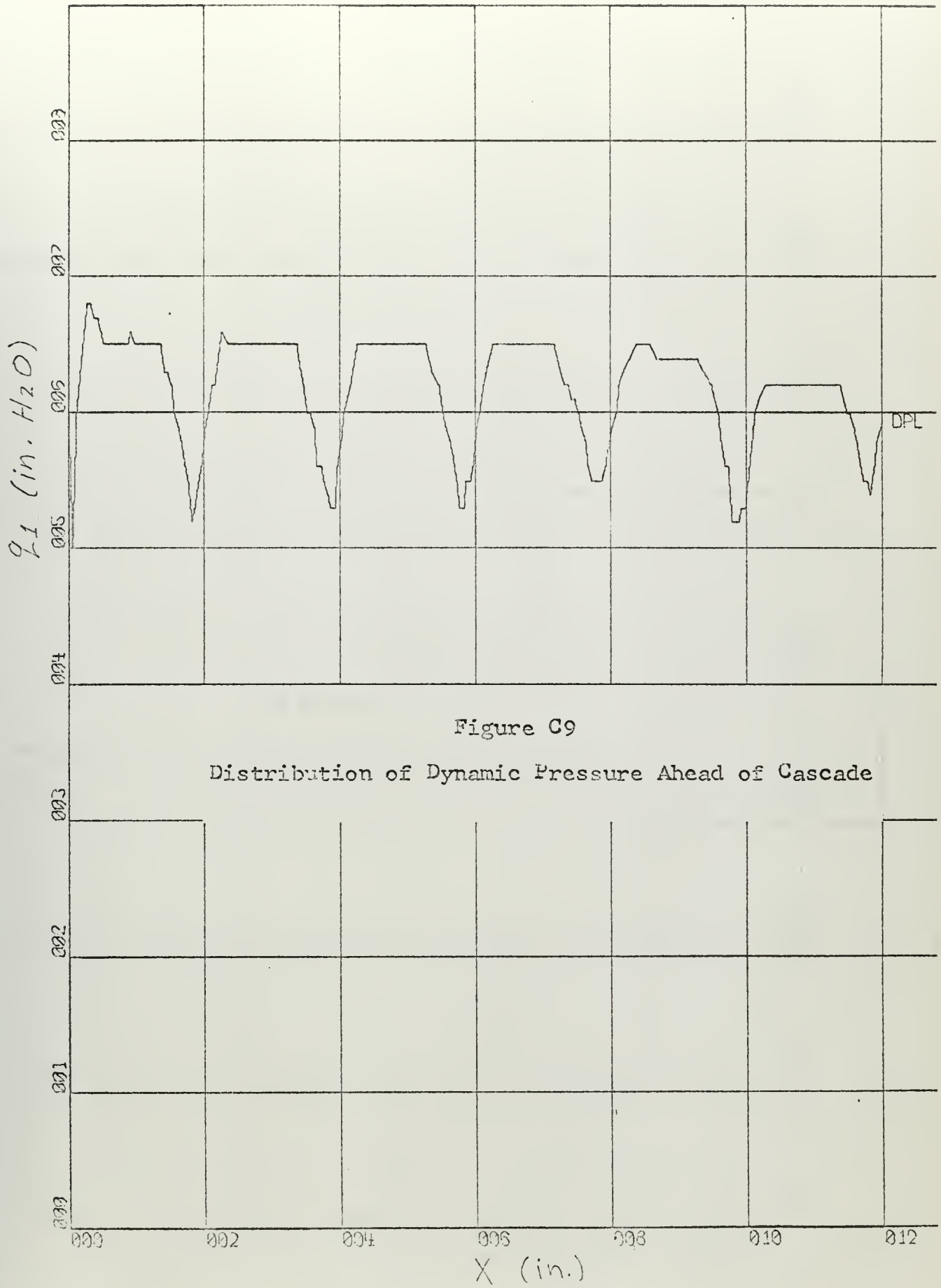

Figure C9

Distribution of Dynamic Pressure Ahead of Cascade

X-SCALE = 2.00E+00 UNITS/INCH.
Y-SCALE = 1.00E-01 UNITS/INCH.

RUN 301

STATOR PROFILES

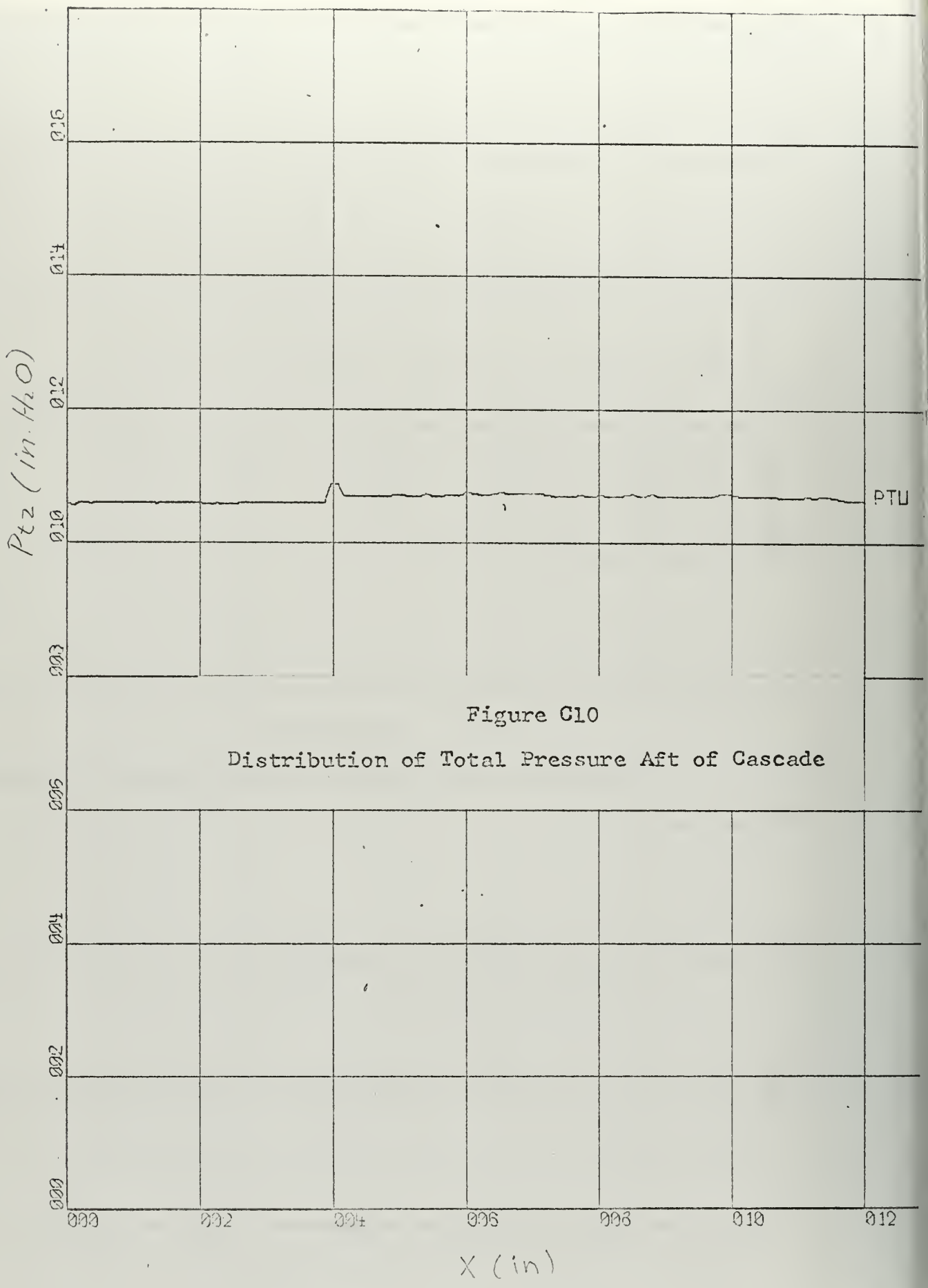

Figure C10

Distribution of Total Pressure Aft of Cascade

X-SCALE = 2.00E+00 UNITS/INCH.
Y-SCALE = 2.00E+00 UNITS/INCH.

RUN 301 STATOR PROFILES

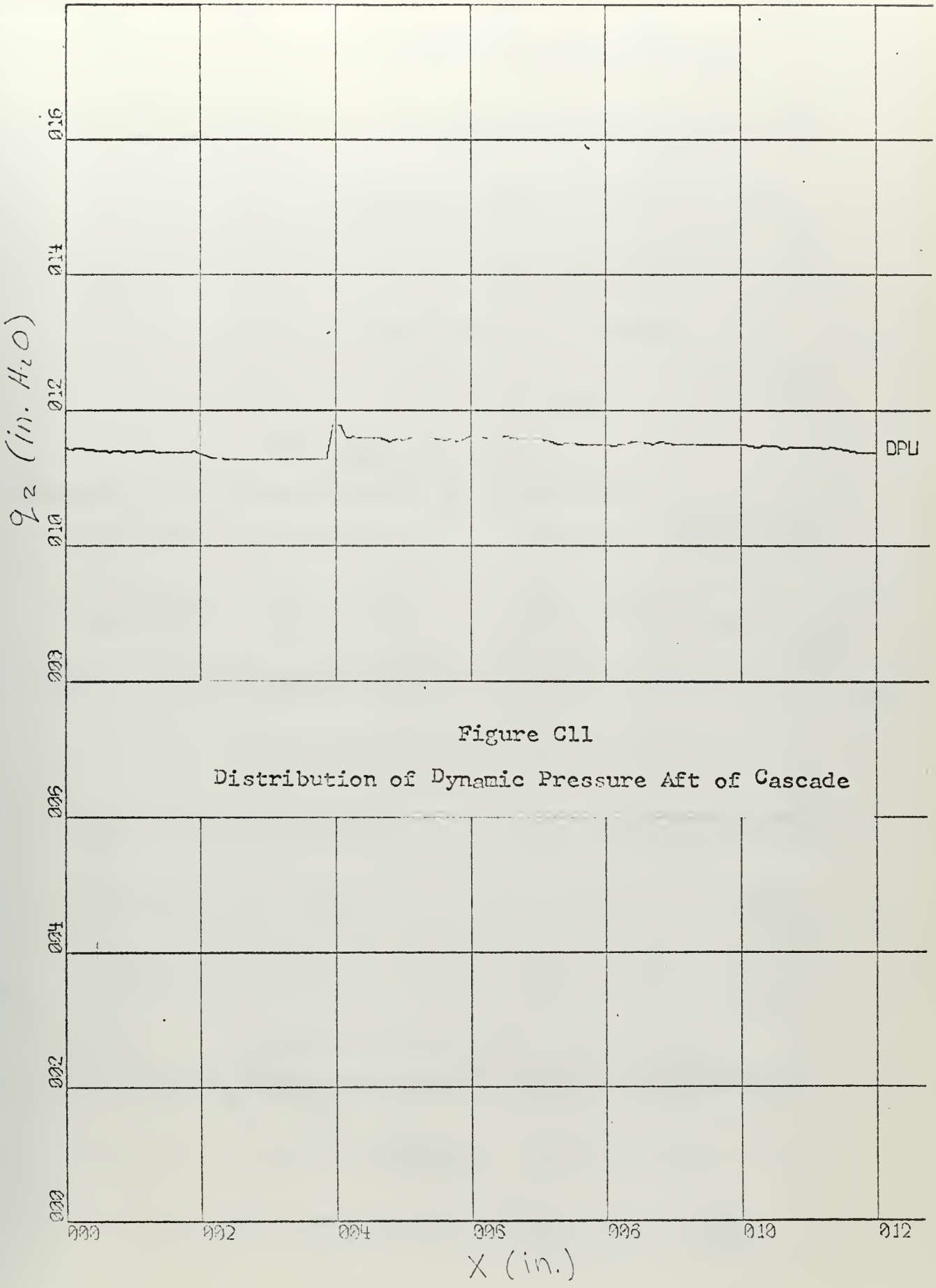

Figure C11

Distribution of Dynamic Pressure Aft of Cascade

X-SCALE = 2.00E+00 UNITS/INCH.
Y-SCALE = 2.00E+00 UNITS/INCH.

RUN 301 STATOR PROFILES

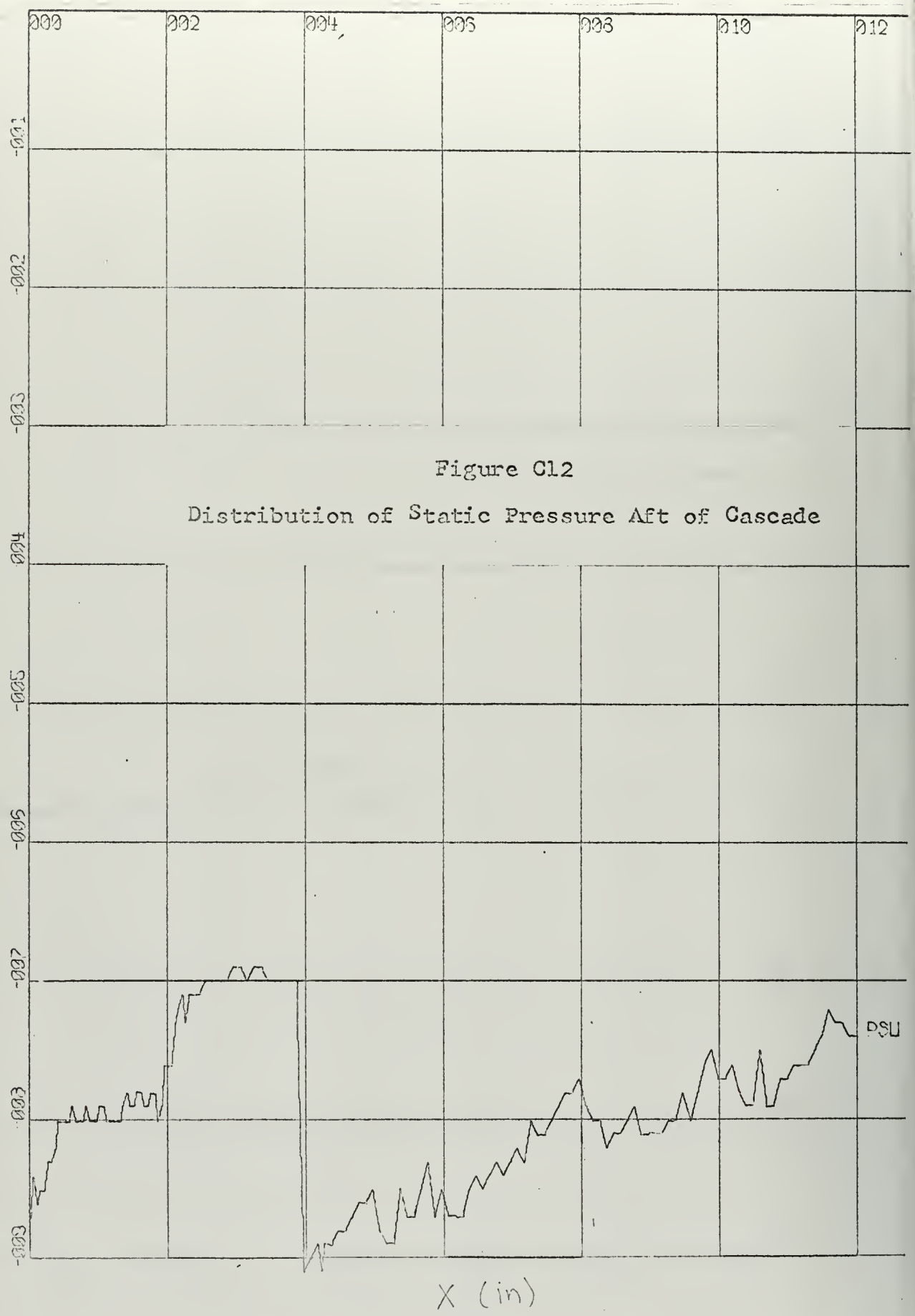

Figure C12

Distribution of Static Pressure Aft of Cascade

X-SCALE = 2.00E+00 UNITS/INCH.
Y-SCALE = 1.00E-01 UNITS/INCH.

RUN 301

STATOR PROFILES

Table C3

PROPULSION LABORATORY
U.S. NAVAL POSTGRADUATE SCHOOL

TEST RUN NO. 302

BAROMETRIC PRESS. = 30.05 IN. HG.

PLENUM TEMP. = 66.7 DEG. F.

STAGGER ANGLE = -4.50DEG.

SOLIDITY = 1.66

BLADE PROFILE =

FAR AHEAD (STATION 0)				FAR AFT (STATION 3)			
V0 (FT/SEC)	ALPHA 0 (DEG)	PT0 (PSF)	PS0 (PSF)	V3 (FT/SEC)	ALPHA 3 (DEG)	PT3 (PSF)	PS3 (PSF)
213.083	62.44	2256.3	2200.1	337.273	-71.88	2246.7	2108.5

CONDITIONS AT THE MEASURING PLANES

LOWER TRAVERSE (STATION 1)		UPPER TRAVERSE (STATION 2)	
PT1 (PSF)	PS1 (PSF)	PT2 (PSF)	PS2 (PSF)
2256.3	2200.1	2246.9	2108.5

FORCES ON THE BLADES IN LBS. PER FT.

AXIAL	TANGENTIAL	LIFT	DRAG
29.78	41.85	51.32	2.27

TOTAL TURNING ANGLE OF THE FLOW (DEG) = 134.33

RUN NO. = 302 CONCLUDED

LOSS COEFFICIENT , MIXING LOSS INCLUDED = .06316

LIFT AND DRAG COEFFICIENTS BASED ON
THE VECTORIAL MEAN OF V0 AND V3

CL	CD
5.2188	.2313

LIFT AND DRAG COEFFICIENTS BASED ON
CONDITIONS FAR AHEAD OF THE CASCADE

CL0	CD0
1.6614	.0736

CONSTRICTION FACTOR = .9701

DELTA X LOWER = 12.00

DELTA X UPPER = 12.00

DENSITY(SLUGS PER CU.FT.) FAR AHEAD = .00245261

DENSITY(SLUGS PER CU.FT.) FAR AFT = .00237540

REYNOLDS NUMBER(CHORD) AND MACH NUMBER

REY	MO
1160648.	.1895

TIME, 5 MINUTES AND 18 SECONDS.

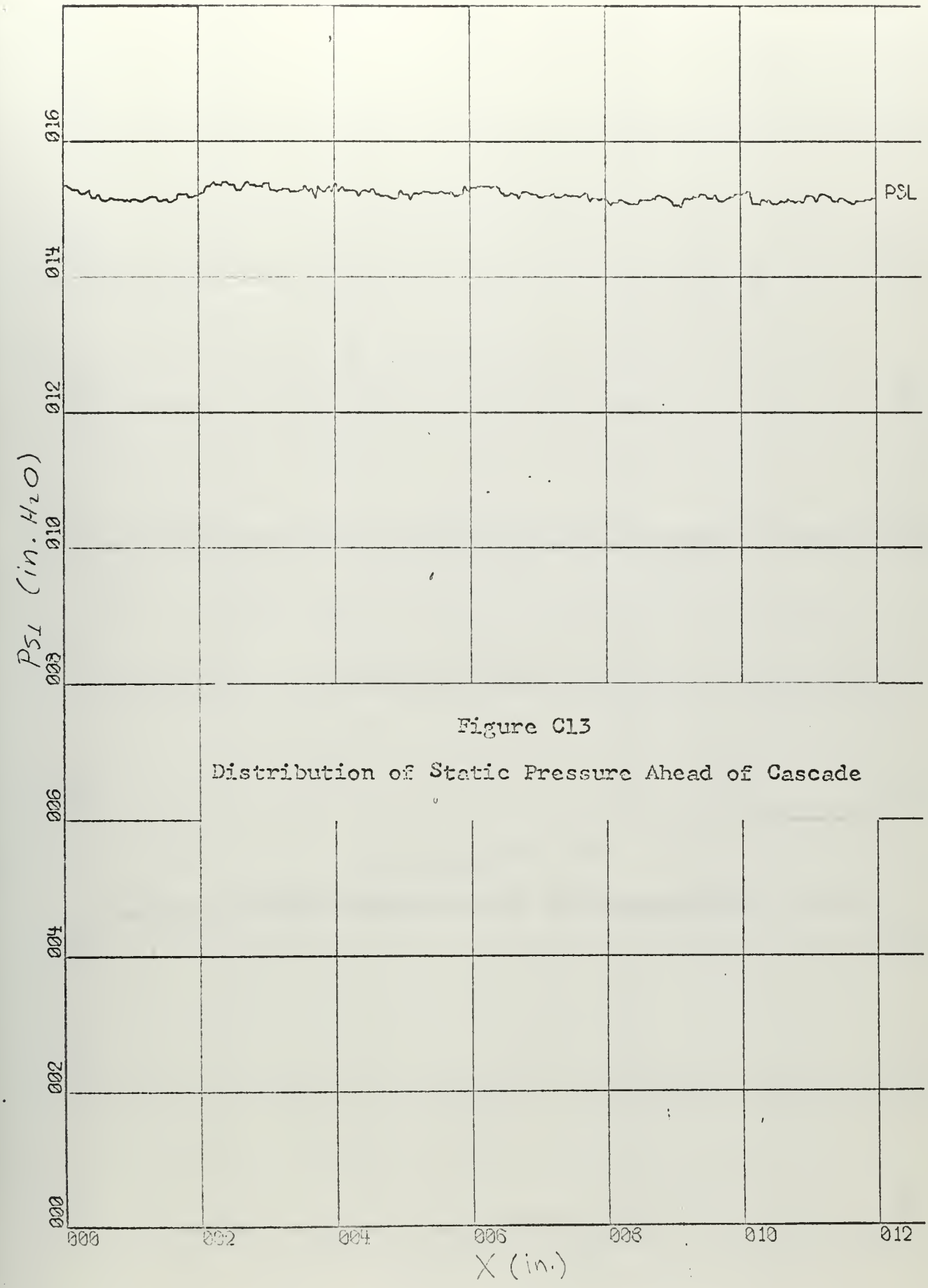

Figure C13

Distribution of Static Pressure Ahead of Cascade

X-SCALE = 2.00E+00 UNITS/INCH.
Y-SCALE = 2.00E+00 UNITS/INCH.

RUN 302 ROTOR PROFILES

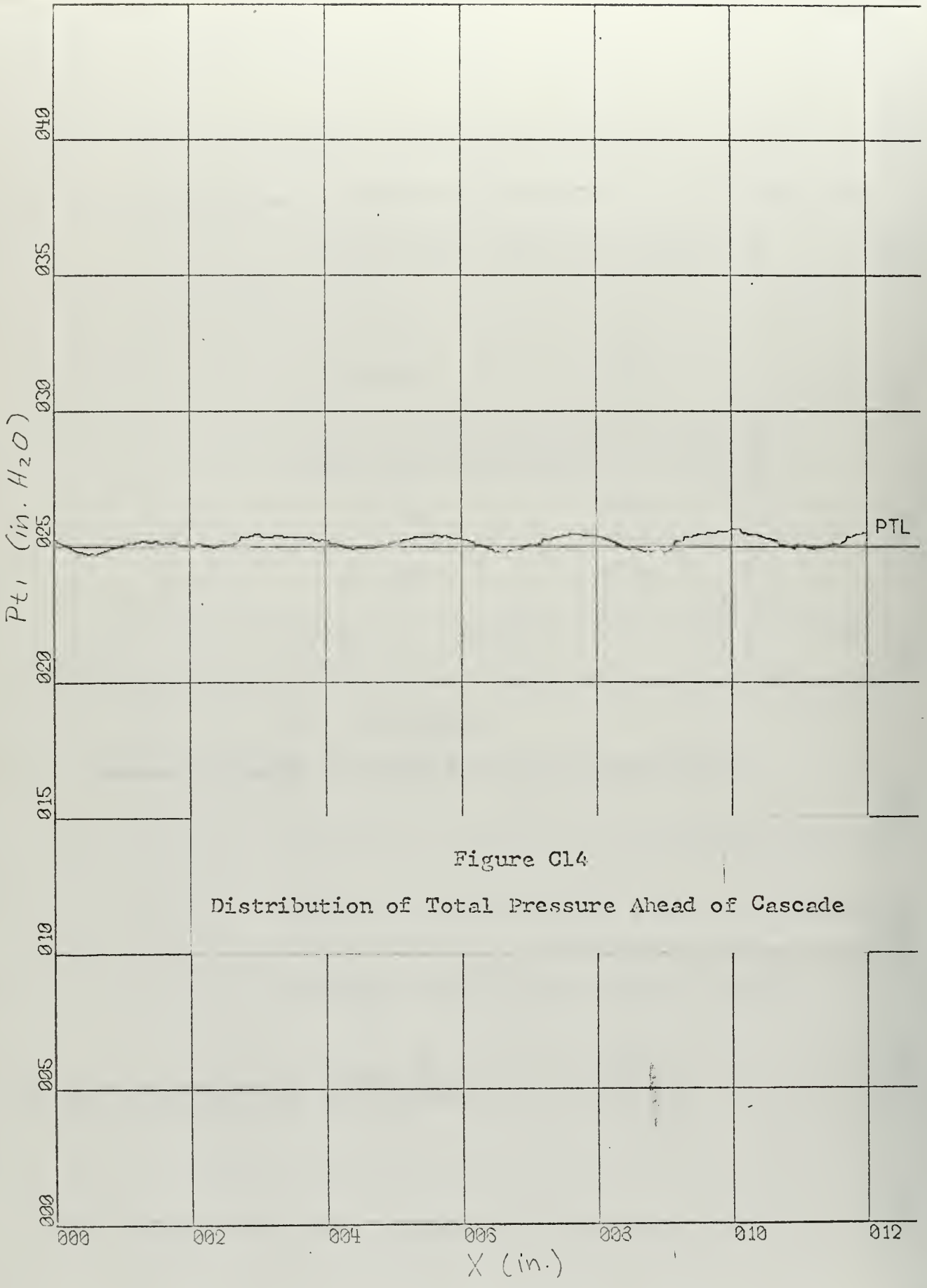

Figure C14

Distribution of Total Pressure Ahead of Cascade

X-SCALE = 2.00E+00 UNITS/INCH.
Y-SCALE = 5.00E+00 UNITS/INCH.

RUN 302 ROTOR PROFILES

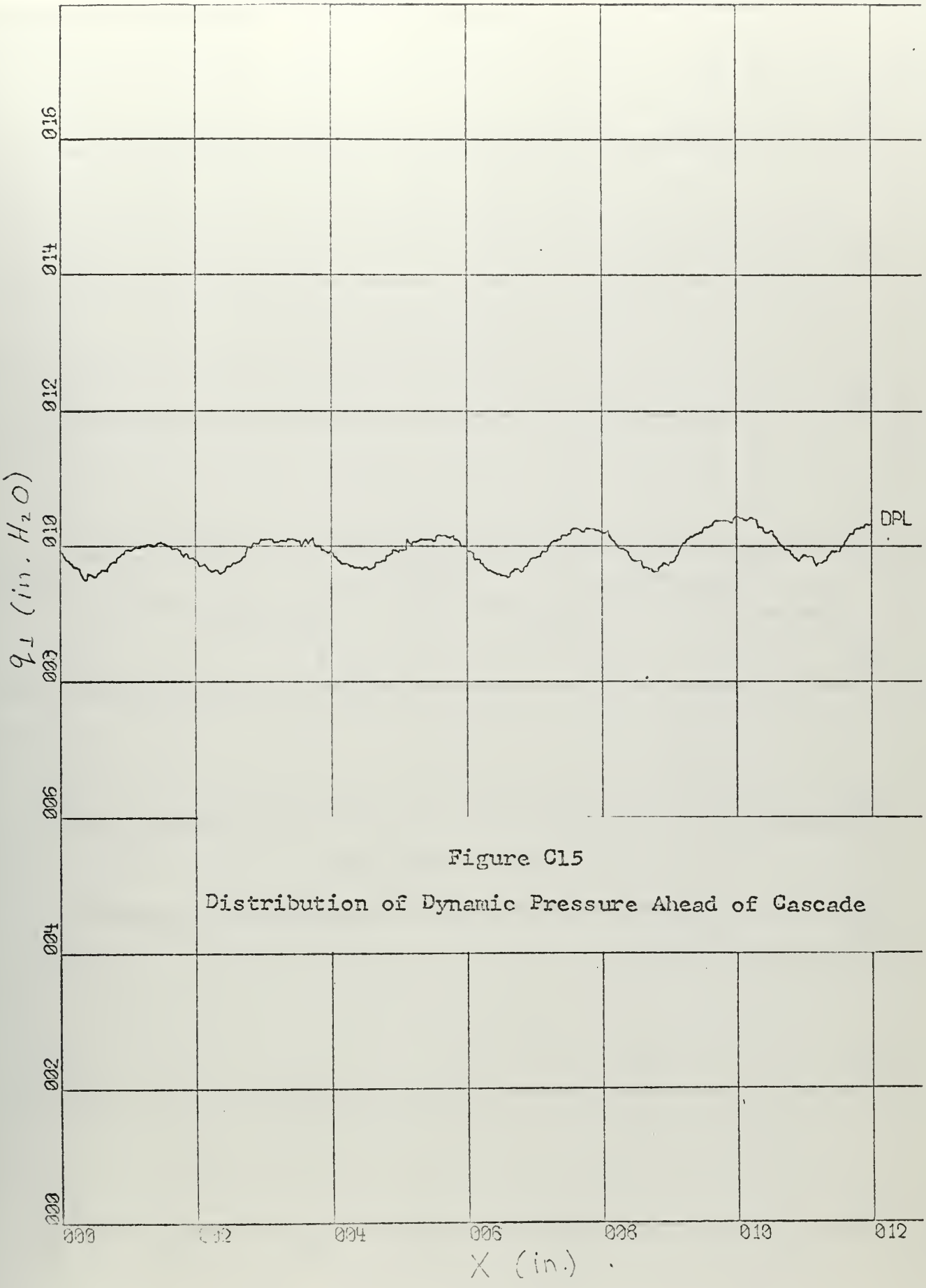

Figure C15

Distribution of Dynamic Pressure Ahead of Cascade

K-SCALE = 2.00E+00 UNITS/INCH.
Y-SCALE = 2.00E+00 UNITS/INCH.

RUN 302 ROTOR PROFILES

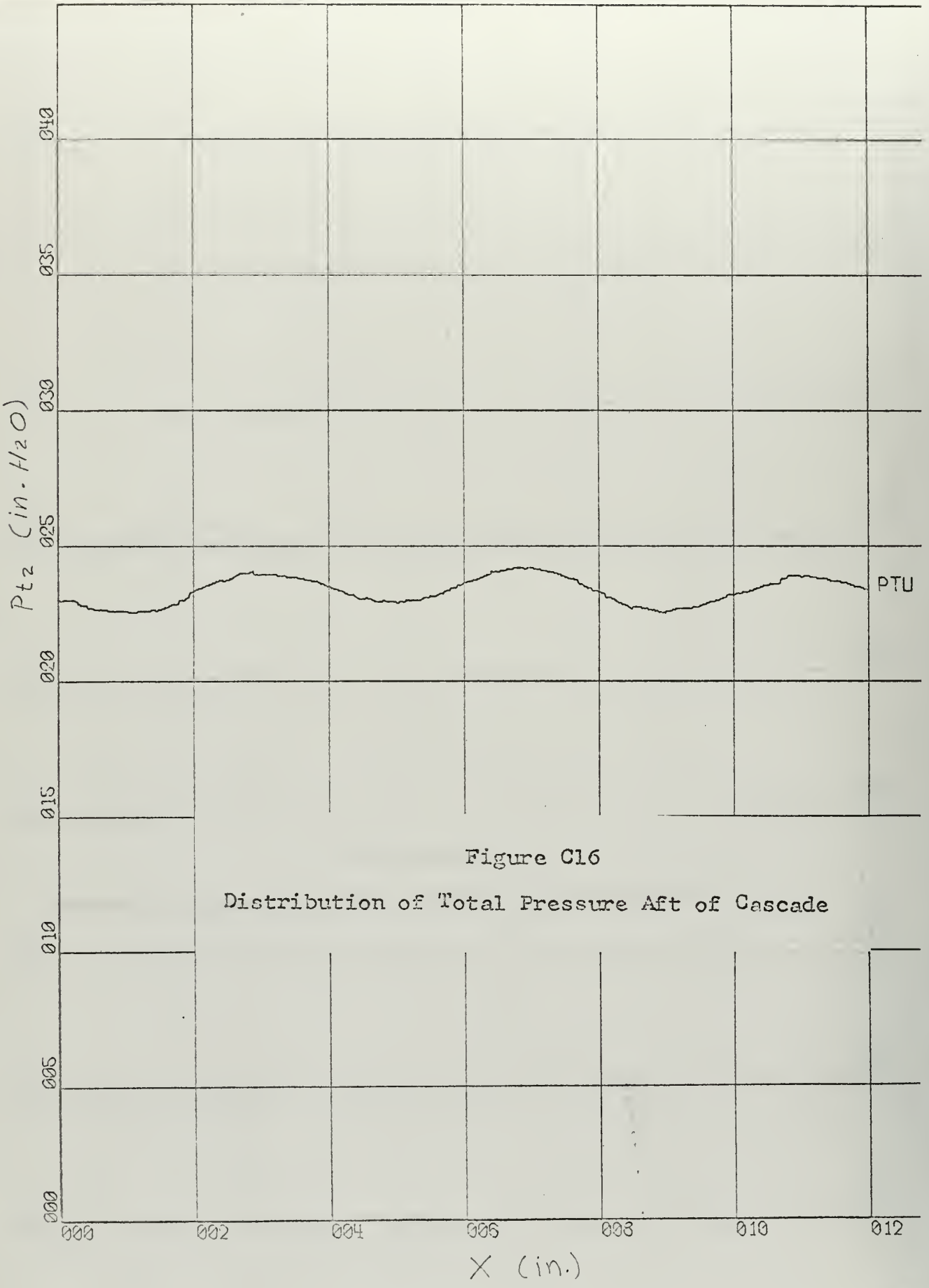

Figure C16

Distribution of Total Pressure Aft of Cascade

X-SCALE = 2.00E+00 UNITS/INCH.
Y-SCALE = 5.00E+00 UNITS/INCH.

RUN 302 ROTOR PROFILES

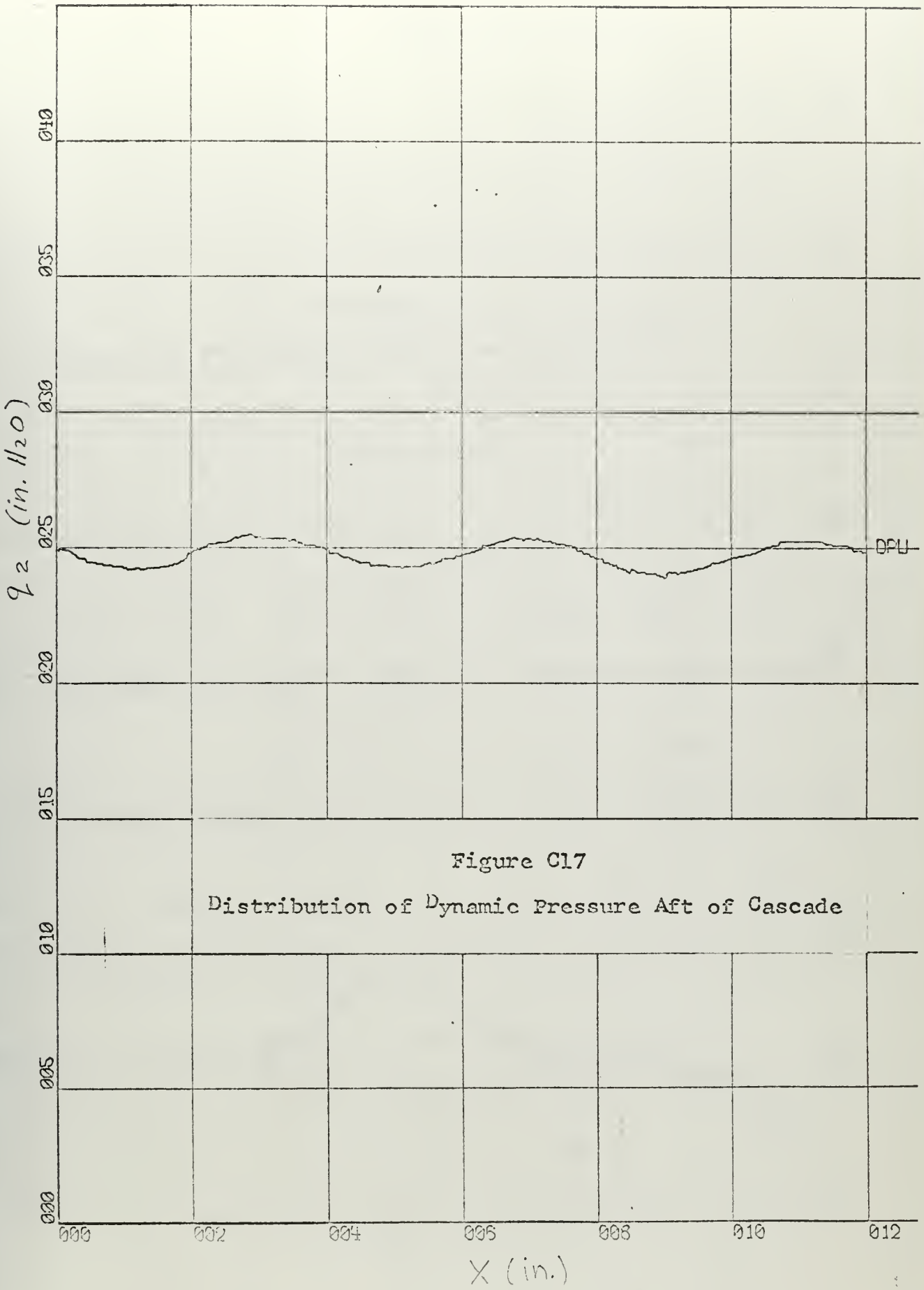

Figure C17

Distribution of Dynamic Pressure Aft of Cascade

X-SCALE = 2.00E+00 UNITS/INCH.
Y-SCALE = 5.00E+00 UNITS/INCH.

RUN 302 ROTOR PROFILES

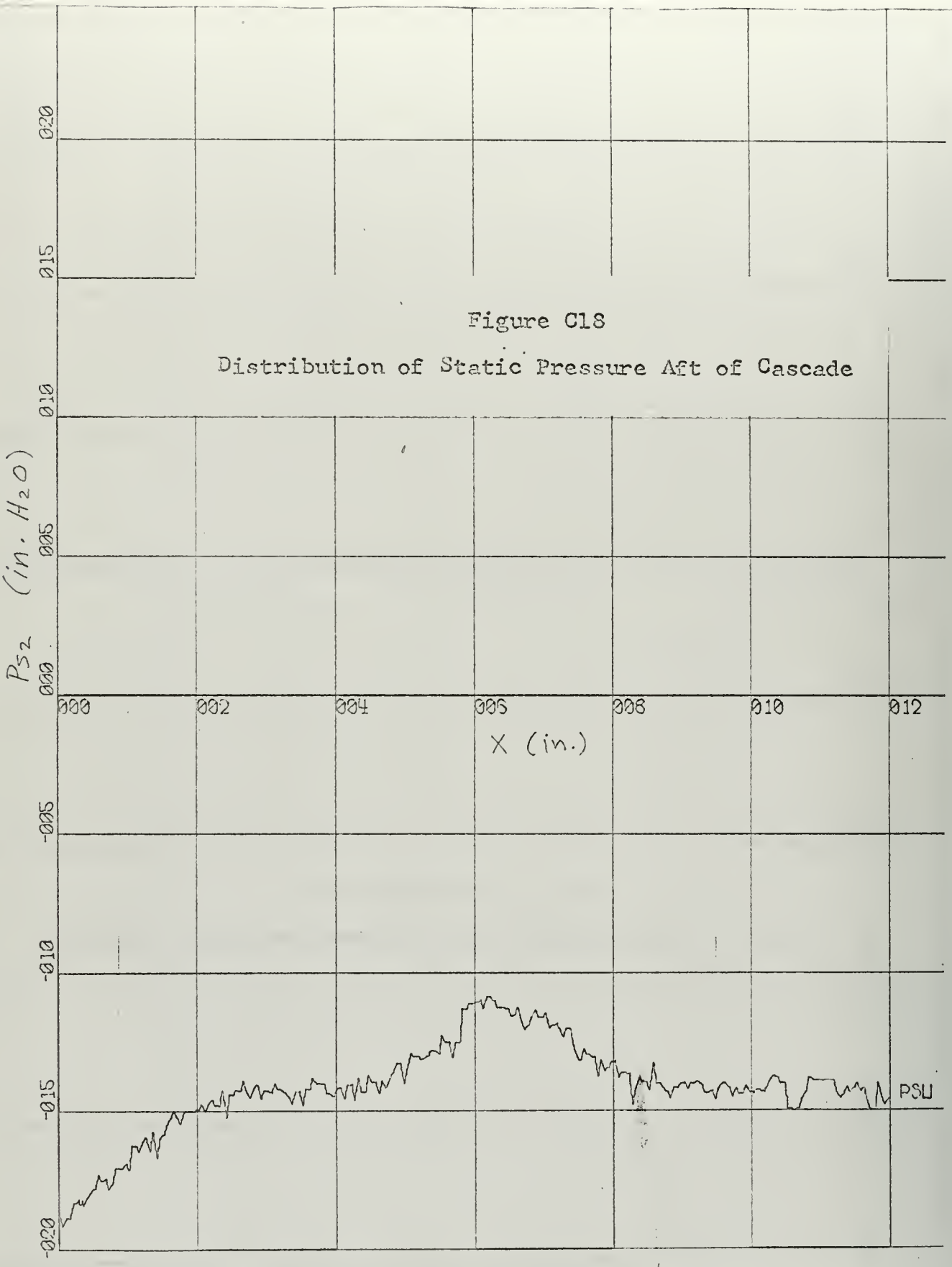

Figure C18

Distribution of Static Pressure Aft of Cascade

X-SCALE = 2.00E+00 UNITS/INCH.

Y-SCALE = 5.00E-01 UNITS/INCH.

RUN 302 ROTOR PROFILES

Table C4

PROPULSION LABORATORY
U.S. NAVAL POSTGRADUATE SCHOOL

TEST RUN NO. 303

BAROMETRIC PRESS. = 30.05 IN. HG.

PLENUM TEMP. = 68.0 DEG. F.

STAGGER ANGLE = -4.50DEG.

SOLIDITY = 1.66

BLADE PROFILE =

FAR AHEAD (STATION 0)				FAR AFT (STATION 3)			
V0 (FT/SEC)	ALPHA 0 (DEG)	PT0 (PSF)	PS0 (PSF)	V3 (FT/SEC)	ALPHA 3 (DEG)	PT3 (PSF)	PS3 (PSF)
238.464	66.23	2256.5	2186.5	336.382	-71.59	2247.2	2109.9

CONDITIONS AT THE MEASURING PLANES

LOWER TRAVERSE (STATION 1)		UPPER TRAVERSE (STATION 2)	
PT1 (PSF)	PS1 (PSF)	PT2 (PSF)	PS2 (PSF)
2256.5	2186.5	2247.3	2109.9

FORCES ON THE BLADES IN LBS. PER FT.

AXIAL	TANGENTIAL	LIFT	DRAG
24.08	43.83	49.97	1.99

TOTAL TURNING ANGLE OF THE FLOW (DEG) = 137.82

RUN NO. = 303 CONCLUDED

LOSS COEFFICIENT , MIXING LOSS INCLUDED = .06190

LIFT AND DRAG COEFFICIENTS BASED ON
THE VECTORIAL MEAN OF V0 AND V3

CL	CD
5.8628	.2333

LIFT AND DRAG COEFFICIENTS BASED ON
CONDITIONS FAR AHEAD OF THE CASCADE

CL0	CD0
1.3007	.0518

CONSTRICTION FACTOR = .9291

DELTA X LOWER = 12.00

DELTA X UPPER = 12.00

DENSITY(SLUGS PER CU.FT.) FAR AHEAD = .00243577

DENSITY(SLUGS PER CU.FT.) FAR AFT = .00237080

REYNOLDS NUMBER(CHORD) AND MACH NUMBER

REY	MO
1153177.	.2118

TIME, 5 MINUTES AND 17 SECONDS

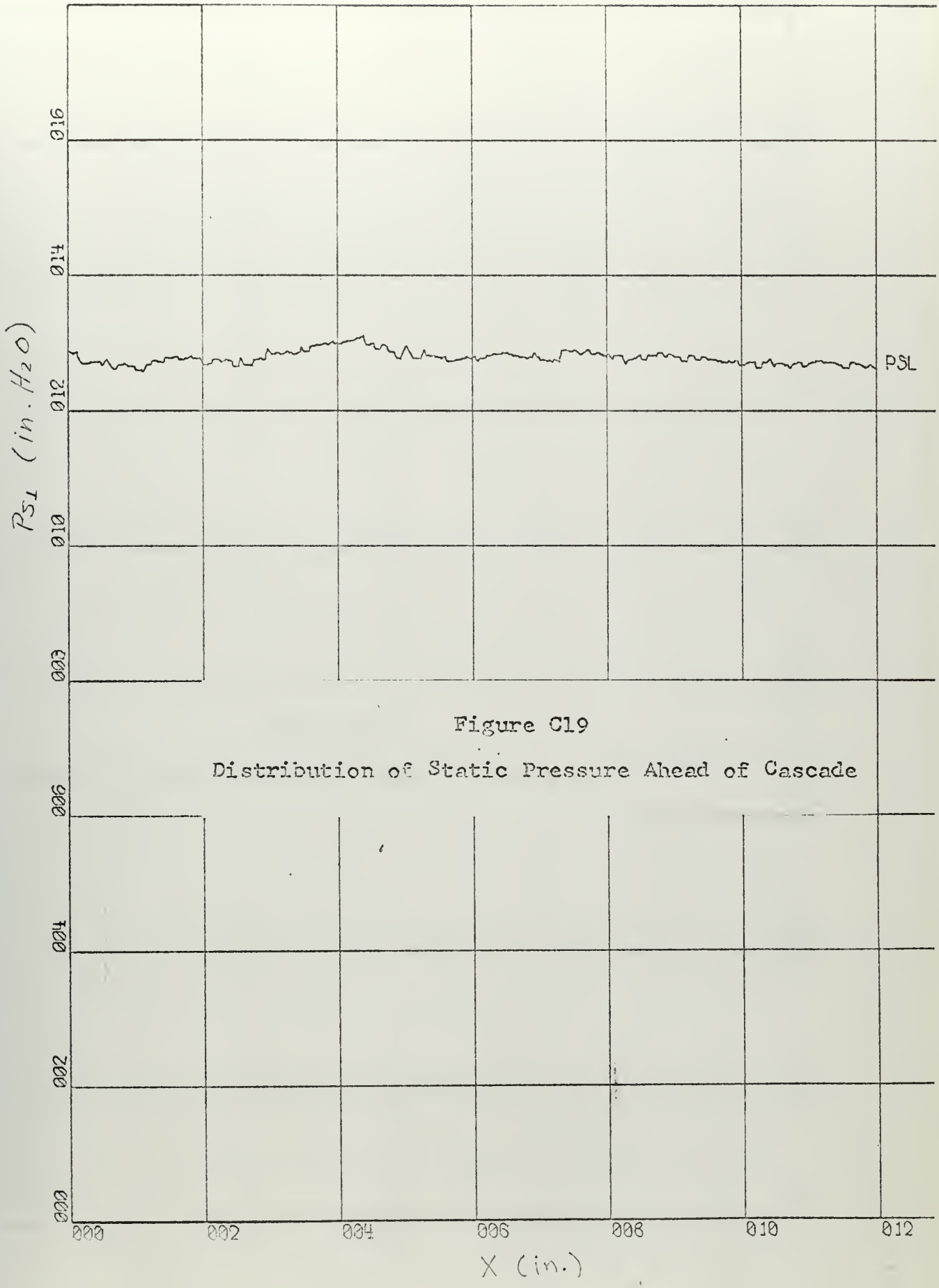

Figure C19

Distribution of Static Pressure Ahead of Cascade

K-SCALE = 2.00E+00 UNITS/INCH.
Y-SCALE = 2.00E+00 UNITS/INCH.

RUN 303

ROTOR PROFILES

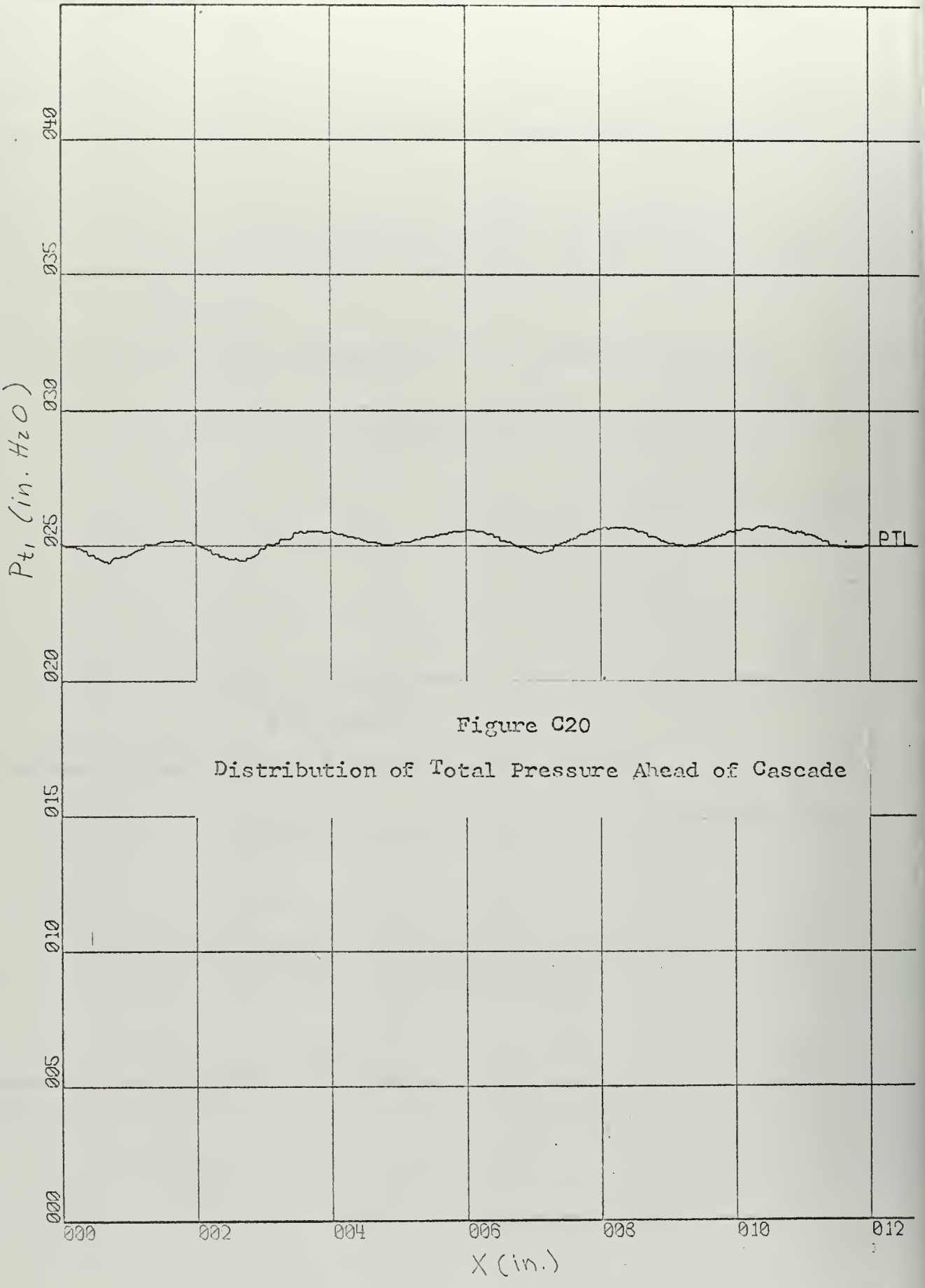

Figure C20

Distribution of Total Pressure Ahead of Cascade

X-SCALE = 2.00E+00 UNITS/INCH.
Y-SCALE = 5.00E+00 UNITS/INCH.

RUN 303 ROTOR PROFILES

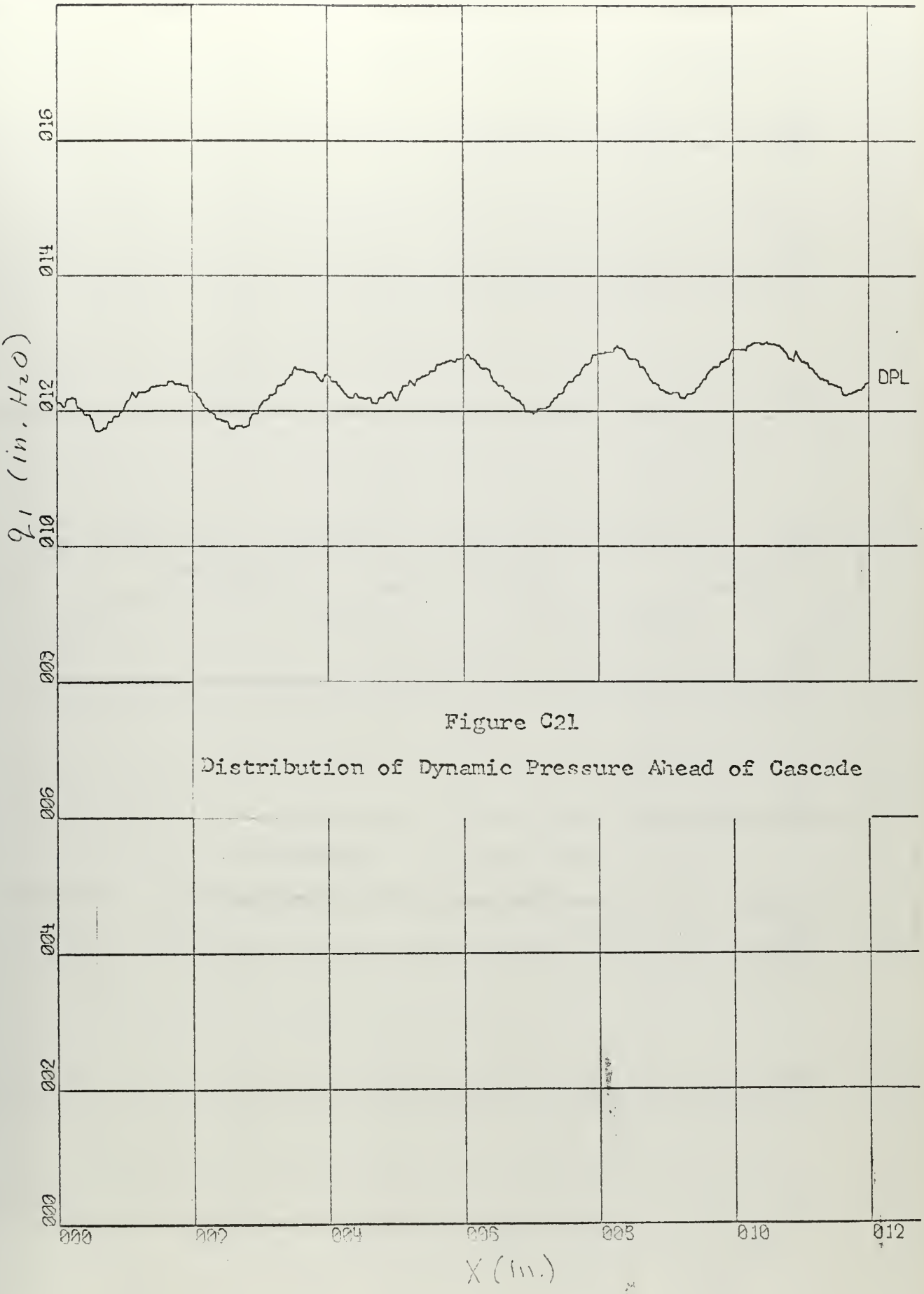

Figure C21

Distribution of Dynamic Pressure Ahead of Cascade

X-SCALE = 2.00E+00 UNITS/INCH.
Y-SCALE = 2.00E+00 UNITS/INCH.

RUN 303 ROTOR PROFILES

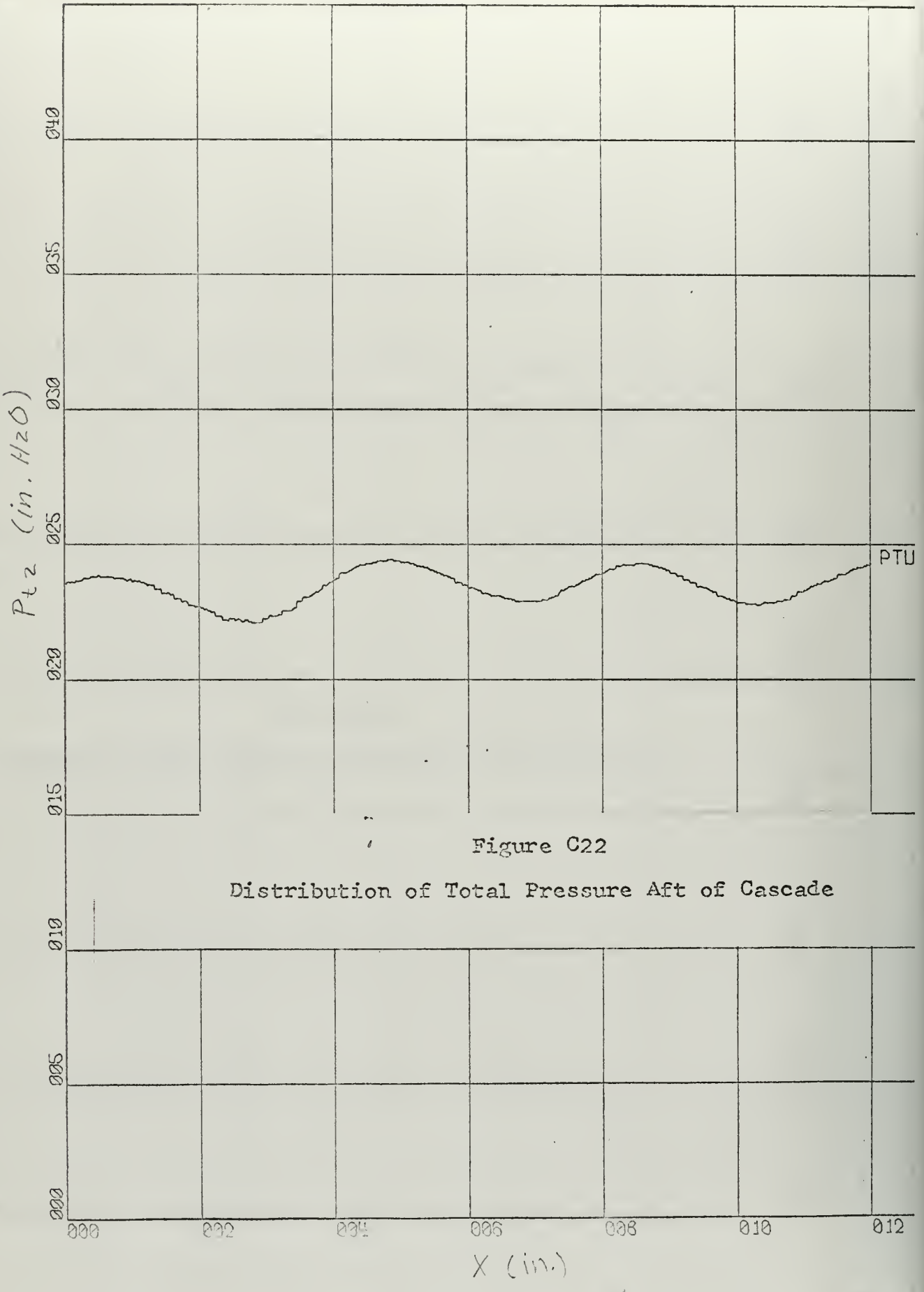

Figure C22

Distribution of Total Pressure Aft of Cascade

K-SCALE = 2.00E+00 UNITS/INCH.
Y-SCALE = 5.00E+00 UNITS/INCH.

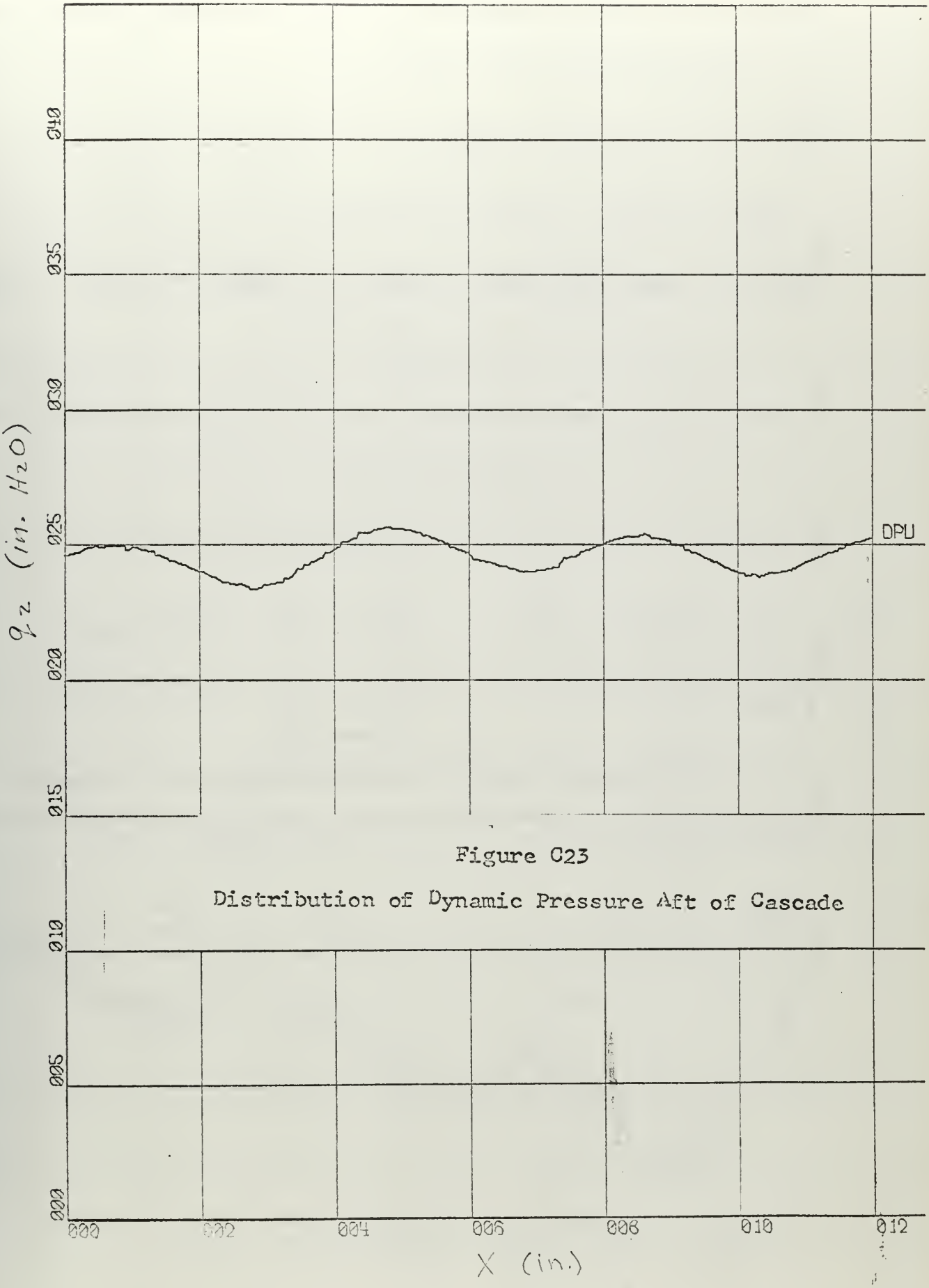

Figure C23

Distribution of Dynamic Pressure Aft of Cascade

K-SCALE = 2.00E+00 UNITS/INCH.
Y-SCALE = 5.00E+00 UNITS/INCH.

RUN 303

ROTOR PROFILES

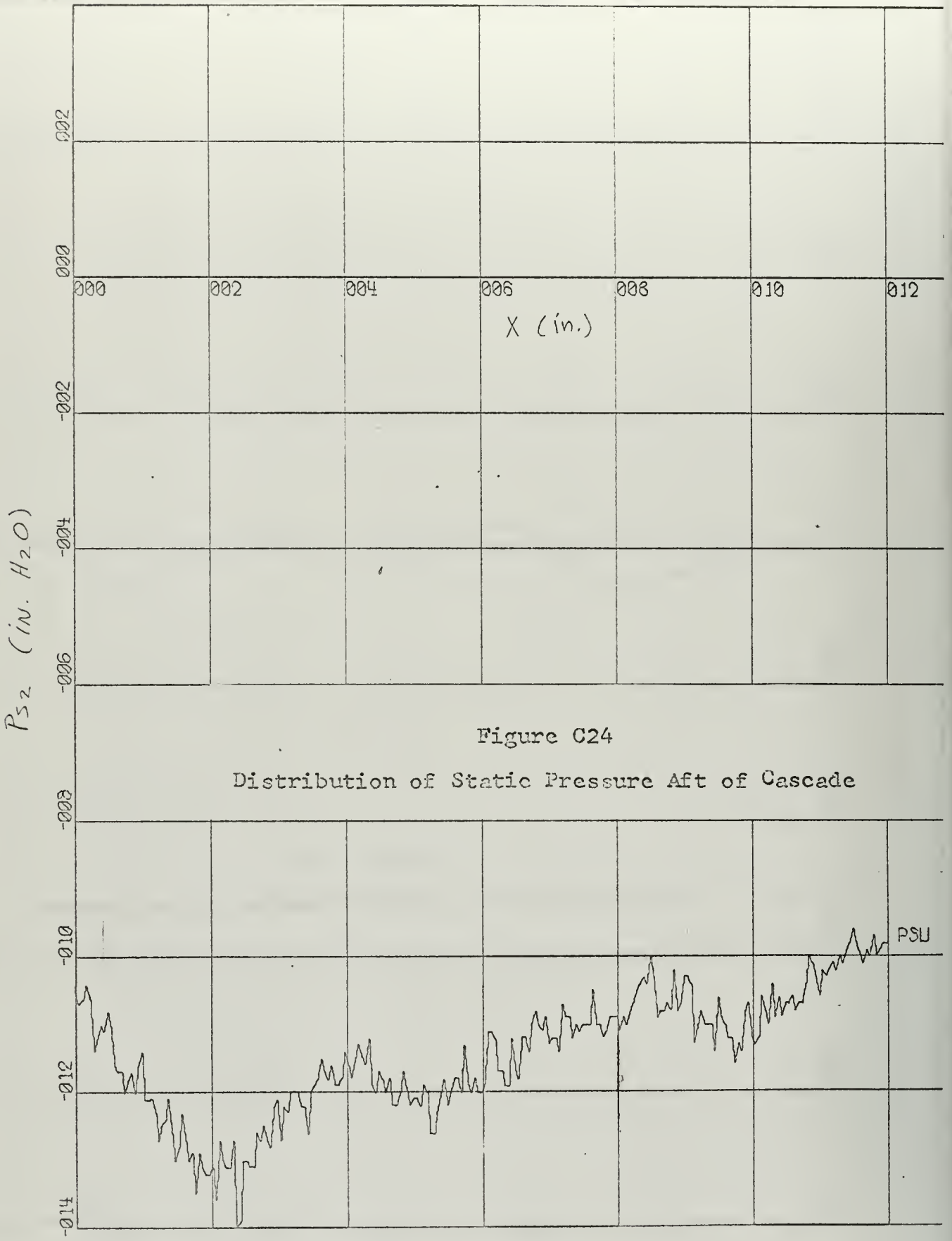

Figure C24

Distribution of Static Pressure Aft of Cascade

X-SCALE = 2.00E+00 UNITS/INCH.
Y-SCALE = 2.00E-01 UNITS/INCH.

RUN 303

Table C5

PROPULSION LABORATORY
U.S. NAVAL POSTGRADUATE SCHOOL

TEST RUN NO. 304

BAROMETRIC PRESS. = 30.10 IN. HG.

PLENUM TEMP. = 71.8 DEG. F.

STAGGER ANGLE = -4.50DEG.

SOLIDITY = 1.66

BLADE PROFILE =

FAR AHEAD (STATION 0)				FAR AFT (STATION 3)			
V0 (FT/SEC)	ALPHA 0 (DEG)	PT0 (PSF)	PS0 (PSF)	V3 (FT/SEC)	ALPHA 3 (DEG)	PT3 (PSF)	PS3 (PSF)
183.870	59.37	2258.4	2216.8	330.799	-72.41	2246.8	2114.9

CONDITIONS AT THE MEASURING PLANES

LOWER TRAVERSE (STATION 1)		UPPER TRAVERSE (STATION 2)	
PT1 (PSF)	PS1 (PSF)	PT2 (PSF)	PS2 (PSF)
2258.4	2216.8	2246.9	2114.9

FORCES ON THE BLADES IN LBS. PER FT.

AXIAL	TANGENTIAL	LIFT	DRAG
33.26	36.85	49.57	2.62

TOTAL TURNING ANGLE OF THE FLOW (DEG) = 131.78

RUN NO. = 304 CONCLUDED

LOSS COEFFICIENT , MIXING LOSS INCLUDED = .08053

LIFT AND DRAG COEFFICIENTS BASED ON THE VECTORIAL MEAN OF V0 AND V3

CL	CD
4.7885	.2528

LIFT AND DRAG COEFFICIENTS BASED ON CONDITIONS FAR AHEAD OF THE CASCADE

CL0	CD0
2.1639	.1142

CONSTRICTION FACTOR = .9708

DELTA X LOWER = 12.00

DELTA X UPPER = 12.00

DENSITY(SLUGS PER CU.FT.) FAR AHEAD = .00244289

DENSITY(SLUGS PER CU.FT.) FAR AFT = .00235770

REYNOLDS NUMBER(CHORD) AND MACH NUMBER

REY	MO
1121636.	.1627

TIME, 4 MINUTES AND 0 SECONDS

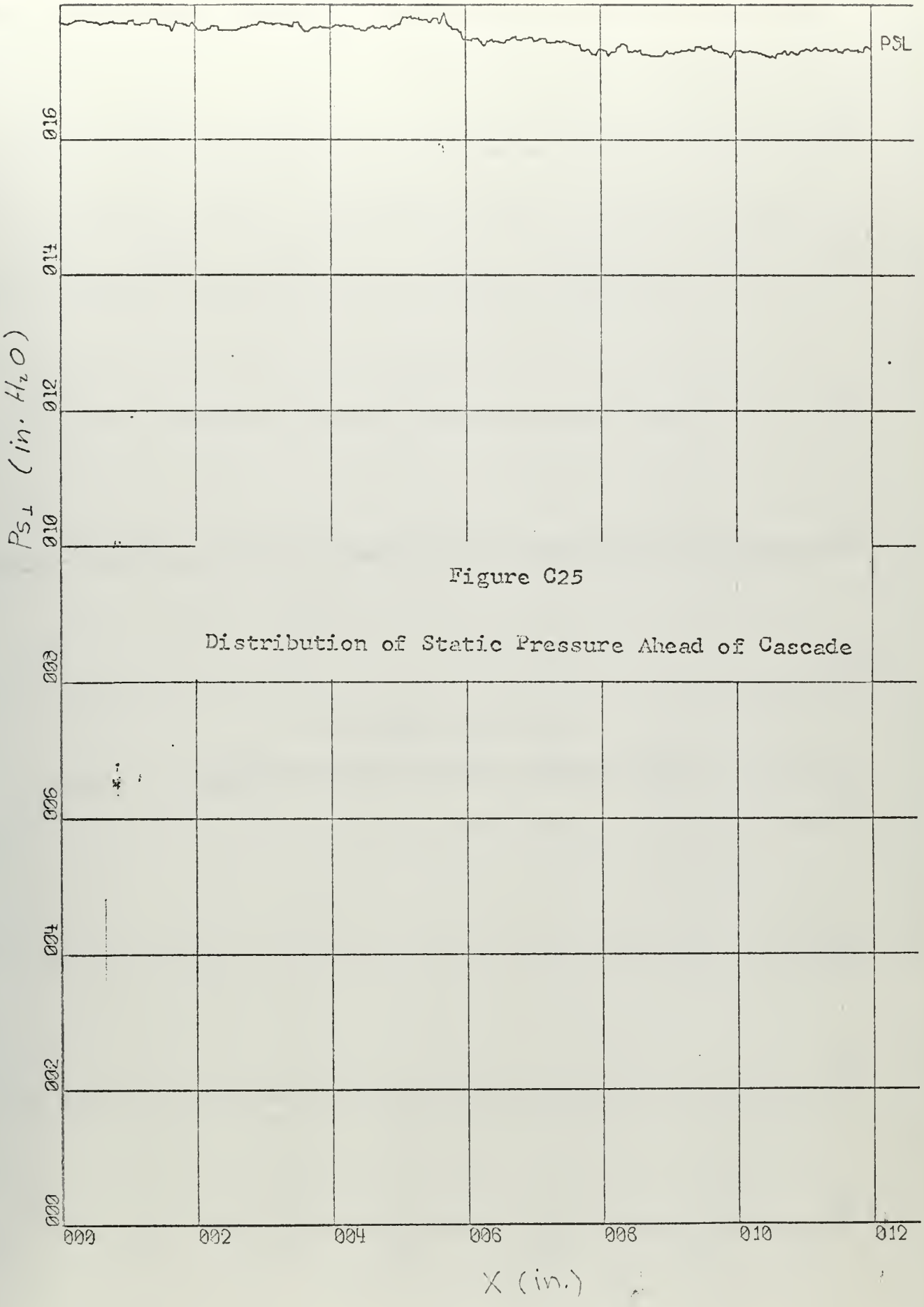

Figure C25

Distribution of Static Pressure Ahead of Cascade

X-SCALE = 2.00E+00 UNITS/INCH.
Y-SCALE = 2.00E+00 UNITS/INCH.

RUN 304 ROTOR PROFILES

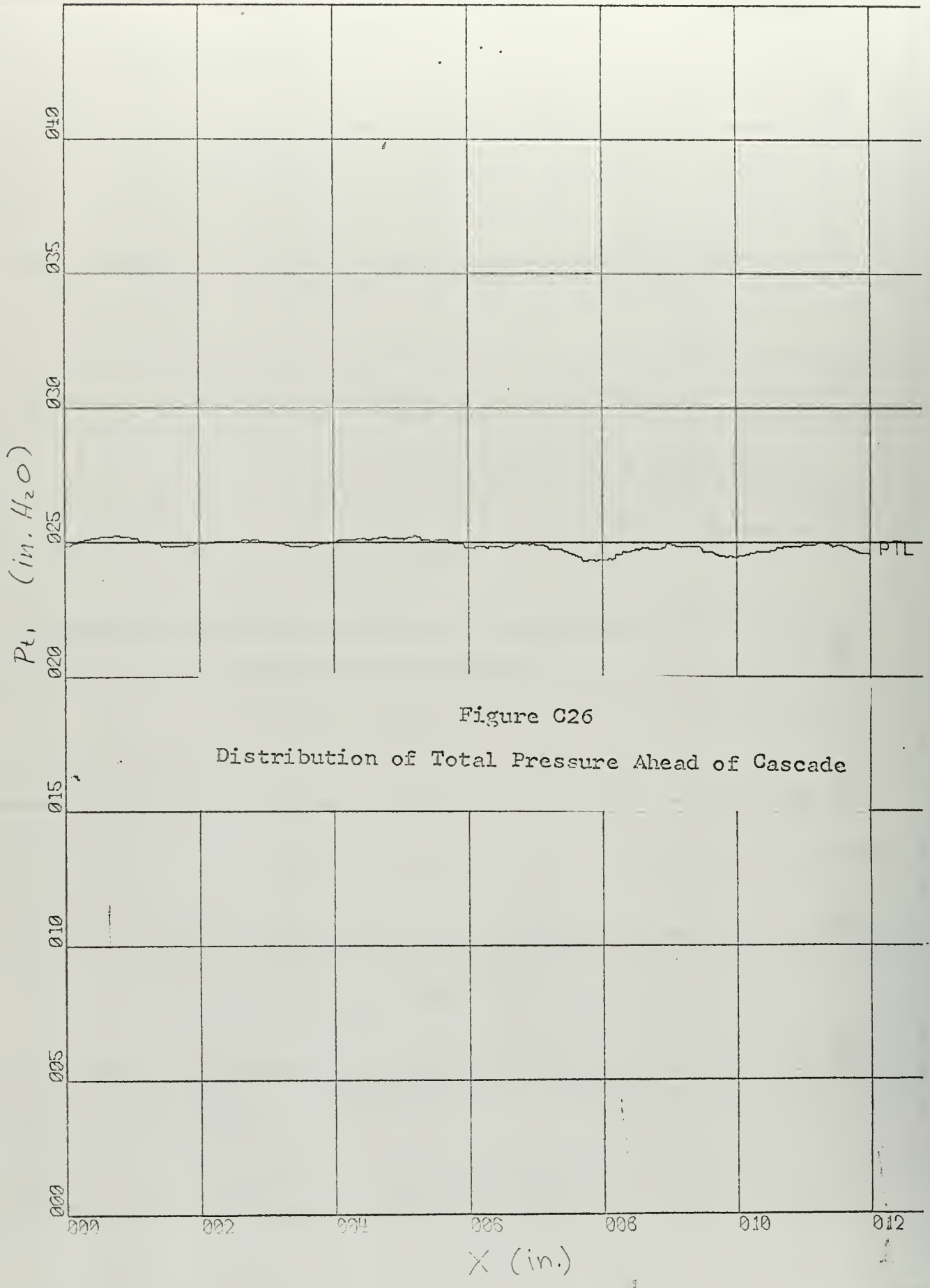

Figure C26

Distribution of Total Pressure Ahead of Cascade

X-SCALE = 2.00E+00 UNITS/INCH.
Y-SCALE = 5.00E+00 UNITS/INCH.

RUN 304 ROTOR PROFILES

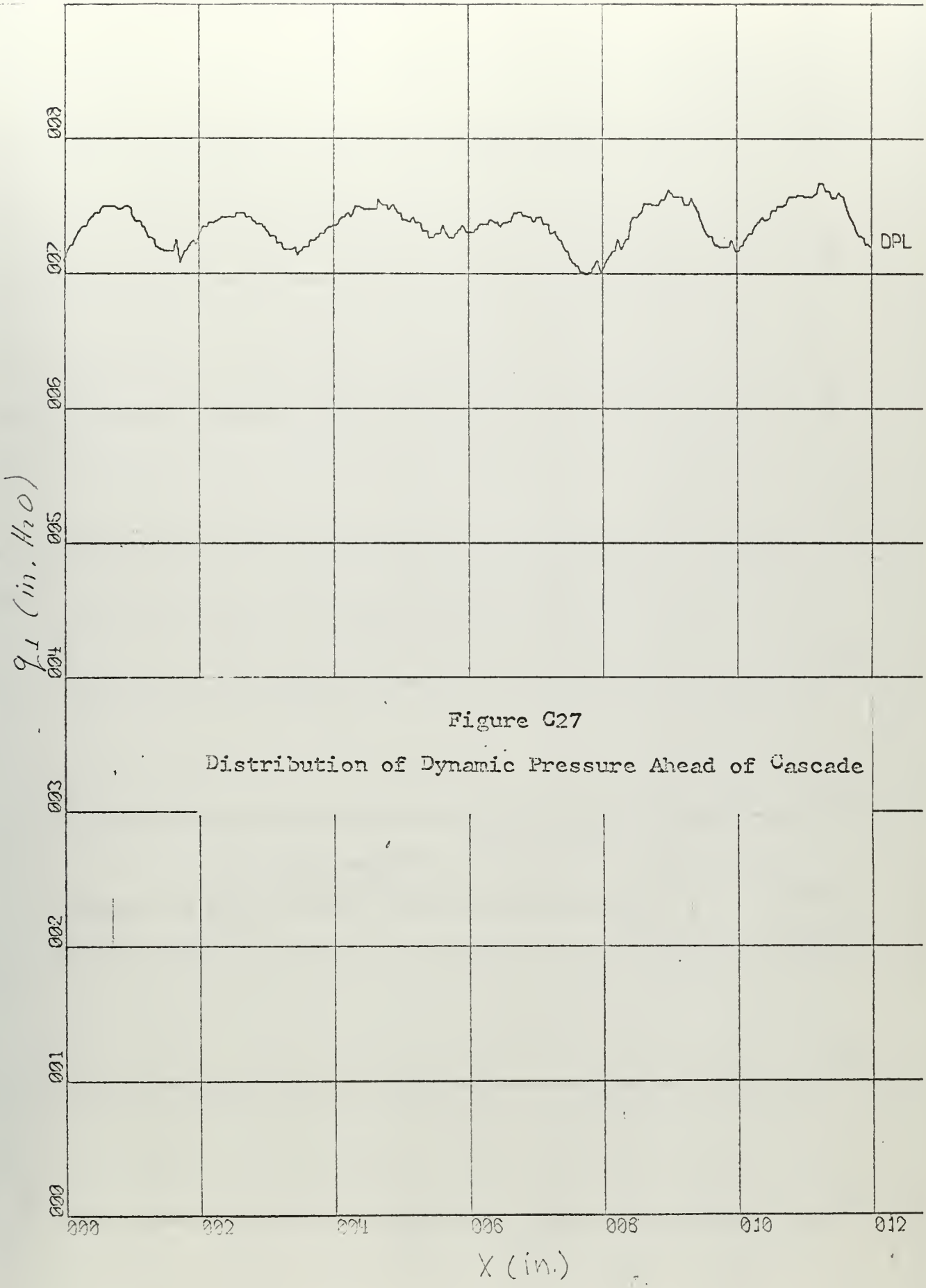

Figure C27

Distribution of Dynamic Pressure Ahead of Cascade

X-SCALE = 2.00E+00 UNITS/INCH.
Y-SCALE = 1.00E+00 UNITS/INCH.

RUN 304 ROTOR PROFILES

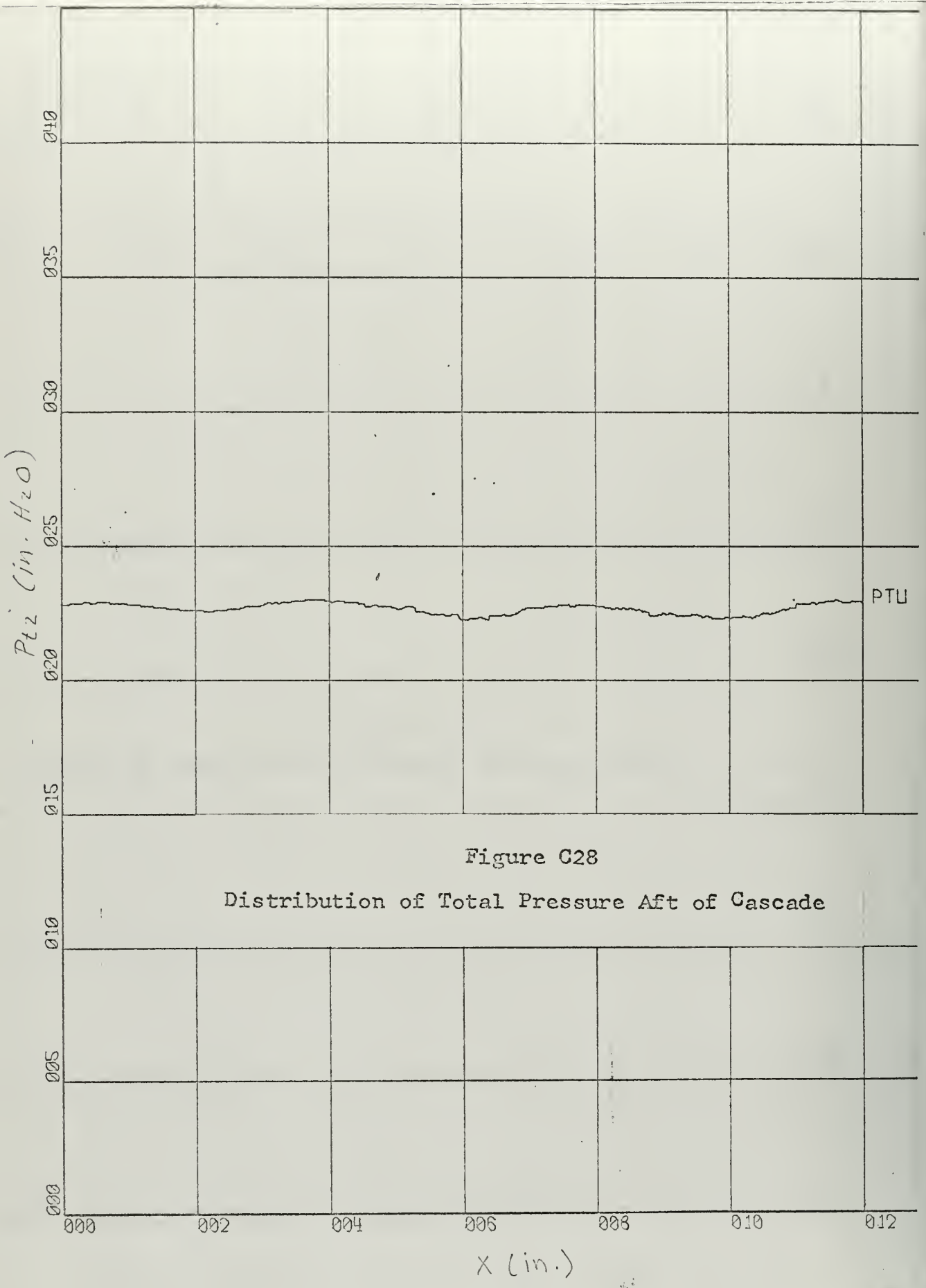

Figure C28

Distribution of Total Pressure Aft of Cascade

X-SCALE = 2.00E+00 UNITS/INCH.
Y-SCALE = 5.00E+00 UNITS/INCH.

RUN 304 ROTOR PROFILES

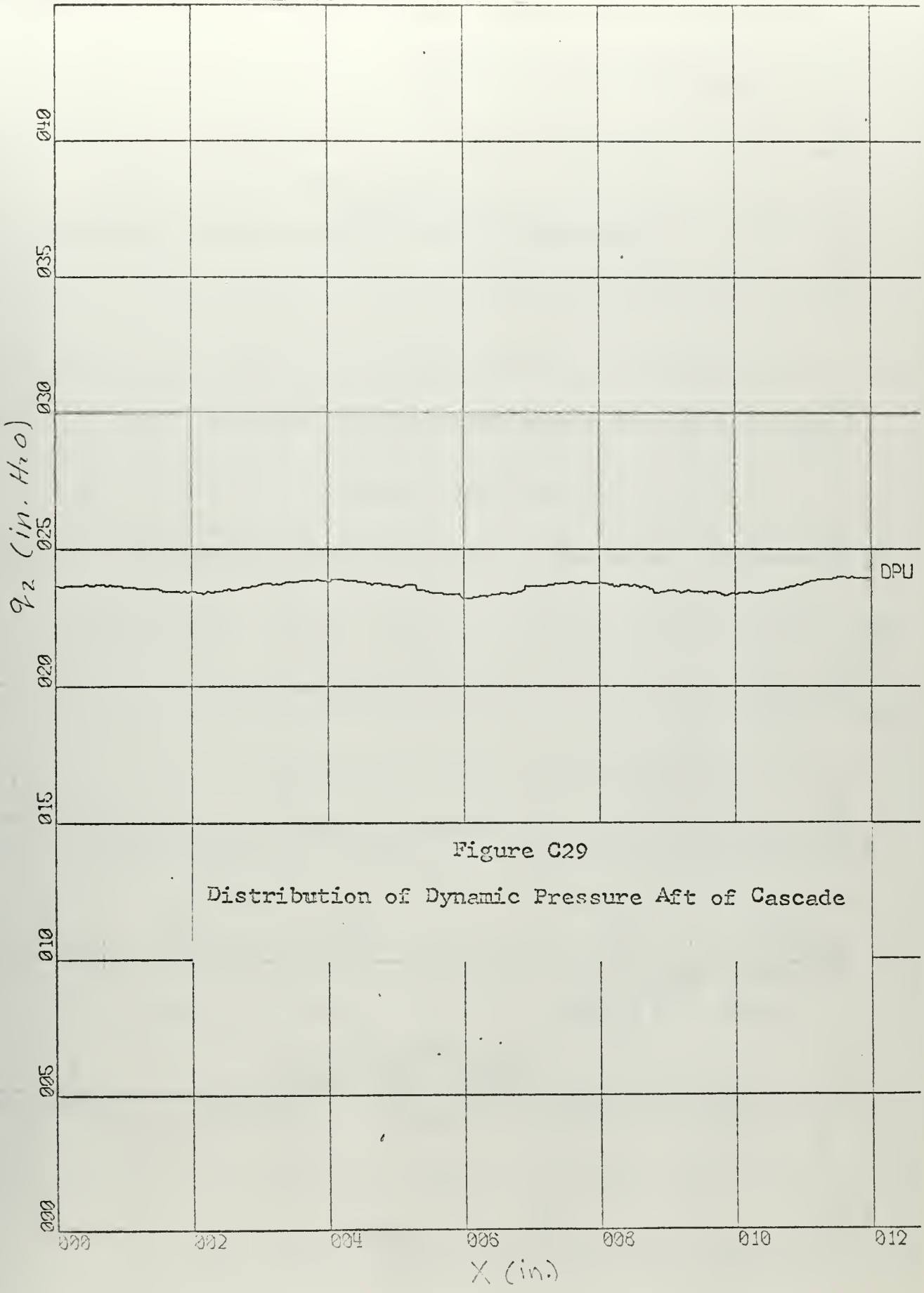

Figure C29

Distribution of Dynamic Pressure Aft of Cascade

X-SCALE = 2.00E+00 UNITS/INCH.
Y-SCALE = 5.00E+00 UNITS/INCH.

RUN 304 ROTOR PROFILES

Figure C30

Distribution of Static Pressure Aft of Cascade

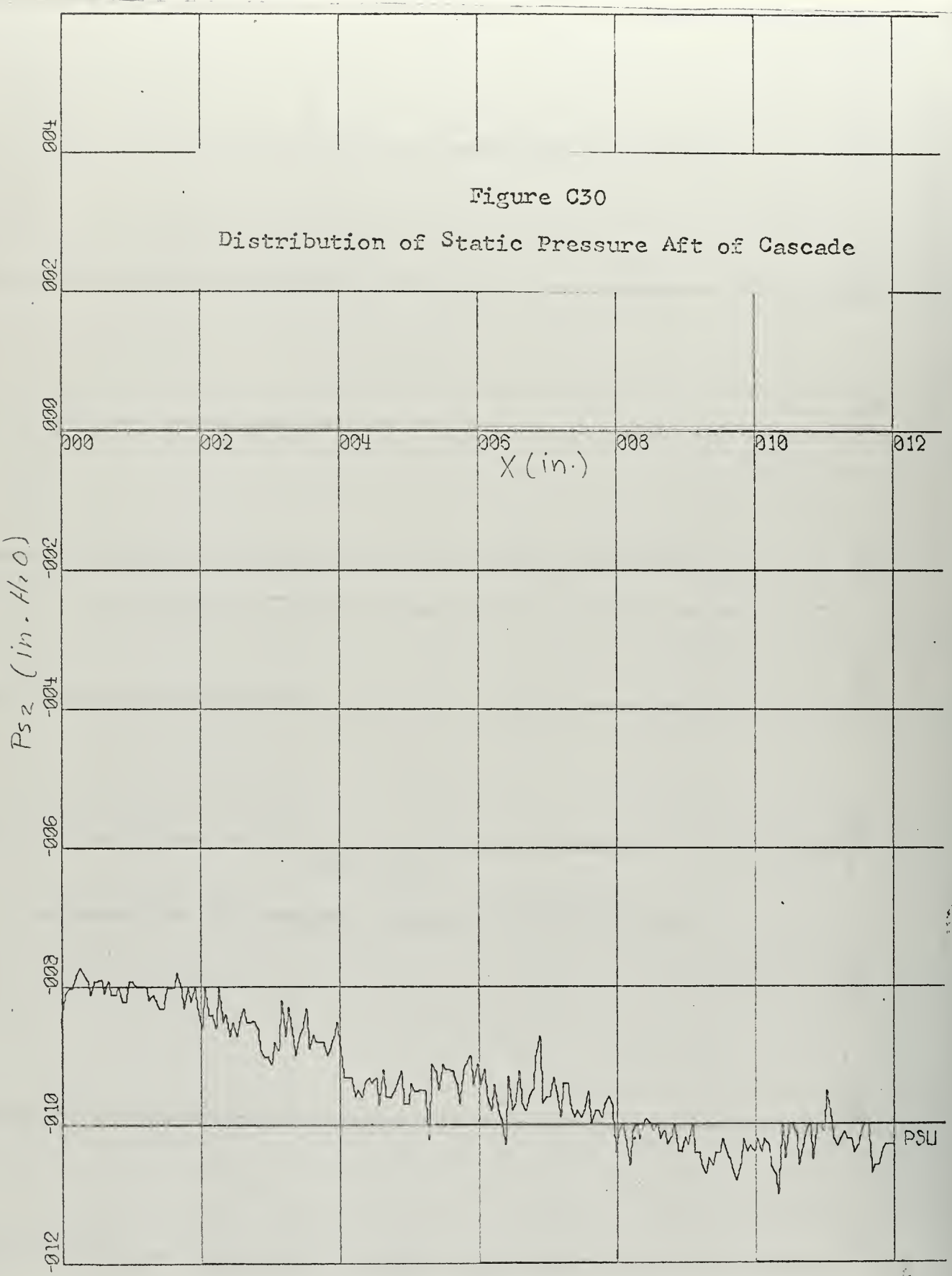

X-SCALE = 2.00E+00 UNITS/INCH.

Y-SCALE = 2.00E-01 UNITS/INCH.

RUN 304 ROTOR PROFILES

Table C6

PROPULSION LABORATORY
U.S. NAVAL POSTGRADUATE SCHOOL

TEST RUN NO. 305

BAROMETRIC PRESS. = 29.79 IN. HG.

PLENUM TEMP. = 71.0 DEG. F.

STAGGER ANGLE = -4.50DEG.

SOLIDITY = 1.66

BLADE PROFILE =

FAR AHEAD (STATION 0)				FAR AFT (STATION 3)			
V0 (FT/SEC)	ALPHA 0 (DEG)	PT0 (PSF)	PS0 (PSF)	V3 (FT/SEC)	ALPHA 3 (DEG)	PT3 (PSF)	PS3 (PSF)
168.254	56.12	2237.9	2203.3	334.858	-71.95	2222.7	2088.8

CONDITIONS AT THE MEASURING PLANES

LOWER TRAVERSE (STATION 1)		UPPER TRAVERSE (STATION 2)	
PT1 (PSF)	PS1 (PSF)	PT2 (PSF)	PS2 (PSF)
2237.9	2203.3	2222.8	2088.9

FORCES ON THE BLADES IN LBS. PER FT.

AXIAL	TANGENTIAL	LIFT	DRAG
36.89	36.30	51.67	3.01

TOTAL TURNING ANGLE OF THE FLOW (DEG) = 128.07

RUN NO. = 305 CONCLUDED

LOSS COEFFICIENT , MIXING LOSS INCLUDED = .10345

LIFT AND DRAG COEFFICIENTS BASED ON
THE VECTORIAL MEAN OF V0 AND V_3

CL	CD
4.4094	.2567

LIFT AND DRAG COEFFICIENTS BASED ON
CONDITIONS FAR AHEAD OF THE CASCADE

CL0	CD0
2.7086	.1577

CONSTRICTION FACTOR = .9412

DELTA X LOWER = 12.00

DELTA X UPPER = 12.00

DENSITY(SLUGS PER CU.FT.) FAR AHEAD = .00242951

DENSITY(SLUGS PER CU.FT.) FAR AFT = .00233320

REYNOLDS NUMBER(CHORD) AND MACH NUMBER

REY	MO
1124886.	.1490

TIME, 4 MINUTES AND 35 SECONDS

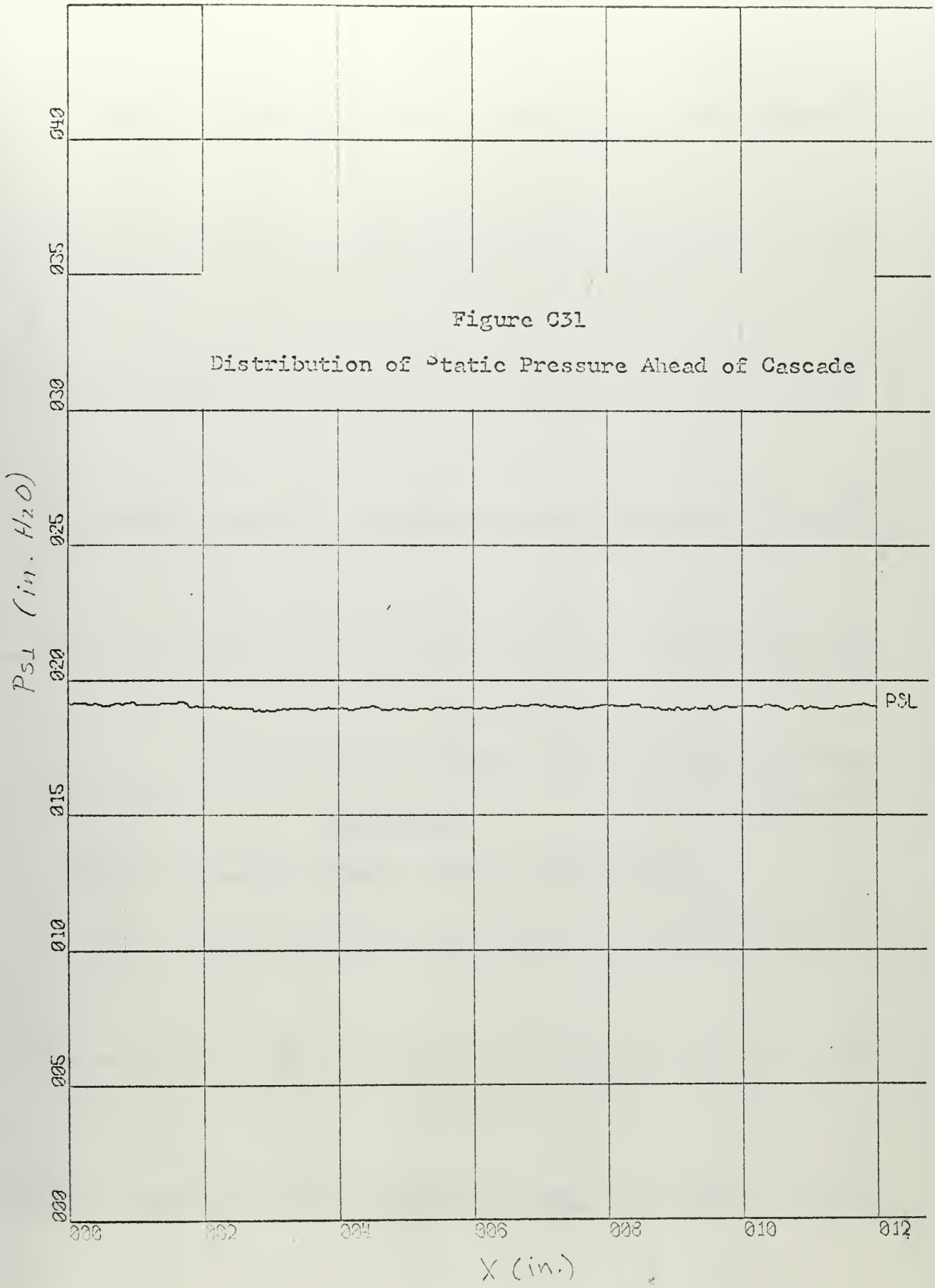

Figure C31

Distribution of Static Pressure Ahead of Cascade

X-SCALE = 2.00E+00 UNITS/INCH.
Y-SCALE = 5.00E+00 UNITS/INCH.

RUN 305 ROTOR PROFILES

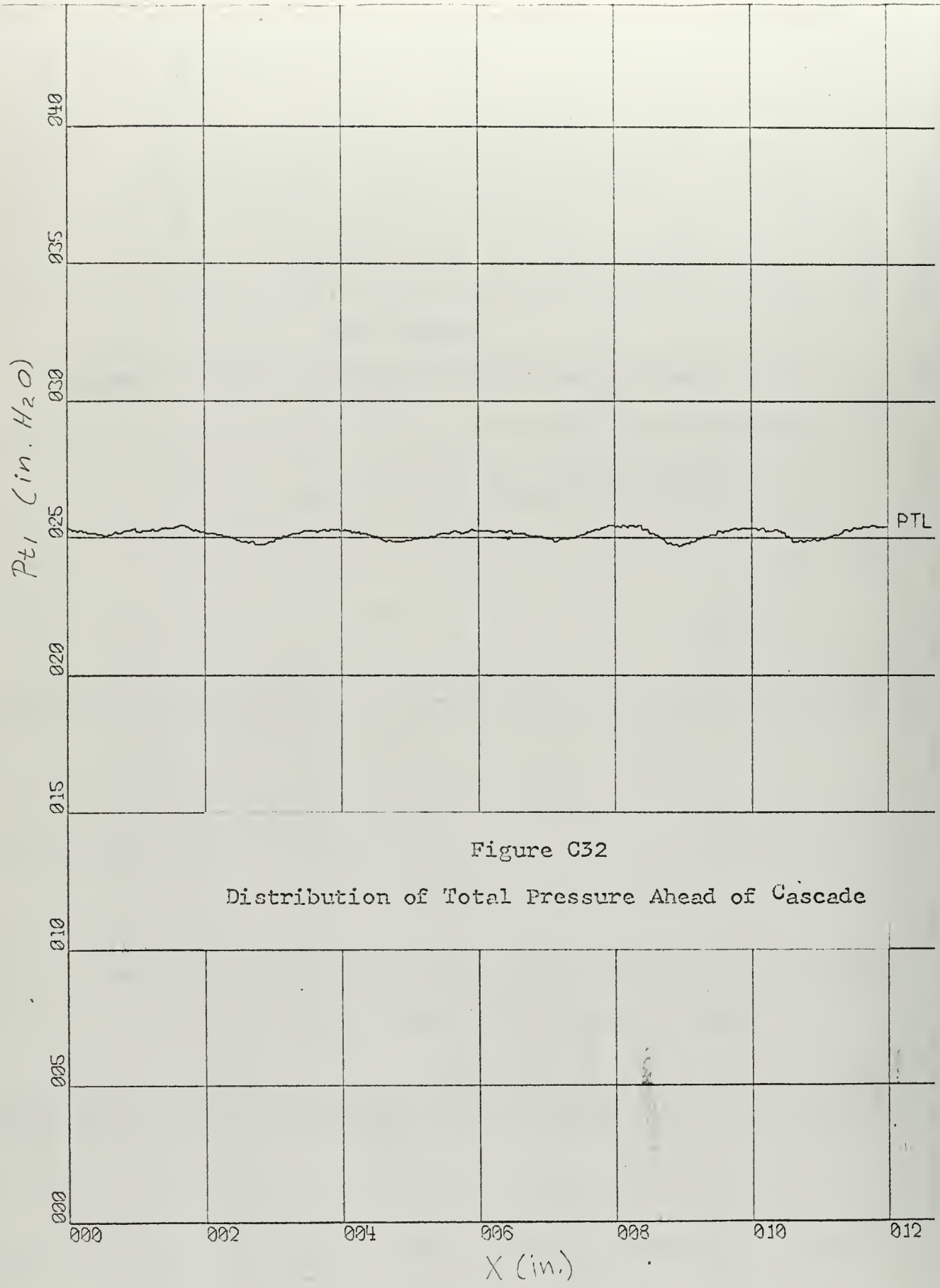

Figure C32

Distribution of Total Pressure Ahead of Cascade

K-SCALE = 2.00E+00 UNITS/INCH.
Y-SCALE = 5.00E+00 UNITS/INCH.

RUN 305 ROTOR PROFILES

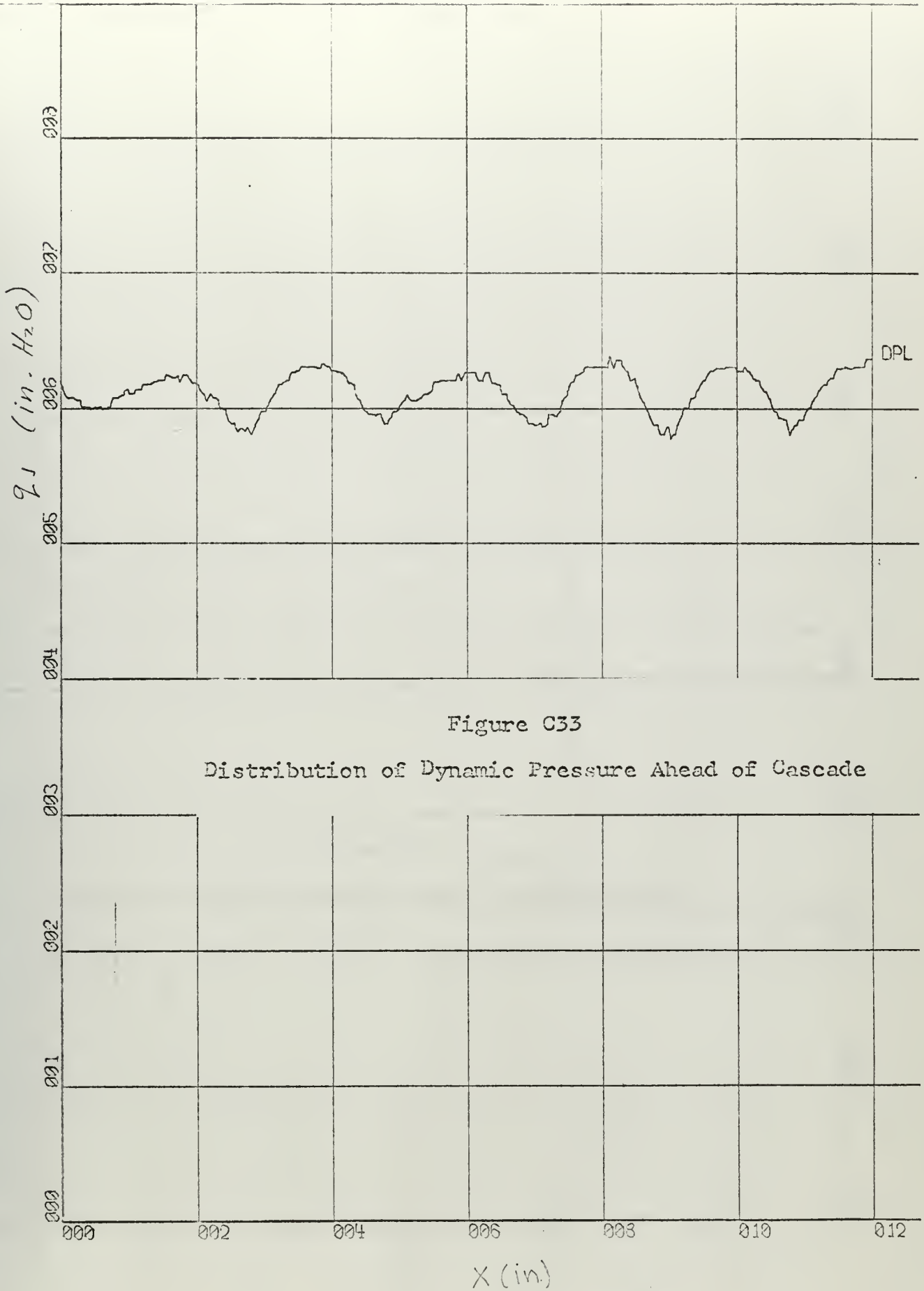

Figure C33

Distribution of Dynamic Pressure Ahead of Cascade

X-SCALE = 2.00E+00 UNITS/INCH.
Y-SCALE = 1.00E+00 UNITS/INCH.

RUN 305 ROTOR PROFILES

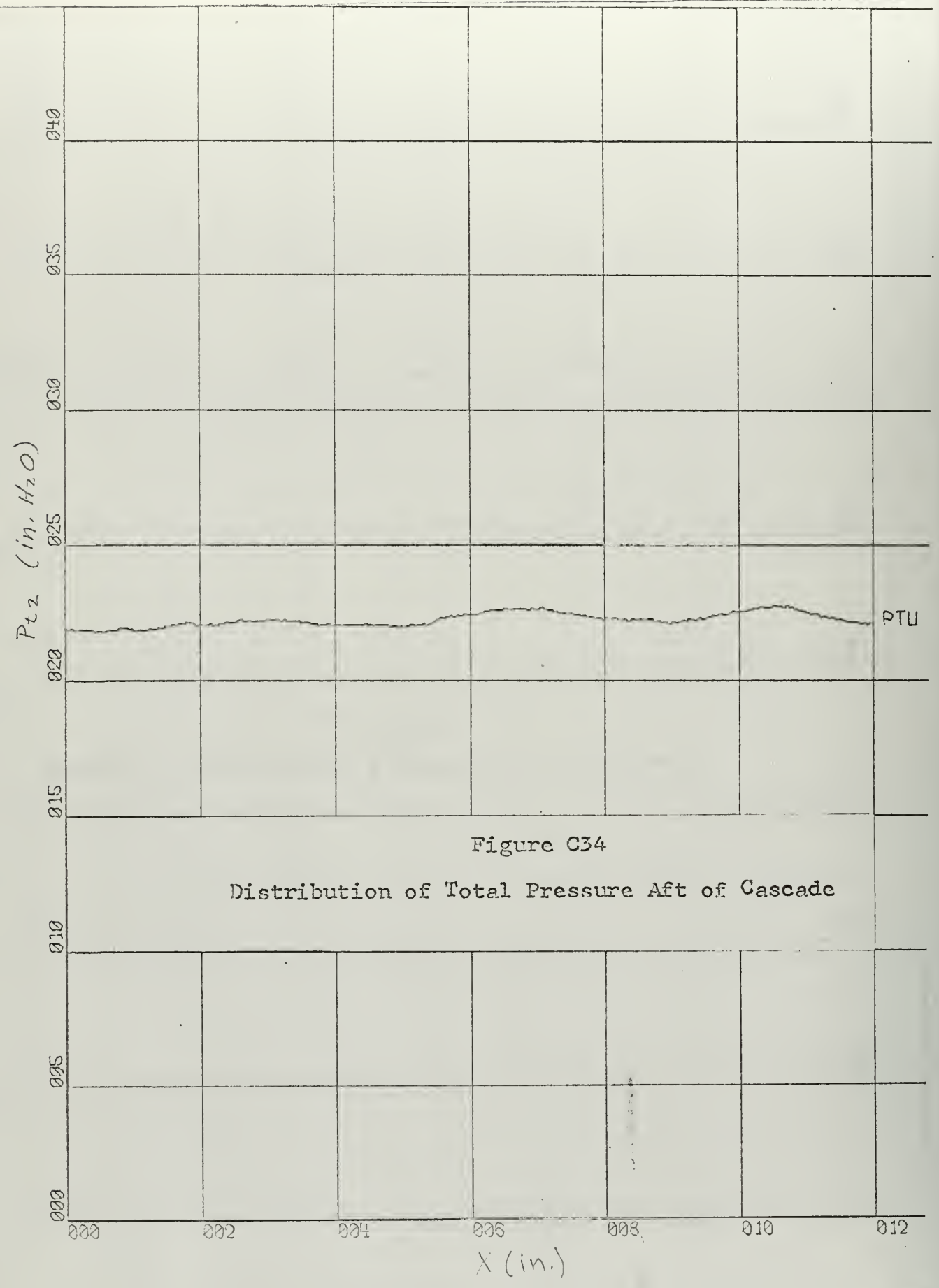

Figure C34

Distribution of Total Pressure Aft of Cascade

X-SCALE = 2.00E+00 UNITS/INCH.
Y-SCALE = 5.00E+00 UNITS/INCH.

RUN 305 ROTOR PROFILES

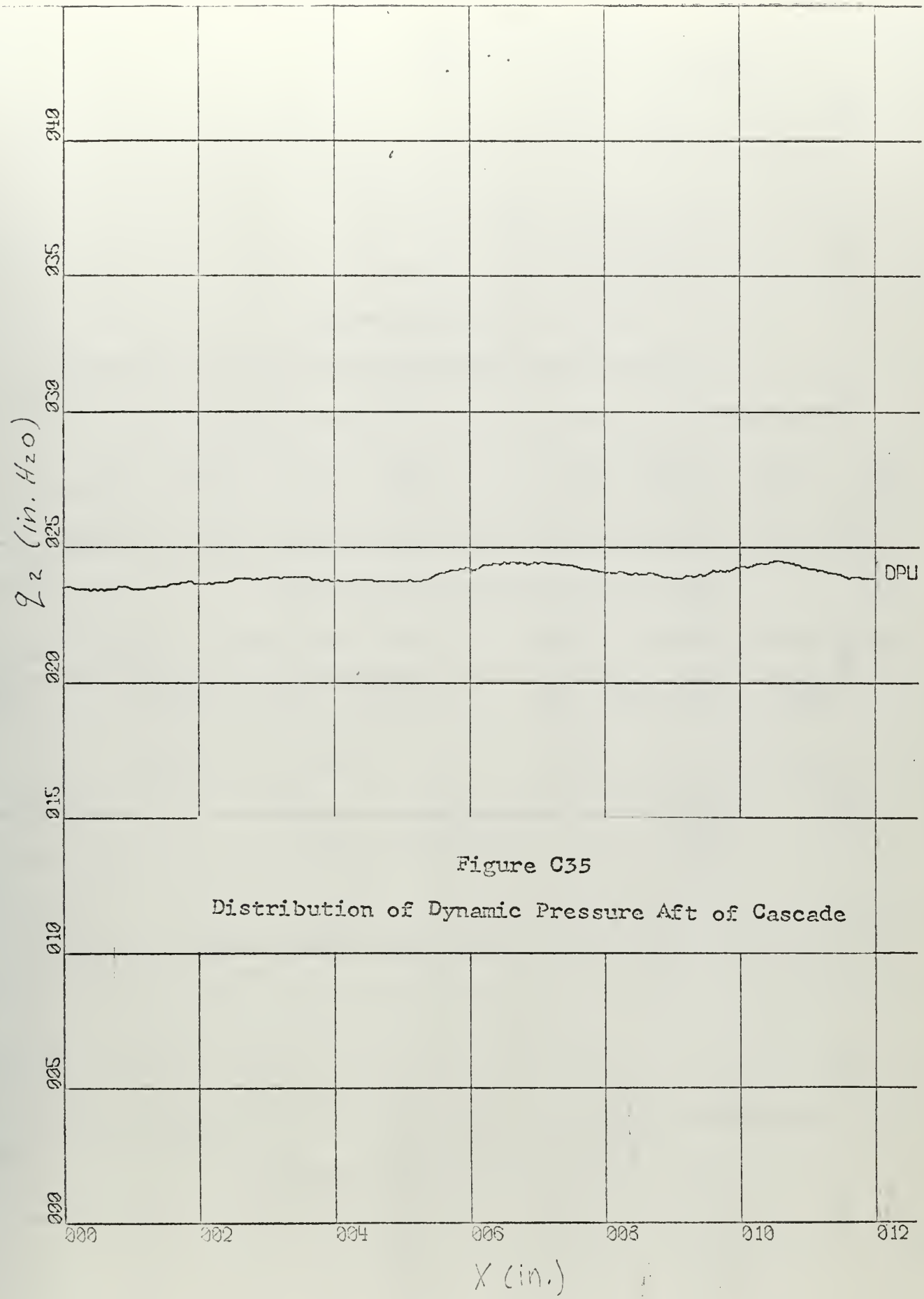

Figure C35

Distribution of Dynamic Pressure Aft of Cascade

X-SCALE = 2.00E+00 UNITS/INCH.
Y-SCALE = 5.00E+00 UNITS/INCH.

RUN 305 ROTOR PROFILES

Figure C36

Distribution of Static Pressure Aft of Cascade

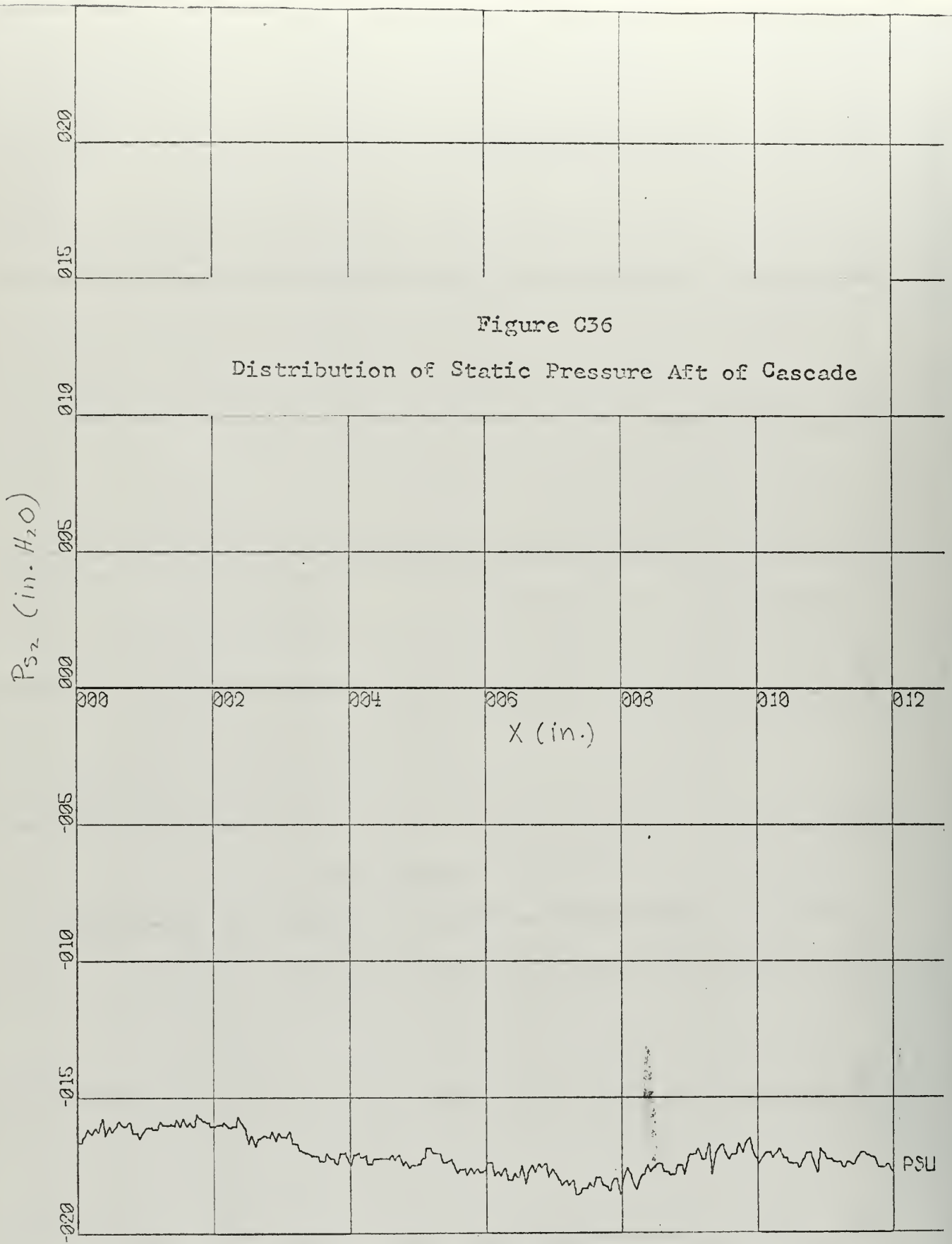

X-SCALE = 2.00E+00 UNITS/INCH.
Y-SCALE = 5.00E-01 UNITS/INCH.

RUN 305 ROTOR PROFILES

Table C7

PROPULSION LABORATORY
U.S. NAVAL POSTGRADUATE SCHOOL

TEST RUN NO. 306

BAROMETRIC PRESS. = 30.10 IN. HG.

PLENUM TEMP. = 71.7 DEG. F.

STAGGER ANGLE = -4.50DEG.

SOLIDITY = 1.66

BLADE PROFILE =

FAR AHEAD (STATION 0)				FAR AFT (STATION 3)			
V0 (FT/SEC)	ALPHA 0 (DEG)	PT0 (PSF)	PS0 (PSF)	V3 (FT/SEC)	ALPHA 3 (DEG)	PT3 (PSF)	PS3 (PSF)
269.861	68.62	2260.4	2171.3	337.933	-70.42	2249.2	2111.5

CONDITIONS AT THE MEASURING PLANES

LOWER TRAVERSE (STATION 1)		UPPER TRAVERSE (STATION 2)	
PT1 (PSF)	PS1 (PSF)	PT2 (PSF)	PS2 (PSF)
2260.4	2171.3	2249.3	2111.5

FORCES ON THE BLADES IN LBS. PER FT.

AXIAL	TANGENTIAL	LIFT	DRAG
17.64	48.18	51.26	2.26

TOTAL TURNING ANGLE OF THE FLOW (DEG) = 139.03

RUN NO. = 306 CONCLUDED

LOSS COEFFICIENT , MIXING LOSS INCLUDED = .07393

LIFT AND DRAG COEFFICIENTS BASED ON THE VECTORIAL MEAN OF V0 AND V3

CL	CD
6.2910	.2772

LIFT AND DRAG COEFFICIENTS BASED ON CONDITIONS FAR AHEAD OF THE CASCADE

CLO	CDO
1.0538	.0464

CONSTRICTION FACTOR = .8878

DELTA X LOWER = 12.00

DELTA X UPPER = 12.00

DENSITY(SLUGS PER CU.FT.) FAR AHEAD = .00240804

DENSITY(SLUGS PER CU.FT.) FAR AFT = .00235620

REYNOLDS NUMBER(CHORD) AND MACH NUMBER

REY	MO
1145262.	.2388

TIME, 4 MINUTES AND 1 SECONDS

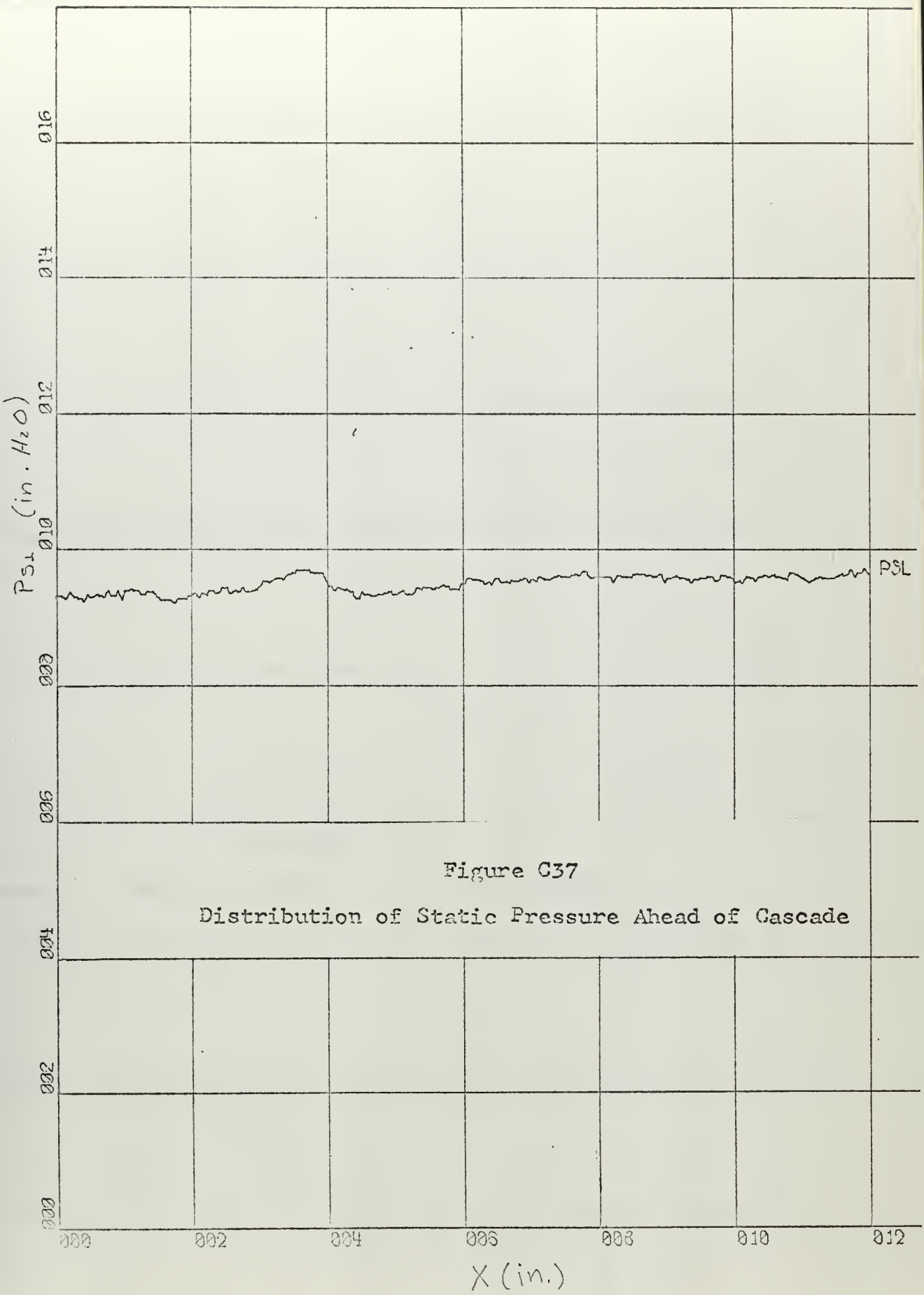

Figure C37

Distribution of Static Pressure Ahead of Cascade

X-SCALE - 2.00E+00 UNITS/INCH.
Y-SCALE - 2.00E+00 UNITS/INCH.

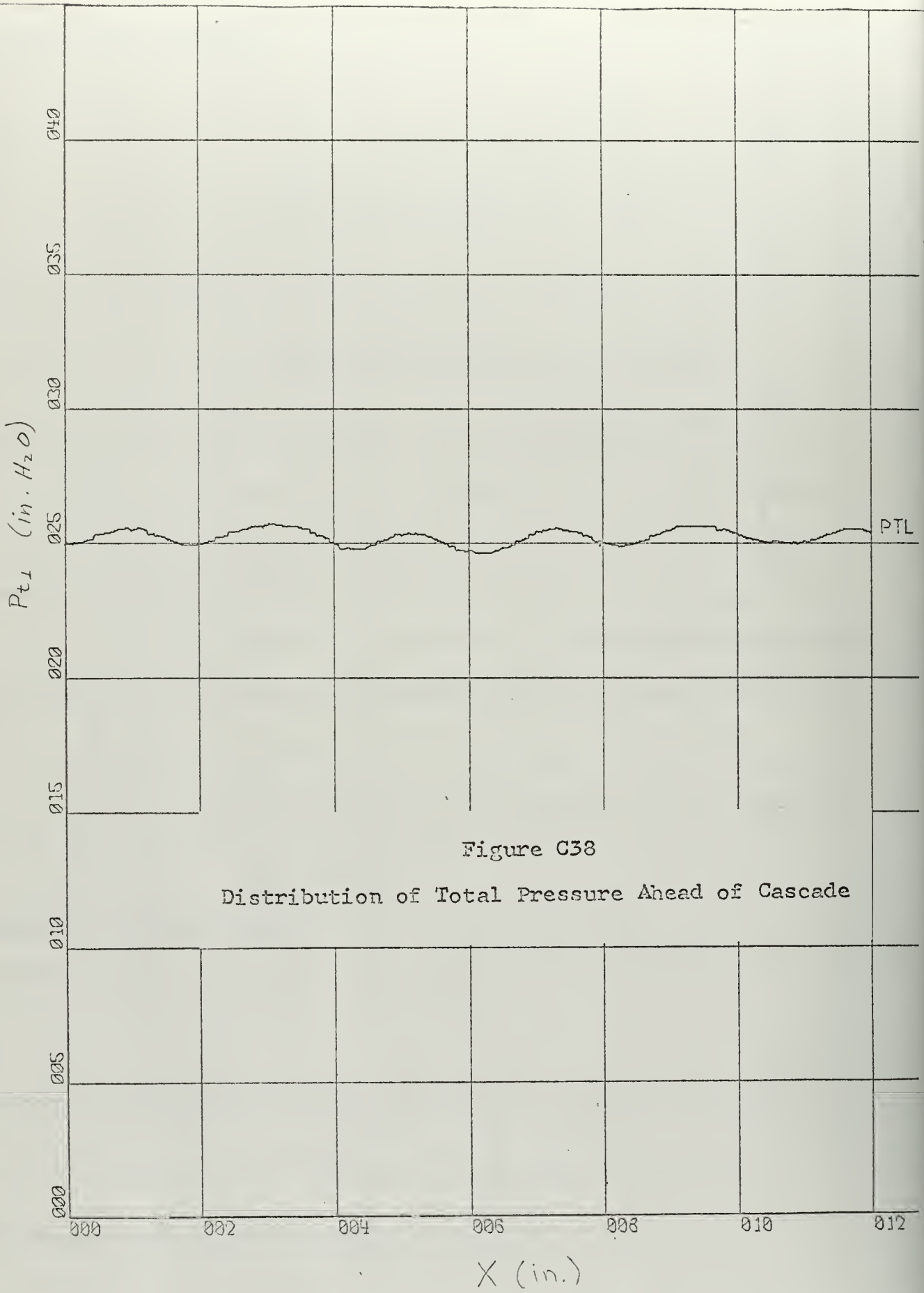

Figure C38

Distribution of Total Pressure Ahead of Cascade

X-SCALE = 2.00E+00 UNITS/INCH.
Y-SCALE = 5.00E+00 UNITS/INCH.

RUN 306 ROTOR PROFILES

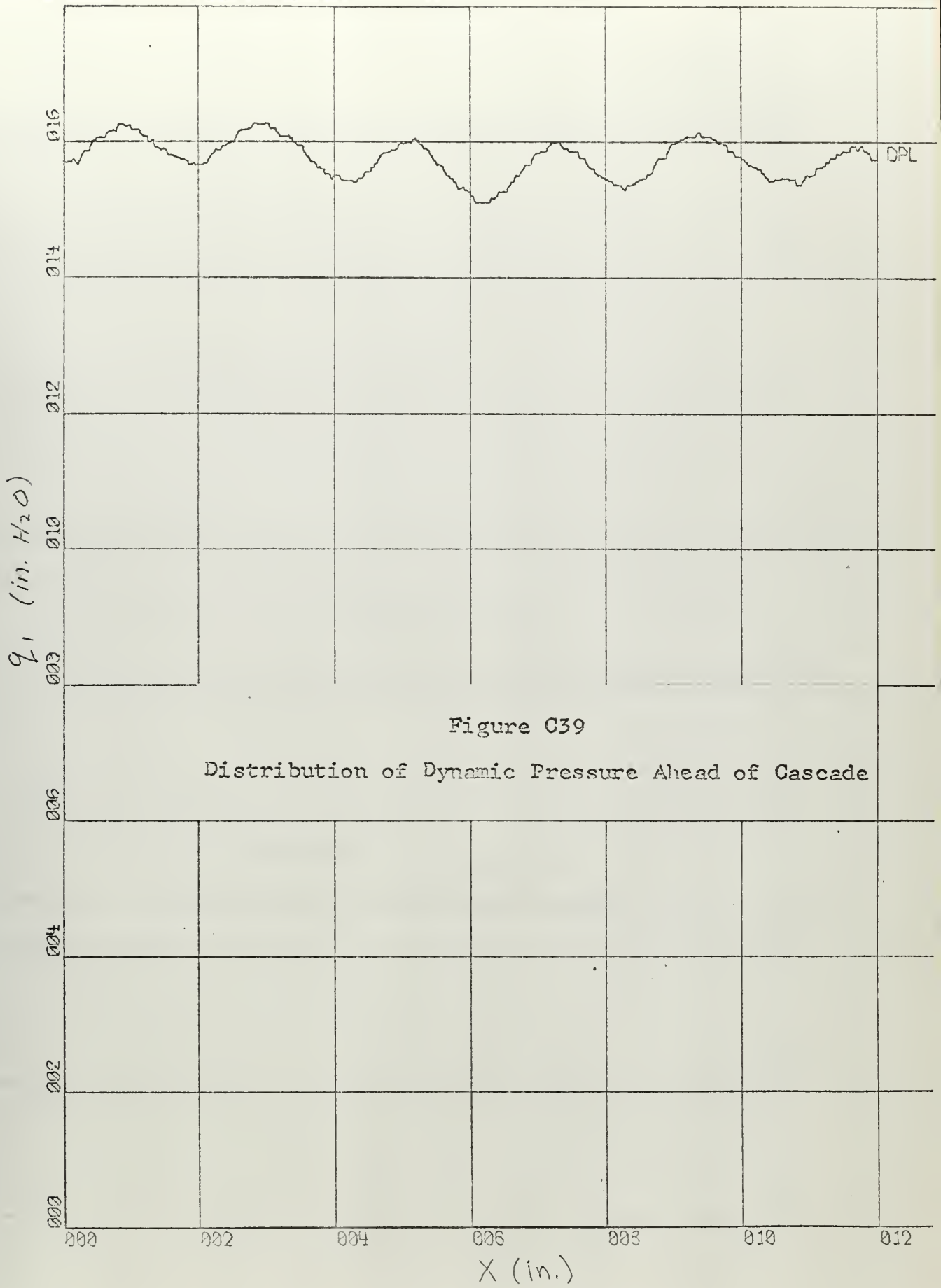

Figure C39

Distribution of Dynamic Pressure Ahead of Cascade

X-SCALE = 2.00E+00 UNITS/INCH.
Y-SCALE = 2.00E+00 UNITS/INCH.

RUN 306

ROTOR PROFILES

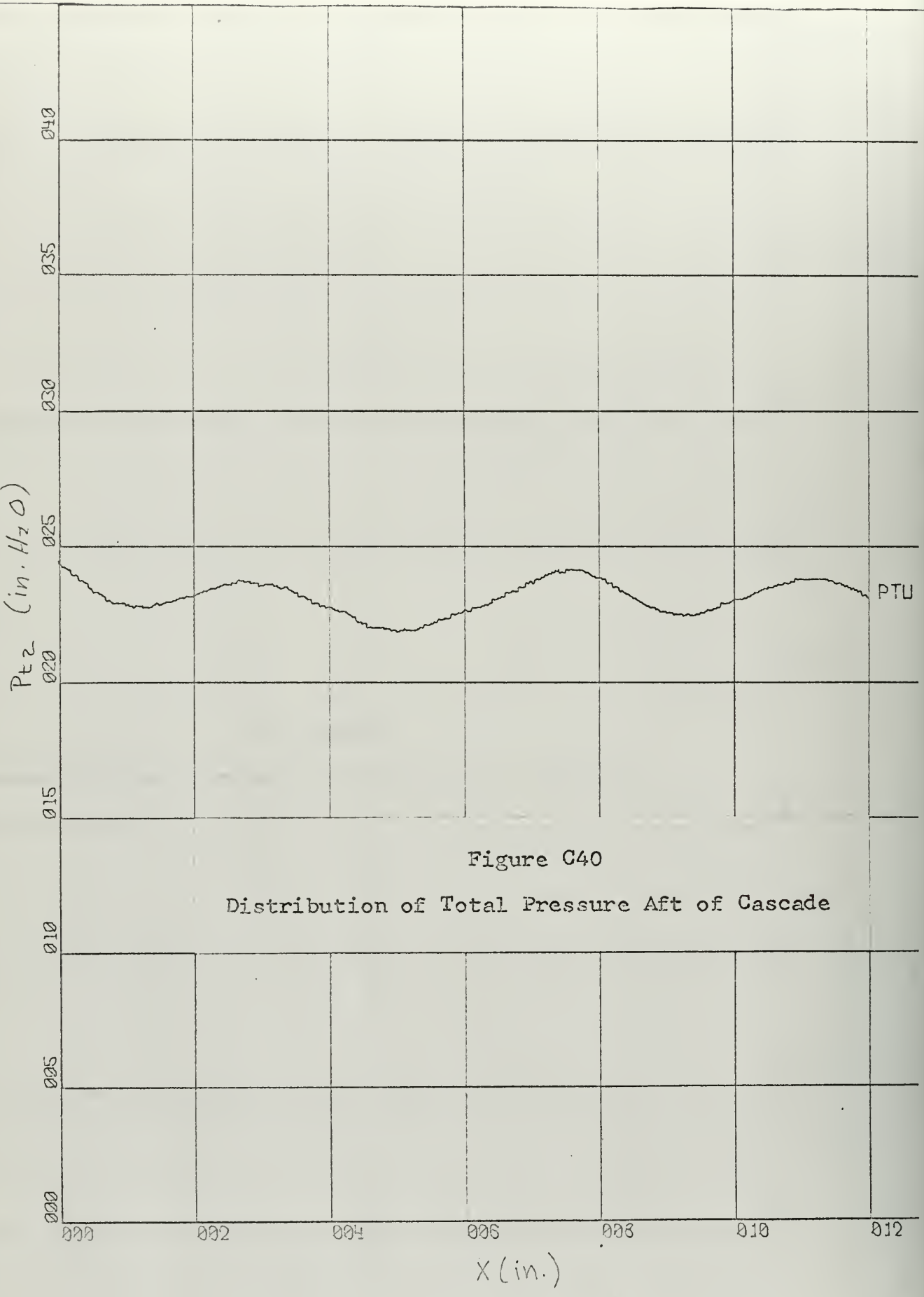

Figure C40

Distribution of Total Pressure Aft of Cascade

X-SCALE = 2.00E+00 UNITS/INCH.
Y-SCALE = 5.00E+00 UNITS/INCH.

RUN 306 ROTOR PROFILES

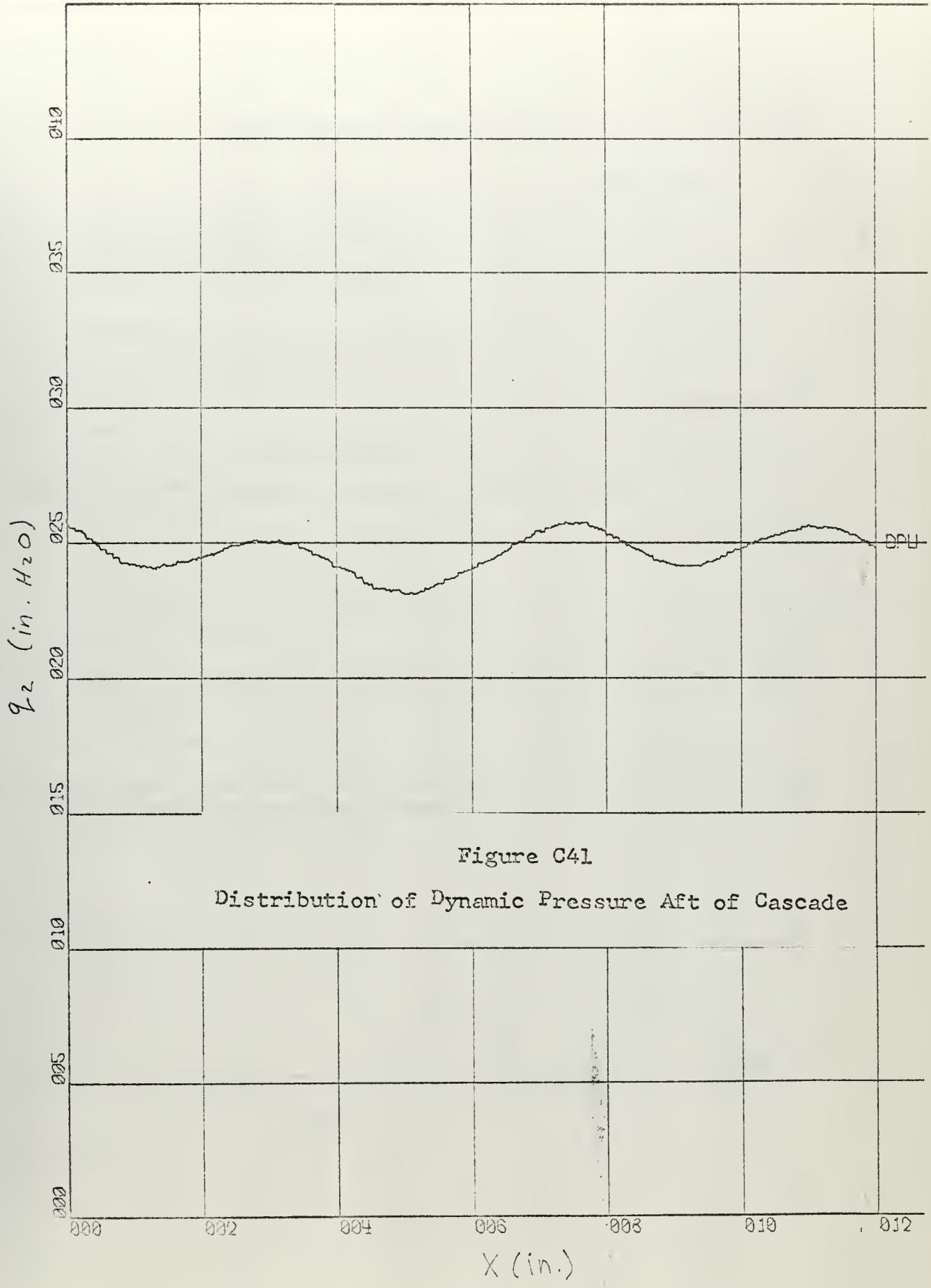

Figure C41

Distribution of Dynamic Pressure Aft of Cascade

X-SCALE = 2.00E+00 UNITS/INCH.
Y-SCALE = 5.00E+00 UNITS/INCH.

RUN 306 ROTOR PROFILES

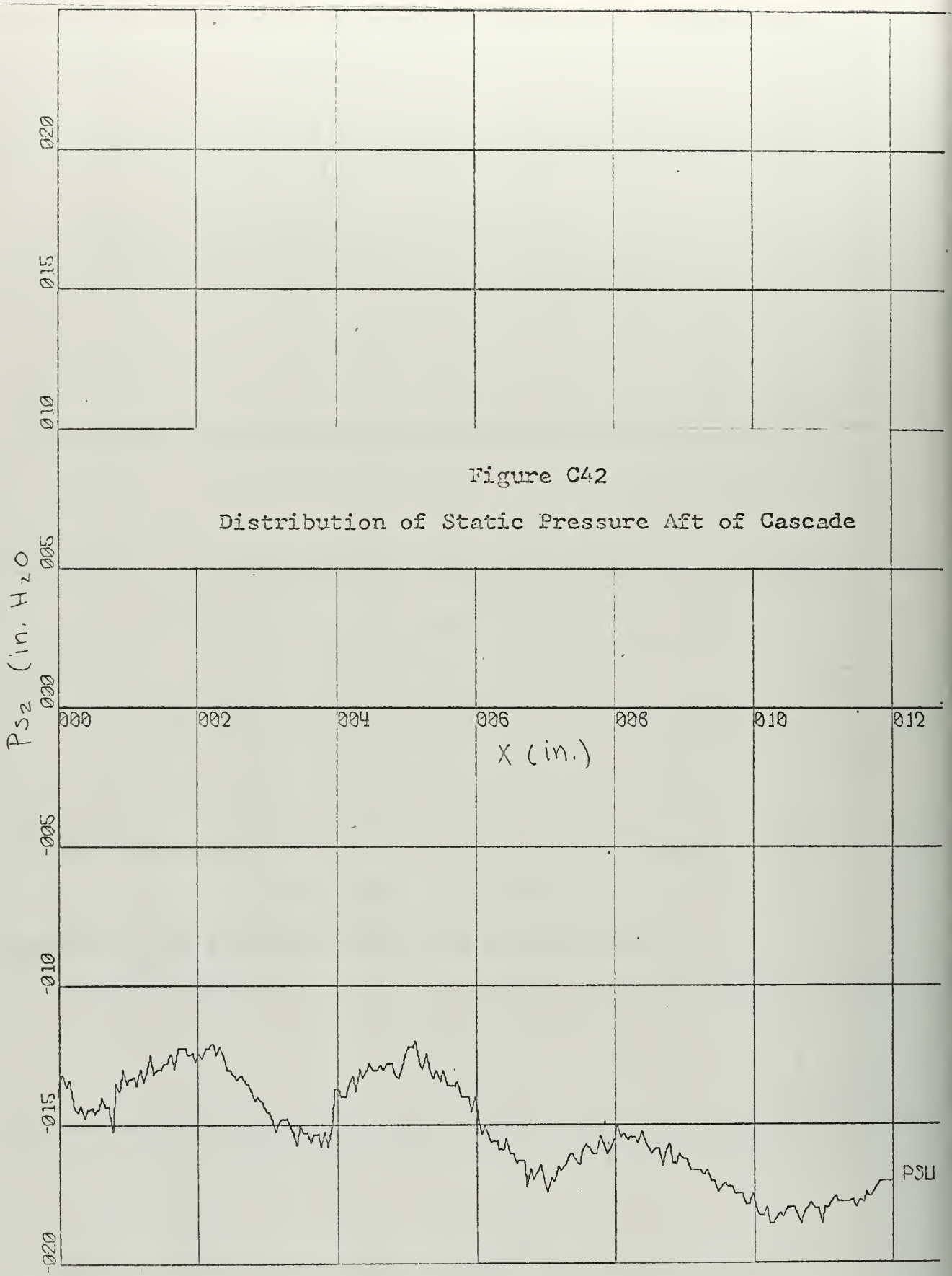

Figure C42

Distribution of Static Pressure Aft of Cascade

X-SCALE = 2.00E+00 UNITS/INCH.
Y-SCALE = 5.00E-01 UNITS/INCH.

RUN 306 ROTOR PROFILES

INITIAL DISTRIBUTION LIST

		No. Copies
1.	Defense Documentation Center Cameron Station Alexandria, Virginia 22314	20
2.	Library U. S. Naval Postgraduate School Monterey, California	2
3.	Commander Naval Air Systems Command Navy Department Washington, D. C.	1
4.	Professor M. H. Vavra Department of Aeronautics U. S. Naval Postgraduate School Monterey, California	2
5.	LCDR John E. Bartocci, USN FITRON 124 NAS Miramar, California	2
6.	Chairman, Department of Aeronautics U. S. Naval Postgraduate School Monterey, California 93940	2

DOCUMENT CONTROL DATA - R&D

(Security classification of title, body of abstract and indexing annotation must be entered when the overall report is classified)

1. ORIGINATING ACTIVITY (Corporate author)	2a. REPORT SECURITY CLASSIFICATION
U. S. Naval Postgraduate School	UNCLASSIFIED
	2b. GROUP N/A

3. REPORT TITLE Cascade Tests of the Blading of a High-Deflection, Single-Stage, Axial-Flow Impulse Turbine and Comparison of Results with Actual Performance

4. DESCRIPTIVE NOTES (Type of report and inclusive dates)
Thesis

5. AUTHOR(S) (Last name, first name, initial)
BARTOCCI, John E.

6. REPORT DATE	7a. TOTAL NO. OF PAGES	7b. NO. OF REFS
May 1966	159 103	12

8a. CONTRACT OR GRANT NO.	9a. ORIGINATOR'S REPORT NUMBER(S)
N/A	
b. PROJECT NO. N/A	N/A
c. N/A	9b. OTHER REPORT NO(S) (Any other numbers that may be assigned this report)
d. N/A	N/A

10. AVAILABILITY/LIMITATION NOTICES
~~Qualified requesters may obtain copies of this report from DDC~~ Memo 10/9/69
This document has been approved for public release and sale; its distribution is unlimited.

11. SUPPLEMENTARY NOTES	12. SPONSORING MILITARY ACTIVITY
N/A	Commander, Naval Air Systems Command, Navy Department, Washington, D. C.

13. ABSTRACT

Cascade tests were performed on models of the stator (nozzles) and rotor blade rows of a high deflection, single-stage, axial-flow impulse turbine. The tests were performed at the Rectilinear Cascade Test Facility of the Propulsion Laboratories, United States Naval Postgraduate School. The results of these tests were compared with the performance data of the actual turbine. The comparison showed that profile and mixing losses, through not negligible, constitute only a small percentage of the overall rotor loss. Also, the inlet flow angle at which the minimum loss occurred for the Cascade flow was significantly different from the inlet flow angle at which minimum actual rotor loss occurred.

DD FORM 1 JAN 64 1473

14. KEY WORDS	LINK A		LINK B		LINK C	
	ROLE	WT	ROLE	WT	ROLE	WT
CASCADE TURBINE						

INSTRUCTIONS

1. ORIGINATING ACTIVITY: Enter the name and address of the contractor, subcontractor, grantee, Department of Defense activity or other organization *(corporate author)* issuing the report.

2a. REPORT SECURITY CLASSIFICATION: Enter the overall security classification of the report. Indicate whether "Restricted Data" is included. Marking is to be in accordance with appropriate security regulations.

2b. GROUP: Automatic downgrading is specified in DoD Directive 5200.10 and Armed Forces Industrial Manual. Enter the group number. Also, when applicable, show that optional markings have been used for Group 3 and Group 4 as authorized.

3. REPORT TITLE: Enter the complete report title in all capital letters. Titles in all cases should be unclassified. If a meaningful title cannot be selected without classification, show title classification in all capitals in parenthesis immediately following the title.

4. DESCRIPTIVE NOTES: If appropriate, enter the type of report, e.g., interim, progress, summary, annual, or final. Give the inclusive dates when a specific reporting period is covered.

5. AUTHOR(S): Enter the name(s) of author(s) as shown on or in the report. Enter last name, first name, middle initial. If military, show rank and branch of service. The name of the principal author is an absolute minimum requirement.

6. REPORT DATE: Enter the date of the report as day, month, year; or month, year. If more than one date appears on the report, use date of publication.

7a. TOTAL NUMBER OF PAGES: The total page count should follow normal pagination procedures, i.e., enter the number of pages containing information.

7b. NUMBER OF REFERENCES: Enter the total number of references cited in the report.

8a. CONTRACT OR GRANT NUMBER: If appropriate, enter the applicable number of the contract or grant under which the report was written.

8b, 8c, & 8d. PROJECT NUMBER: Enter the appropriate military department identification, such as project number, subproject number, system numbers, task number, etc.

9a. ORIGINATOR'S REPORT NUMBER(S): Enter the official report number by which the document will be identified and controlled by the originating activity. This number must be unique to this report.

9b. OTHER REPORT NUMBER(S): If the report has been assigned any other report numbers *(either by the originator or by the sponsor)*, also enter this number(s).

10. AVAILABILITY/LIMITATION NOTICES: Enter any limitations on further dissemination of the report, other than those imposed by security classification, using standard statements such as:

(1) "Qualified requesters may obtain copies of this report from DDC."

(2) "Foreign announcement and dissemination of this report by DDC is not authorized."

(3) "U. S. Government agencies may obtain copies of this report directly from DDC. Other qualified DDC users shall request through _____."

(4) "U. S. military agencies may obtain copies of this report directly from DDC. Other qualified users shall request through _____."

(5) "All distribution of this report is controlled. Qualified DDC users shall request through _____."

If the report has been furnished to the Office of Technical Services, Department of Commerce, for sale to the public, indicate this fact and enter the price, if known.

11. SUPPLEMENTARY NOTES: Use for additional explanatory notes.

12. SPONSORING MILITARY ACTIVITY: Enter the name of the departmental project office or laboratory sponsoring *(paying for)* the research and development. Include address.

13. ABSTRACT: Enter an abstract giving a brief and factual summary of the document indicative of the report, even though it may also appear elsewhere in the body of the technical report. If additional space is required, a continuation sheet shall be attached.

It is highly desirable that the abstract of classified reports be unclassified. Each paragraph of the abstract shall end with an indication of the military security classification of the information in the paragraph, represented as *(TS), (S), (C), or (U)*.

There is no limitation on the length of the abstract. However, the suggested length is from 150 to 225 words.

14. KEY WORDS: Key words are technically meaningful terms or short phrases that characterize a report and may be used as index entries for cataloging the report. Key words must be selected so that no security classification is required. Identifiers, such as equipment model designation, trade name, military project code name, geographic location, may be used as key words but will be followed by an indication of technical context. The assignment of links, roles, and weights is optional.

DD FORM 1 JAN 64 1473 (BACK)